CHAPTER (5)

EXPERIMENTAL RESULTS AND DISCUSSION

CHAPTER (5)

EXPERIMENTAL RESULTS AND DISCUSSION .

INTRODUCTION :-

Parameters of the DC glow discharge in the three different regions (i.e. cathode fall , negative glow and positive column regions) have been investigated . The electron temperature and density , the floating potential , the plasma potential , the potential distributions , the electric field distributions , the electron energy distribution functions (EEDF) and the degree of ionization have been obtained using electric probes and spectroscopic techniques .

5.1-Electrical Characteristics of The Glow Discharge.

5.1.1-The Current-Voltage (I_a - V_a) Characteristic Curves of the Glow Discharge :-

The (I_a - V_a) characteristic curves of the gas discharge were measured using the electric circuit as shown in Fig. (12) . The measurements have been carried out in the pressure range of 0.5 - 4.0 mbar for Ar gas , and in the range of 2.7- 6 mbar for He gas , whereas

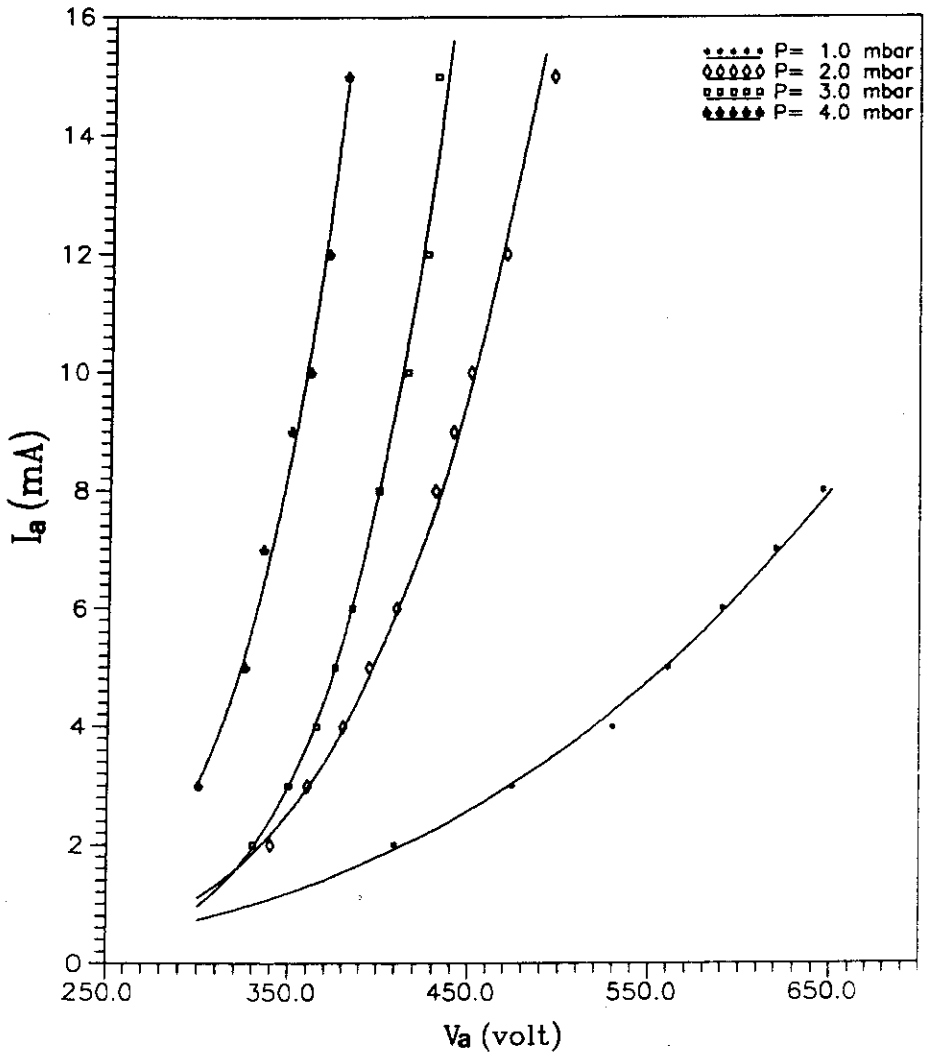

Fig.(12) The I–V characteristics curves for Ar discharge in the pressure range of (1–4) mbar .

the distance between the two discharge electrodes was fixed at 3.2 cm . This distance is long enough for the existence of the three regions (***Parker , 1963***) . The I_a-V_a characteristic curves for Ar gas at pressures of (1 , 2 , 3 and 4 mbar) are shown in Fig. (12) . Similar I_a-V_a characteristic curves were obtained for He discharge , see Fig. (13) . The upper limits of I_a and V_a were limited by the power of the DC power supply . The I_a-V_a characteristic curves shown in Figs. (12 , 13) covers the region DEFG in Fig. (1) . Since at low pressure , the probability of electron ionizing collisions with atoms will decrease (therefore the mean free path will increase) , large value of the discharge voltage will be required to maintain the discharge . Thus , small discharge current I_a is expected . This confirms the measurements in Figs. (12,13) . At high pressures number of electron-atom ionizing collisions increases . Thus , more electrons and positive ions are produced and consequently , the discharge current is increased at the same voltage . (see ***Yumoto et al. 1989*** and ***Schweer et al. , 1990***) .

5.1.2- Effect of Gas Pressure on the Discharge Voltage .

Effect of the gas pressure P , on the discharge voltage V_a , at discharge currents of 2.0 , 6.0 and 10.0 mA , for Ar discharge , is shown in Fig. (14) . The discharge voltage V_a decreases by increasing gas pressure since at low pressures large values of the discharge voltage V_a (at a constant I_a) is required for maintaining the discharge . For He-discharge the same variation was obtained {see Fig.(15) } , although gas pressure range was higher than that of Ar-discharge .

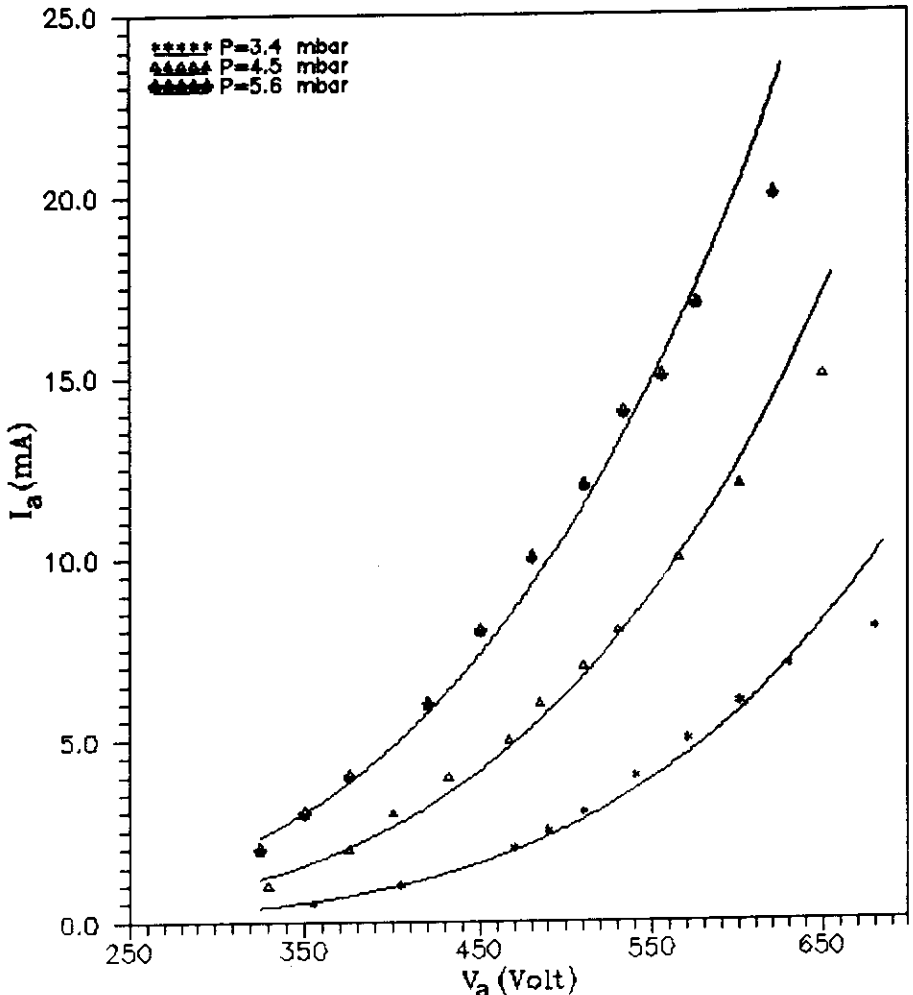

Fig.(13) The I–V charcteristic curves of He discharge for the pressure range of (3.4–5.6) mbar .

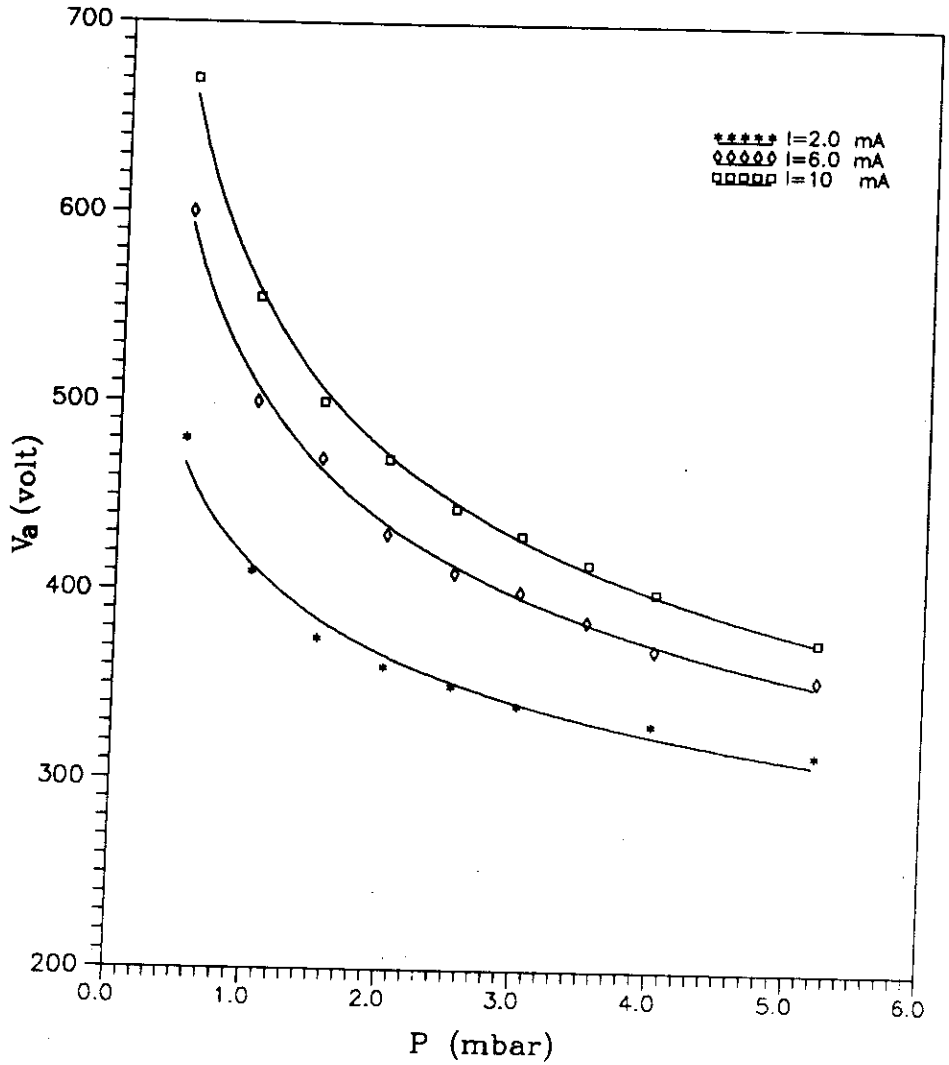

Fig.(14) The relation between the discharge voltage and the Ar gas pressures at different values of I_a

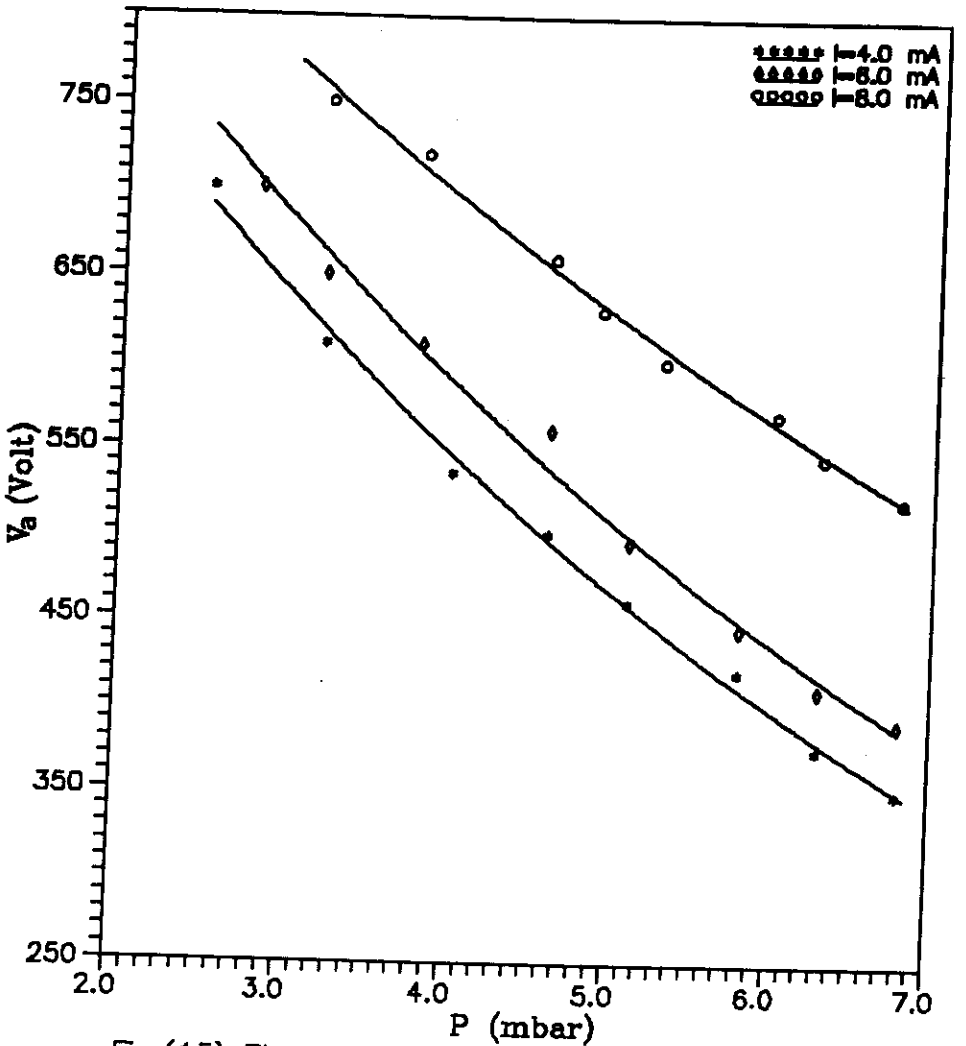

Fig.(15) The relation between the discharge voltage and the He gas discharge at constant I_a.

This can be attributed to the higher ionization potential of He (24.6 eV) than that of Ar (15.76 eV) and hence the breakdown voltage of He will be high . Nevertheless , if He pressure is increased , the breakdown voltage can be reduced over the same distance between the two electrodes (***Parker , 1963***) .

5.1.3- Potential Distribution Measurements .

An important character of the glow discharge is the variation of the potential difference (P.D.) across the two electrodes between the cathode to the anode . The measurements of the potential distribution was carried out by moving a single probe (of 0.15 cm radius) between the cathode and the anode (the cathode was fixed at ground potential) . At the beginning of the measurements in Ar- discharge , the potential distribution was measured at discharge current of 5.0 mA as a function of the gas pressure {see Fig. (16)}. Effect of increasing discharge current on the potential distribution (at constant gas pressure of 2.0 mbar) is shown in Fig. (17) . Figure (16) shows that the potential distribution can be divided into three regions . In region I (AB) , the potential increases sharply within a small discharge length . Whenever , gas breakdown takes place in the tube , a sudden increase in the rate of ionization , particularly near the cathode is observed . Since positive ions move in the electric field much more slowly than the electrons (due to their masses) , the electrons are swept rapidly towards the anode leaving a dense positive space charge near the cathode . Thus , the electric field is distorted and most of the applied potential is dropped

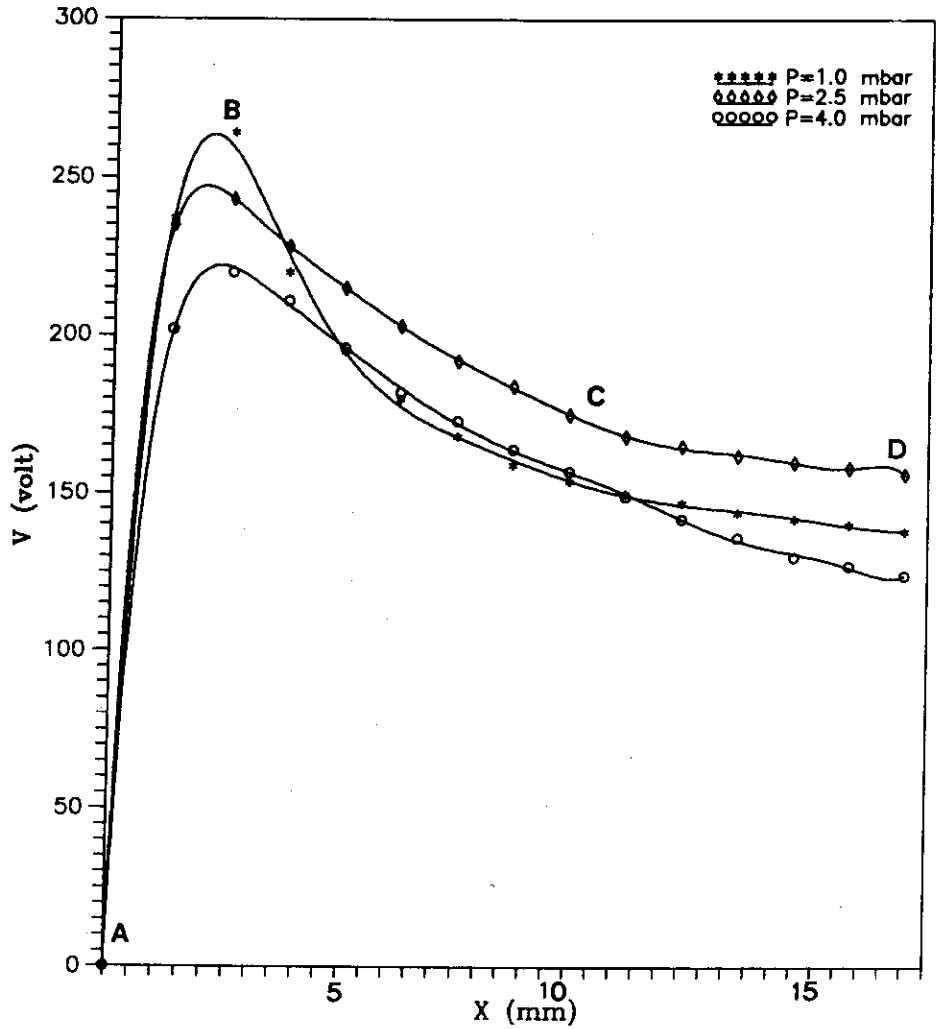

Fig.(16) The axial potential distribution along the Ar glow discharge at different pressures .

across a narrow space in front of the cathode , which is called "cathode fall region" . Region II (BC) in Fig. (16) indicates that the .potential decreases steadily and hence the electric field will be weak , since this region contains many free electrons , this region is called the "negative glow" . In region III (CD) , however the potential distribution is nearly constant and linear since the positive and negative carriers densities are closely. equal this region is called the "positive column" . The positive column can be extended to any length to fill the remaining space between the end of the negative glow and the anode , as shown in Fig. (16) .

The potential distributions behaviour in He discharge were also measured and shown in Figs. (18) and (19) . Curves in Figs. (16) , (17) , (18) and (19) , agree with the expected potential distribution in the cylindrical discharge tubes (see ***Hintz , 1990***) . Although , the general behaviour of the present results agree with that of ***Hintz (1990)*** , they differ in the detail values under the different conditions . This can be attributed to the presence of a magnet placed under the cathode in the present experiment . This produced magnetic field which confined the discharge between the two electrodes and thus charged particles were diffuse out , of the discharge area to the container walls , with very small rate .

5.1.4- The Electric Field Distribution .

Values of the electric field are obtained by differentiating the measured potential distribution curves in the preceding section , i.e. by computing (dV/dX) using BASIC computing program . Figures (20) and

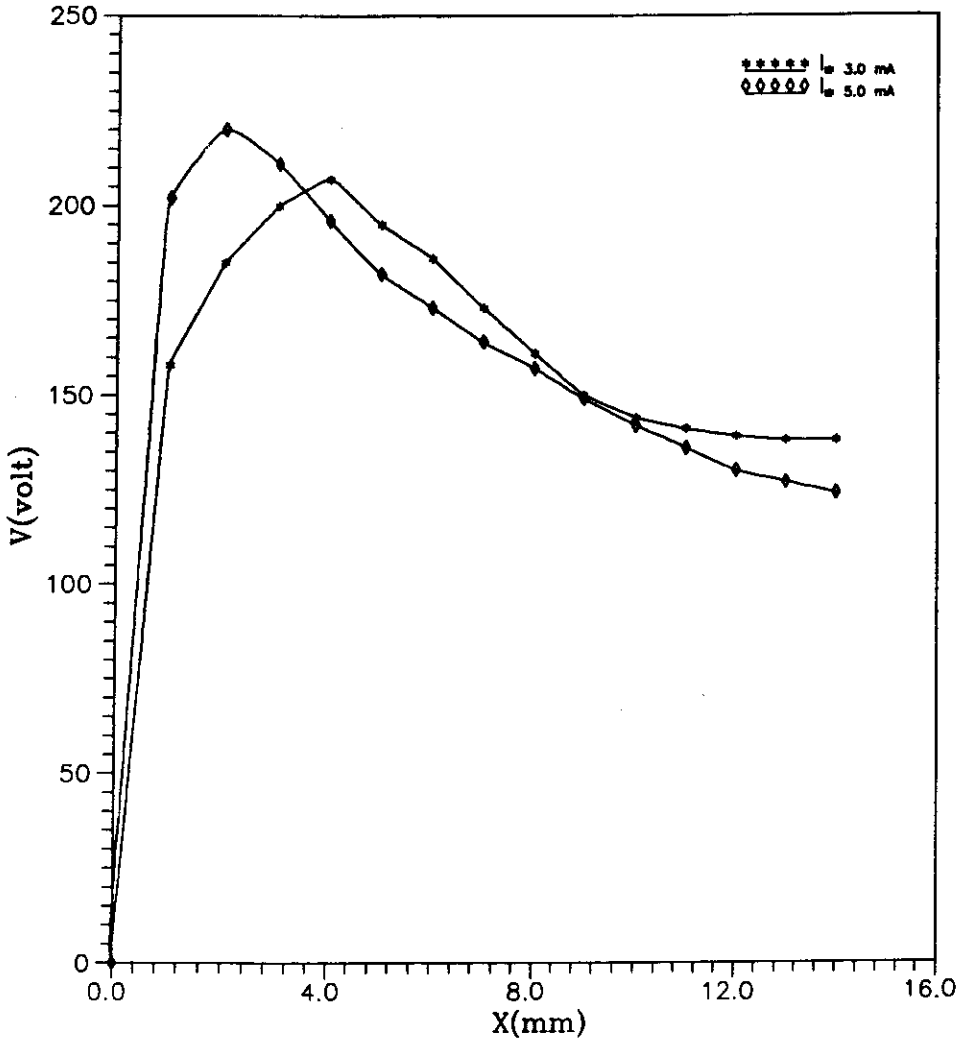

Fig.(17) The potential distribution of Ar dischorge at constant pressure (P=2 mbar) .

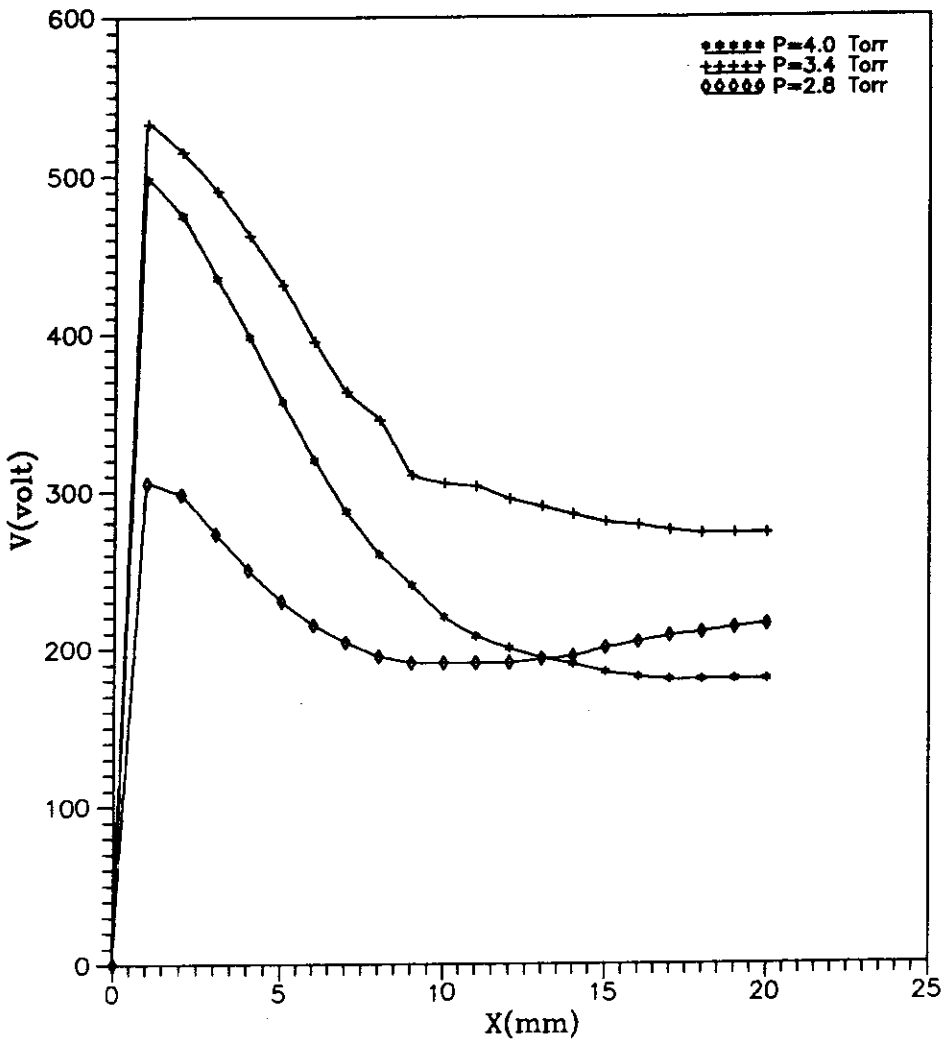

Fig.(18) The potential distribution of He discharge at constant I_a (= 5.0 mA) .

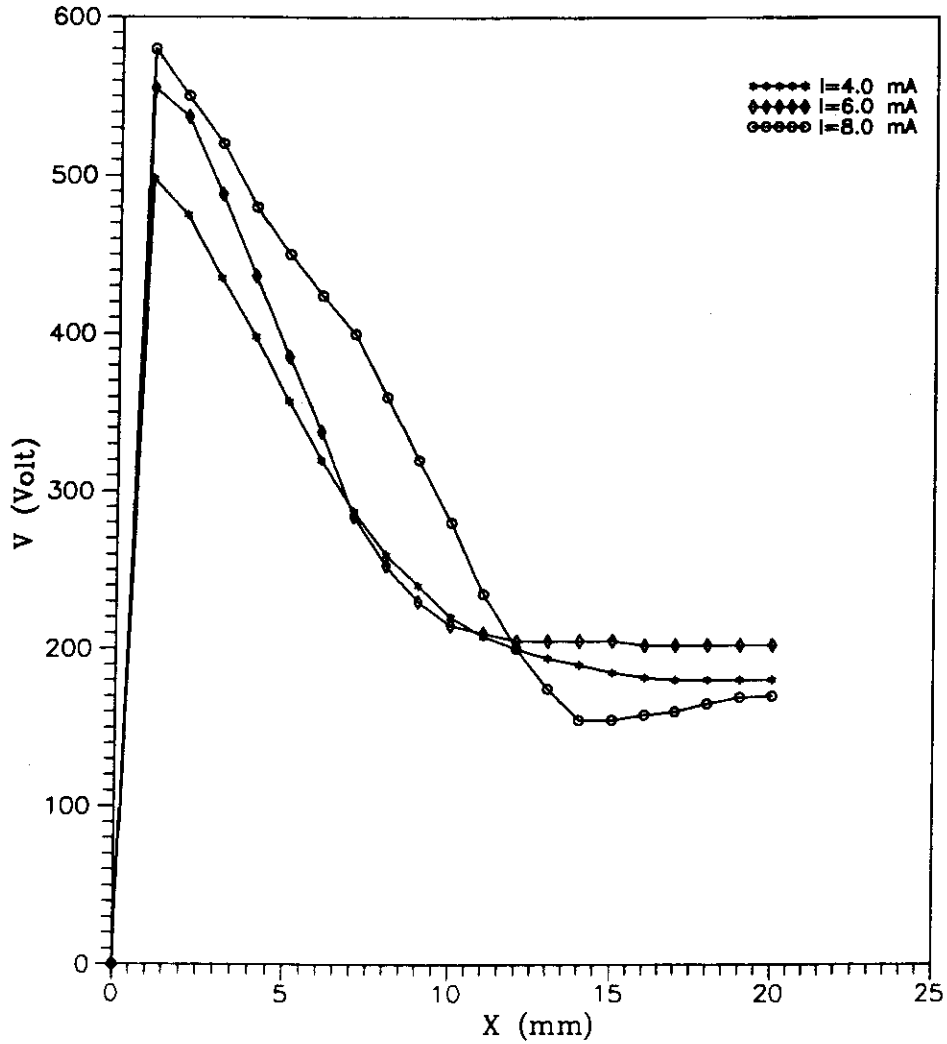

Fig.(19) The potentail distribution of He discharge ot constant pressure (P= 4 mbar) .

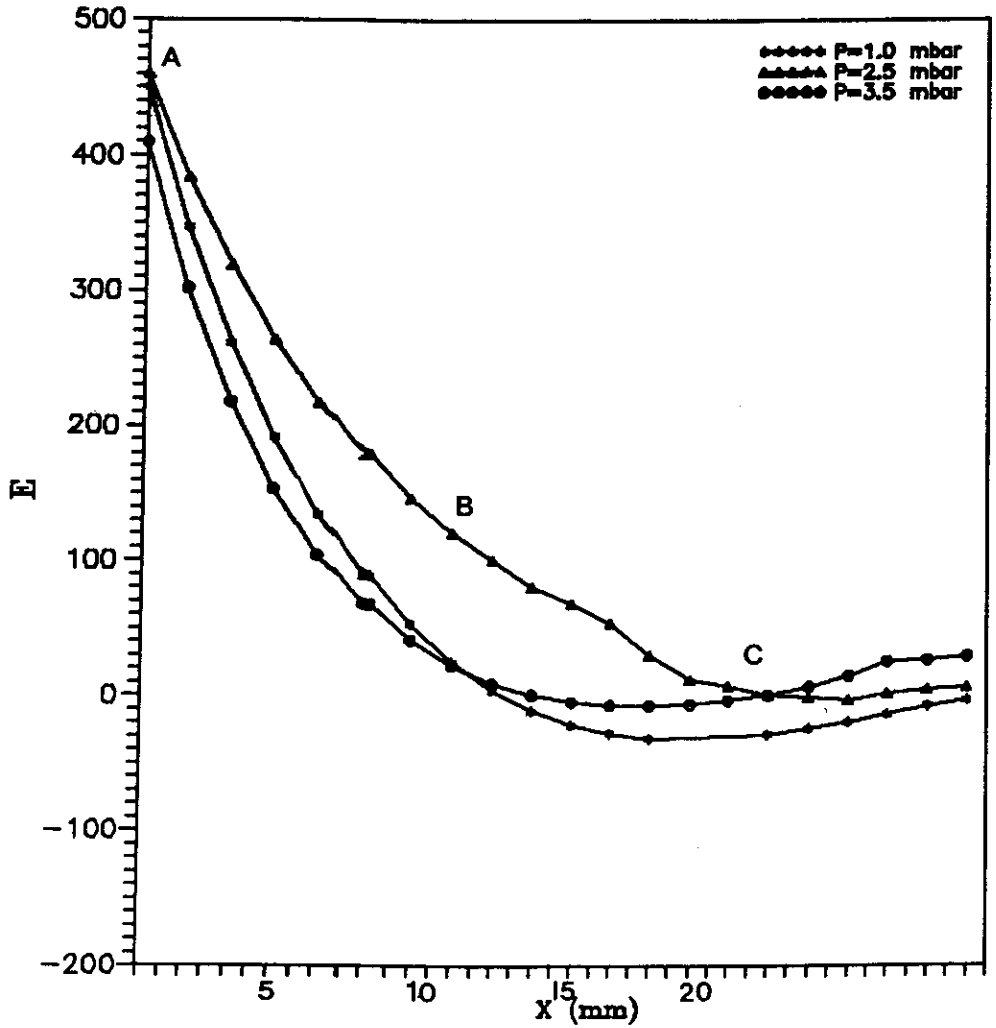

Fig.(20) The Electric field distribution of Ar discharge at constant I_a.

(21) show the electric field distribution for Ar and He discharges, respectively , at three different gas pressures (and at $I_a = 5.0$ mA) . The effect of increasing discharge current on the electric field distribution is also shown in Figs. (22) and (23) for Ar and He , respectively .

At the cathode fall region , the electric field is high and falls sharply with large slope away from the cathode , this is related to the intense positive space charge which lies in front of the cathode . This acts as an accelerator for the electrons . Thus the electrons emitted from the cathode are then accelerated away , until they reach the negative glow region where the electric field becomes weak (zero and sometimes it reaches a negative value) . In this region , the gained kinetic energy of the electrons is dissipated in collisions with the atoms of the gas and thus secondary electrons would be produced . In the positive column region constant and linear electric field is needed to maintain discharge along the large length of the column which is required to carry the discharge current .

The present measurements agree fairly with measurements of ***Den Hartog et al. , 1988*** and ***Barbeau and Jolly , 1991*** . The latter used Laser induced fluorescence technique which produced accurate measurements of the absolute electric field intensity in the cathode fall region . Also , ***Fujii et al. (1989)*** calculated the electric field distribution E in the cathode fall region by using a recent formula proposed of the ionization coefficient "α" which would be more suitable in this region . They concluded that E changes linearly with position and reaches an extremely high value near the cathode surface .

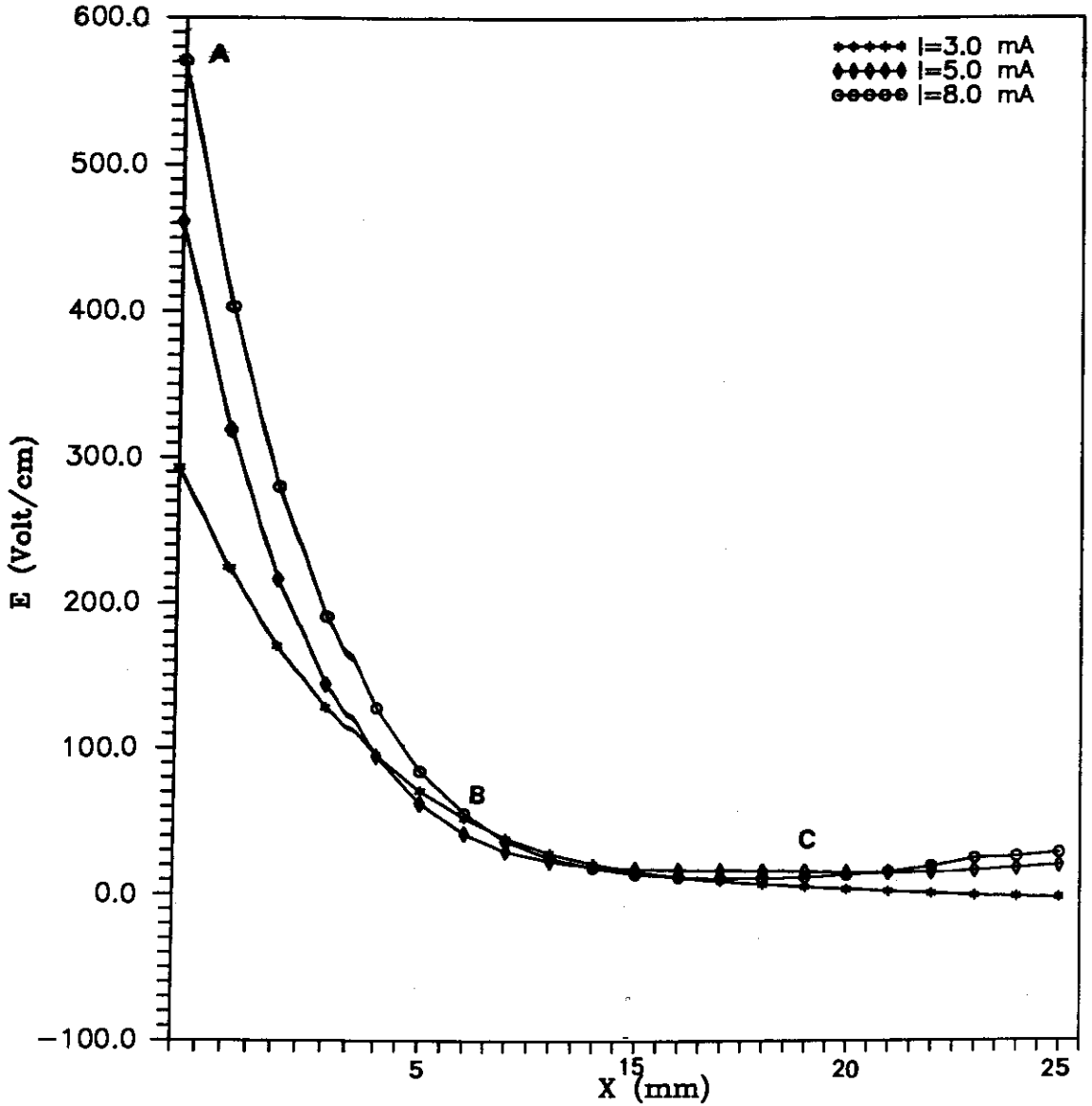

Fig.(21) The axial electric field distribution along the He glow discharge at different values of I_o.

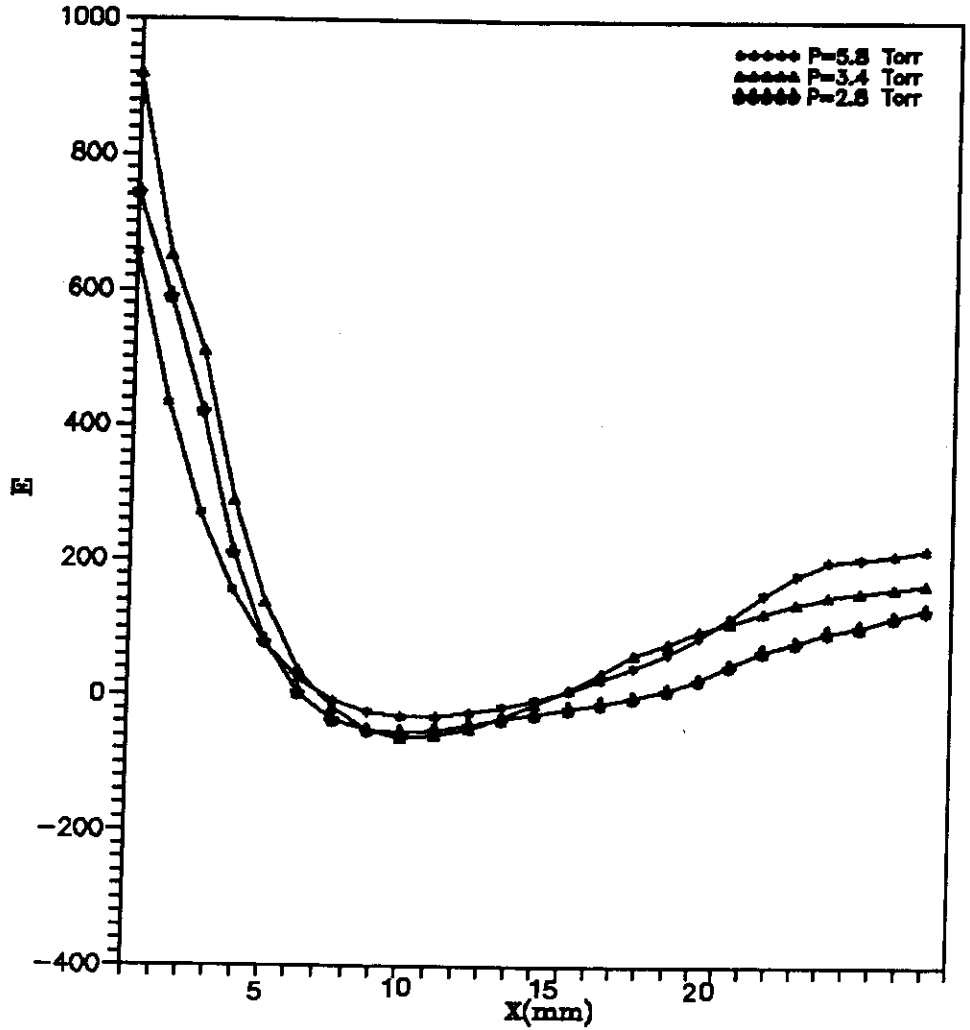

Fig.(22) The Electric field distribution of Ar discharge at constant I_e .

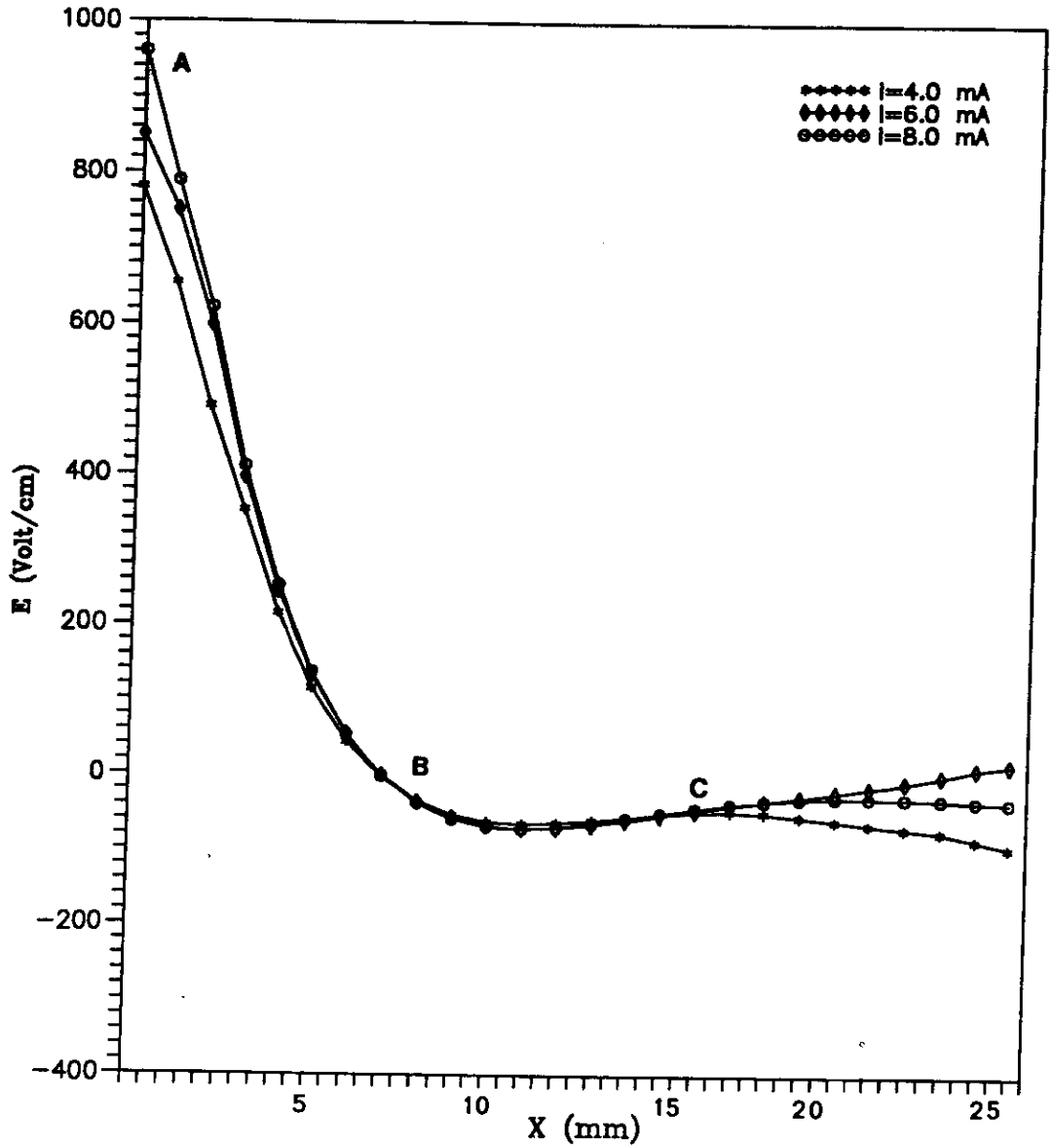

Fig.(23) The electric field distribution of He discharge at Ia= 4.0,6.0 and 8.0 mA (P= 4.0 mbar).

5.2- ELECTRON ENERGY DISTRIBUTION MEASUREMENTS .

Introduction :-

In most plasma diagnostic techniques , the electron energy distribution function (EEDF) is usually assumed to be Maxwellian . This assumption holds only for the case where the charged particles are in equilibrium with the gas atoms . It is of interest to verify this since it is important also in the definition of the plasma model . On the other hand , discussion of the energy distribution helps to explain the mechanism of the glow discharge in the different regions (i.e. :- cathode fall , negative glow and positive column regions) .

In the present work two methods are used to investigate the electron energy distribution using single probe .

The first method depends on the plotting of the semi-log curve of the electron current I_e as a function of the probe voltage V_p . For a Maxwellian energy distribution , a straight line with a slope of $(-\frac{e}{kT_e})$ is expected . A departure from linearity , however, doesn't necessarily mean that the distribution is not Maxwellian . It must be remembered that the departures from linearity could also be caused by a spread in the work function over the surface of the probe , a drift in the work function of the probe , effect of the finite probe size and by fluctuations of electron temperature (***Swift and Schwar , 1970***) .

The second method , depends on measuring the second derivatives of the electron current $(\frac{d^2I_e}{dV_p^2})$. The energy distribution may be obtained using the relationship :-

$$F(E) = -\frac{4}{e^2 A_p}\left(-\frac{m_e V_p}{2e}\right)^{1/2}\frac{d^2I_e}{dV_p^2} \qquad (V_p < 0) \qquad (5\text{-}1)$$

Several methods are used to determine $(\frac{d^2I_e}{dV_p^2})$, one of these methods is to superimpose an a.c.small signal to the probe circuit (***Sloane and MacGregor , 1934*** and **Konuma , 1992)** . The direct current component of the probe would increased by a fraction ΔI_t , where :-

$$\Delta I_t = \left(\frac{A^2}{4}\right).\left(\frac{d^2I_e}{dV_p^2}\right) \qquad (5\text{-}2)$$

A is the amplitude of the a.c.signal .

The used probe circuit is shown in Fig. (24) . A 600 Hz signal has an amplitude between (0.4-0.8 volts) , was introduced to the probe circuit using a 1:1 transformer (T) . The current ΔI_t was thus measured using a resistance R_p , where $\Delta I_t = \frac{\Delta V_t}{R_p}$. The second derivative was thus estimated using equation (5-2) . The EEDF was calculated using equation (5-1) at different gas pressure and in the different glow discharge regions .

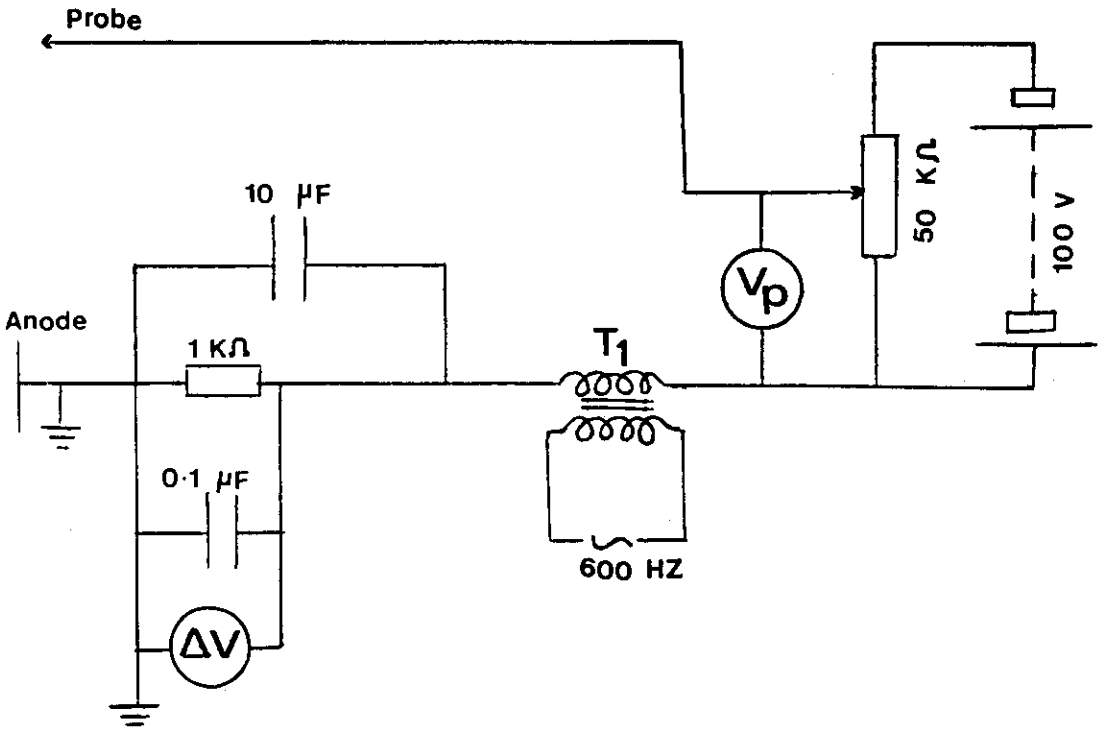

Fig.(24) The Single Probe Circuit used for the Superimposition of an A.C. Signal .

The measured electron energy distribution functions were compared with the Maxwellian distribution function . The latter was computed using the relationship :-

$$F(E) = \text{const.}\, V_p^{1/2} . \exp(-\frac{eV_p}{kT_e}) \qquad (5\text{-}3)$$

Moreover , the presence of a Maxwellian distribution was tested by plotting the semi-log curves of the second derivative , against V_p . Equations (5-1) and (5-3) show that a plot of $\ln(\frac{d^2I_e}{dV_p^2})$ as a function of V_p would produce a straight line having a slope of $(-\frac{e}{kT_e})$ whenever the distribution is Maxwellian . This method is more sensitive test for the Maxwellian distribution function.

EEDF was thus measured by using of Langmuir single probe , which was placed in the three regions of the discharge (i.e. cathode fall , negative glow and positive column regions) . The spherical probe , which was made of phosphor-bronze and has a diameter of 3 mm and the cylindrical probe which was made of tungsten wire and has a diameter of 0.8 mm and a length of 4.8 mm were used in Ar and He glow discharges.

5.2.1- Cathode Fall and Negative Glow Region :-

The I-V characteristic curves of the single probe at the edge of the cathode fall and in the negative glow region , for Ar and He discharges , at different pressures are shown in Figs. (25) , (26) , (27) and (28) , respectively .

Figures (29) , (30) , (31) and (32) show the semi-log curves of the electron current for the cathode fall and negative glow regions of Ar-discharge (at I_a = 4.0 mA) at a pressure range of (0.5 - 4.0 mbar) , and He-discharge (at I_a = 5.0 mA) at a pressure range of (2.7-5.6 mbar) . The discontinuity in the semi-log curves may represent the space potential V_S . This is the point at which the electron saturation current starts in an ideal I-V characteristic of a single probe {see Fig.(7) , chapter (3)} . At this potential , the collector receives the random electron and positive ion currents . The electron current I_e in the retarding region ($Vp < 0$) is given by :-

$$I_e = I_0 . \exp(-\frac{eV_p}{kT_e})$$

Where :-

V_p is the probe potential ($= V - V_S$) with respect to the sheath edge , V is the applied potential and V_S is the space potential . When the probe potential reaches the space potential , the current I is equal to a constant value and a horizontal line is obtained . At this point the electron current derivatives with respect to the probe voltage , are equal to zero . In practice , secondary effects like reflection from the probe surface may prevent the horizontal line from being obtained . Nevertheless , the

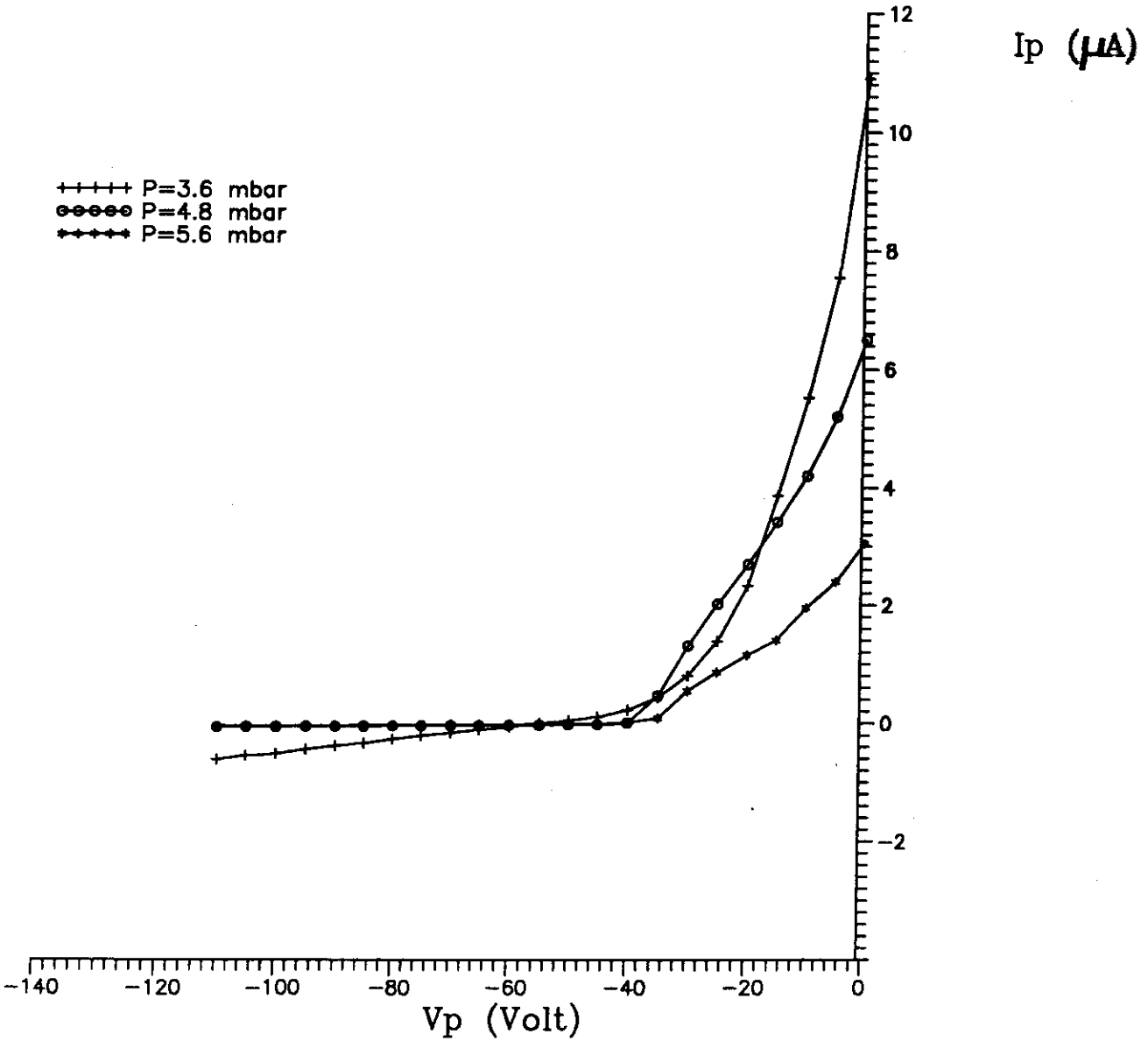

Fig.(26) I–V curves of the single probe for cathode fall region at different He perssures .

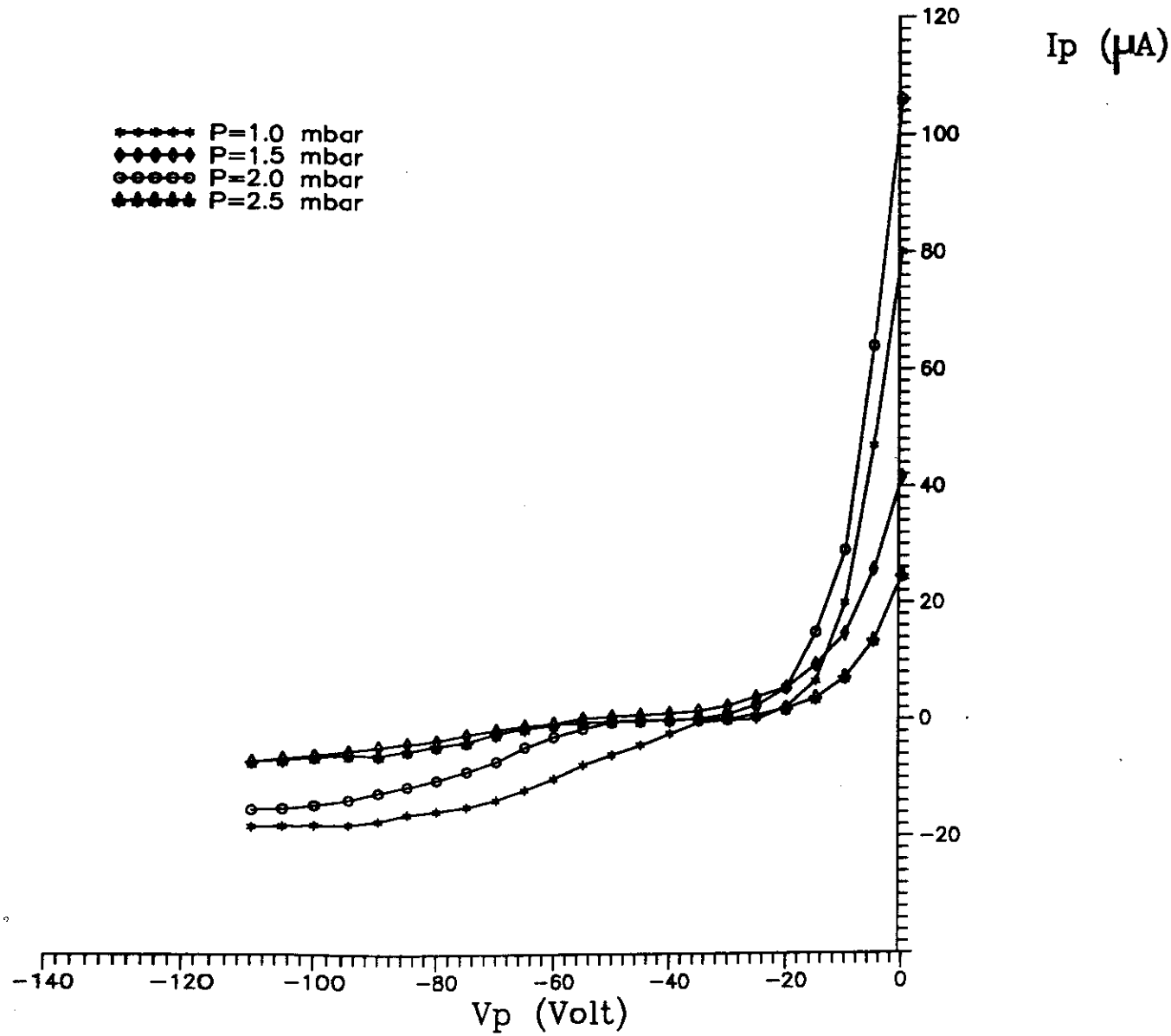

Fig.(27) I–V curves of the single probe for negotive glow region at different Ar perssures .

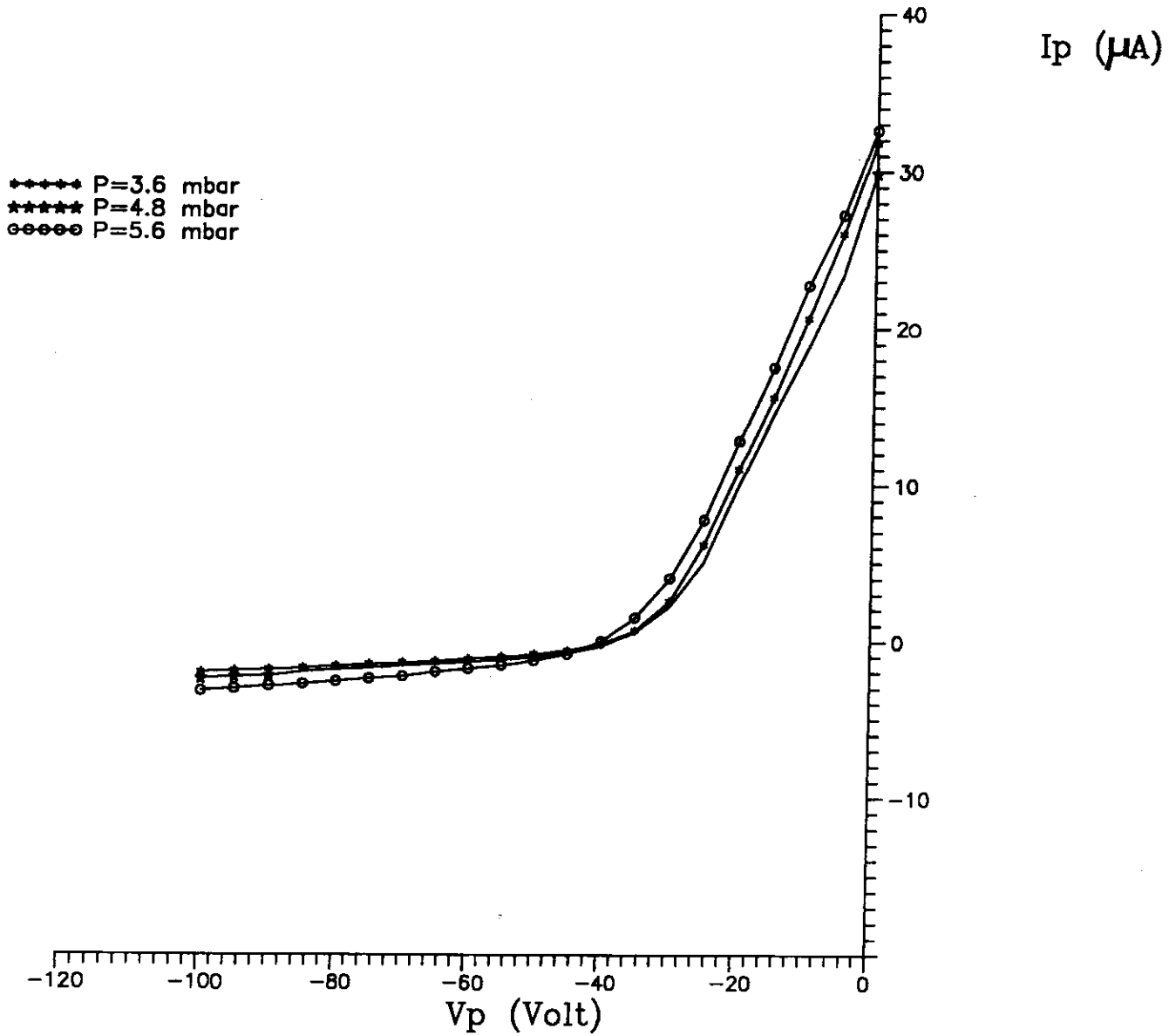

Fig.(28) I–V curves of the single probe for negative glow region at different He perssures .

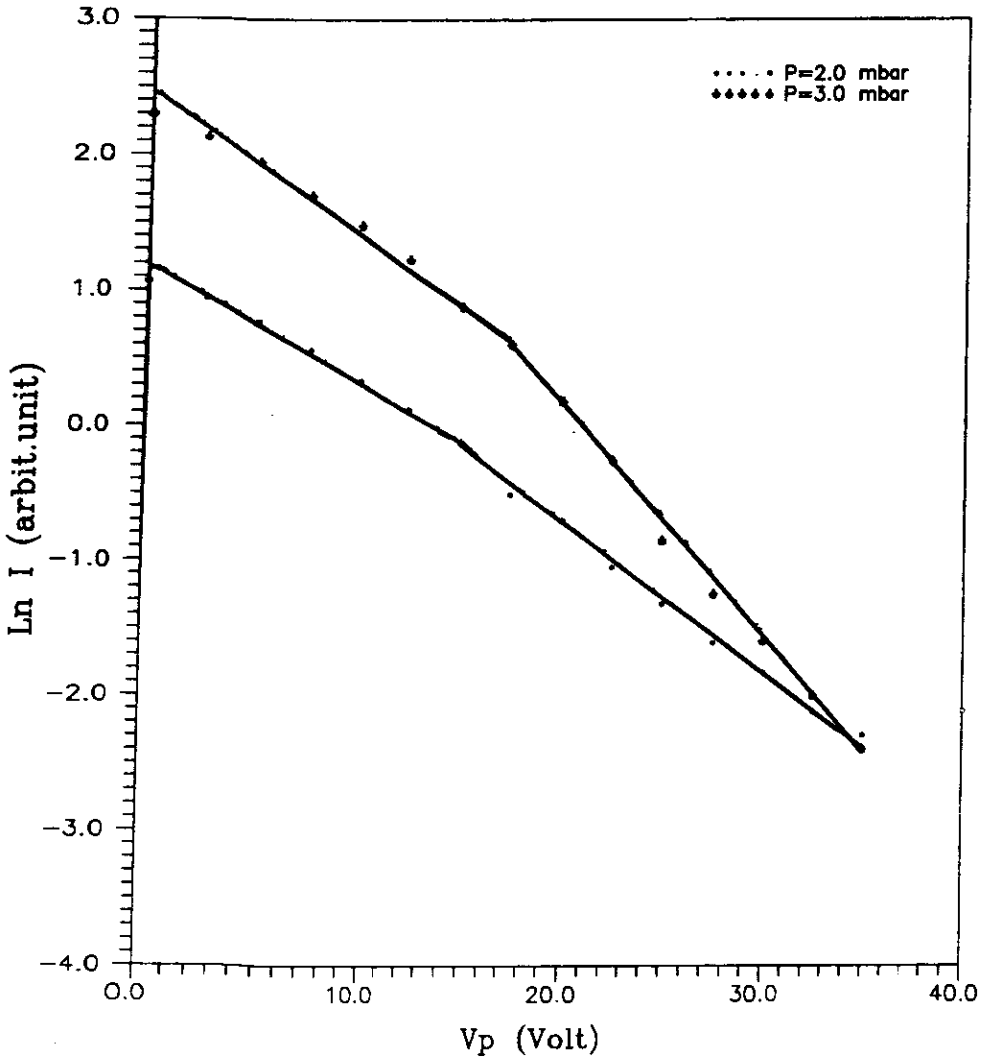

Fig.(29) Semi–log curves for the electron current as a function of the probe retarding potentoil , meosured in the cathode fall region of Ar glow discharge.

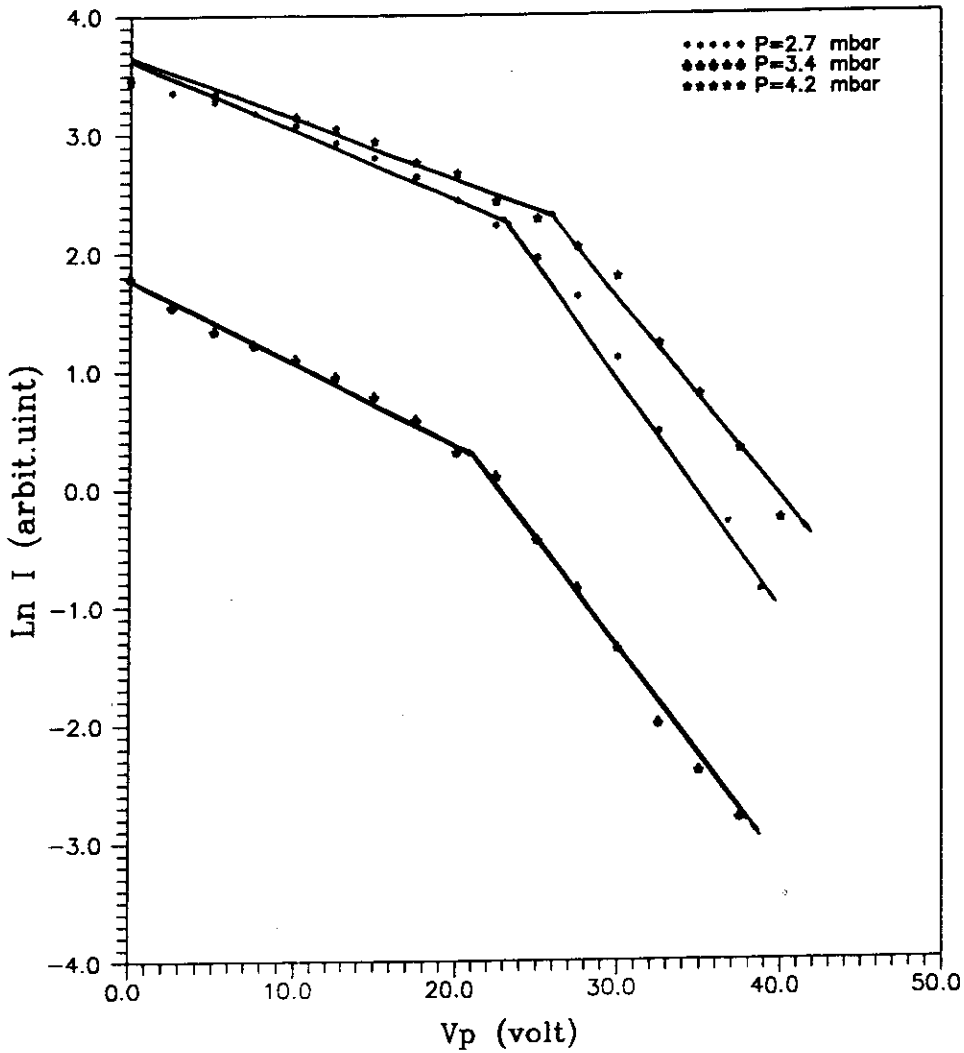

Fig.(30) Semi–log curves for the electron current as a function of the probe retarding potentail, measured in the cath. fall region of He glow discharge .

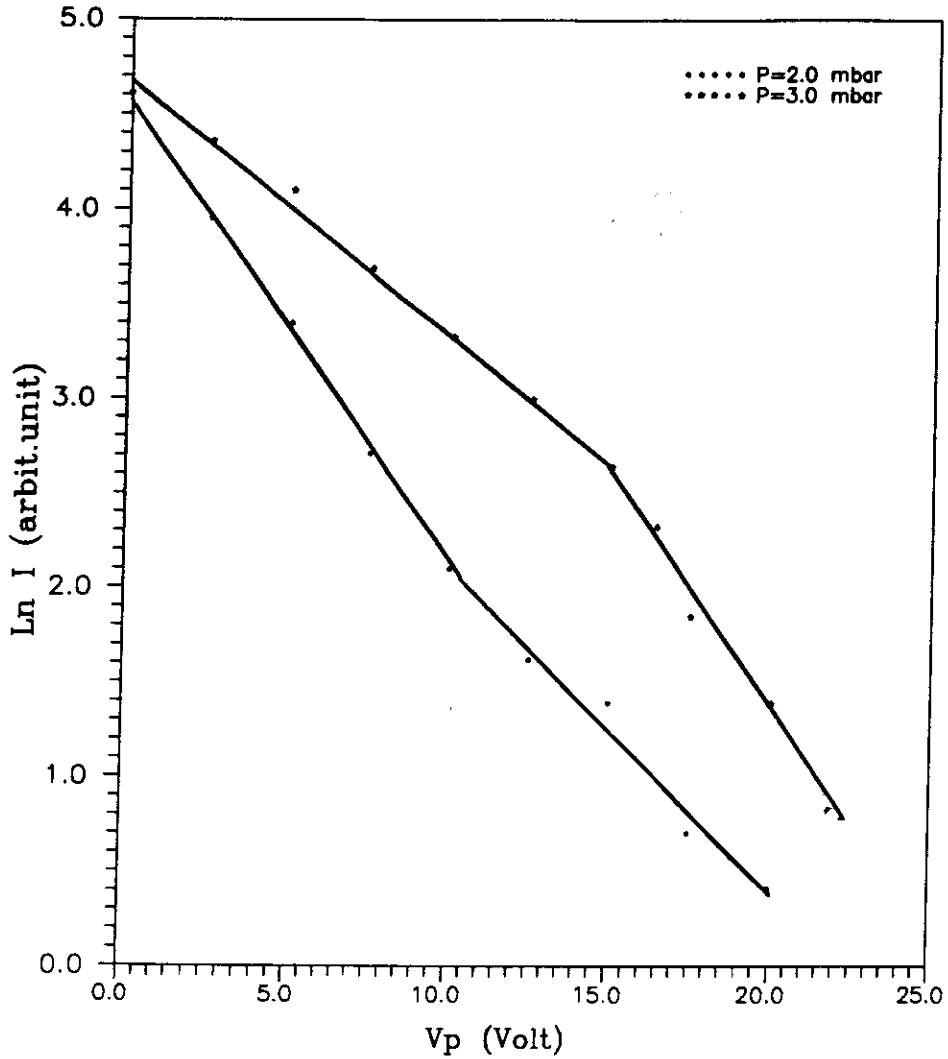

Fig.(31) Semi–log curves for the electron current as a function of the probe retarding potentail , measured in the negative glow region of Ar glow discharge .

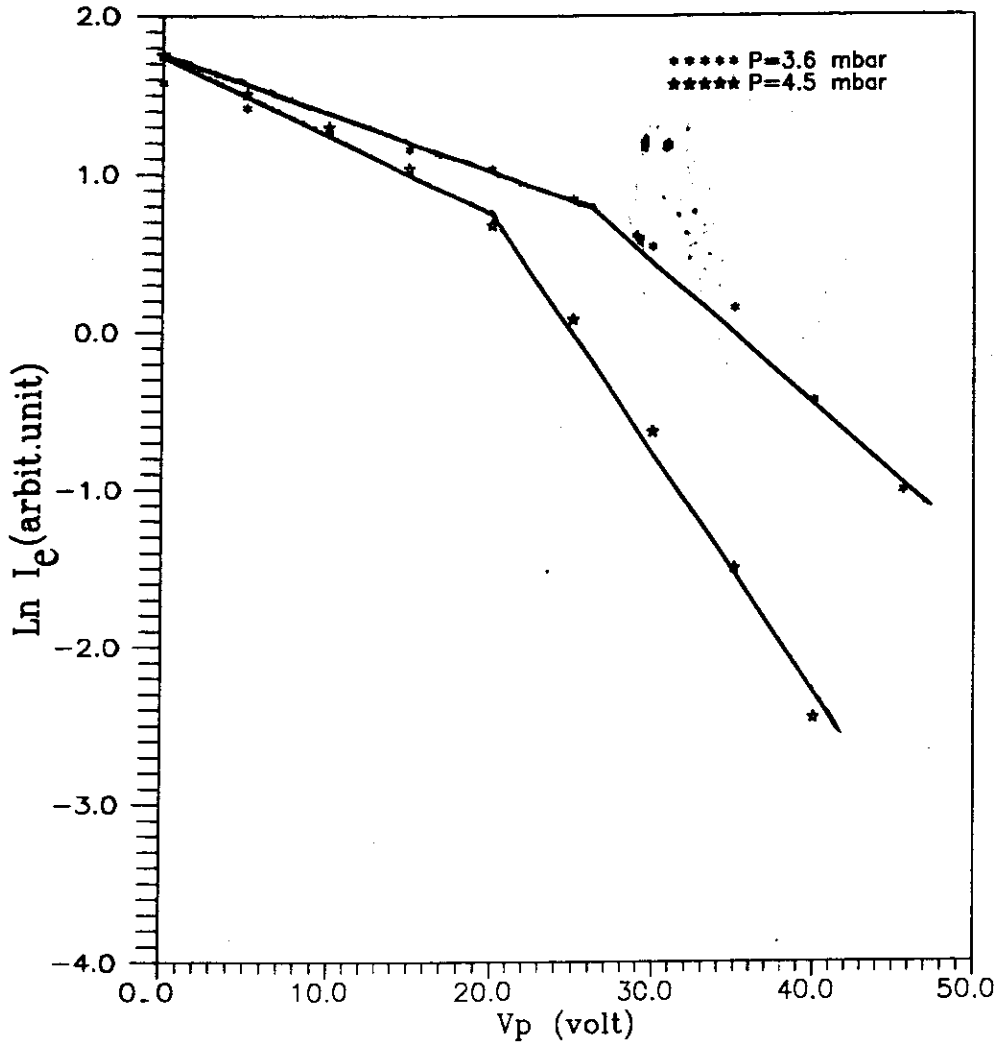

Fig.(32) Semi–log curves for the electron current as a function of the probe retarding potentail , measured in the negative glow region of He discharge .

straight lines in themselves are insufficient to prove the presence of Maxwellian distribution . ***Mott-Smith and Langmuir , (1926)*** found that , a straight line may also be obtained when a beam of electrons having a common drift velocity is superimposed on the Maxwellian distribution of a relatively low temperature .

The semi-log curves of the second derivative of the electron current $\ln(\frac{d^2I_e}{dV_p^2})$ as a function of the probe voltage V_p are shown in Figs. (33) , (34) , (35) and (36) for the cathode fall and the negative glow region of the Ar and He-discharges , respectively . Two linear parts are noticed which may related to the existence of two groups of electrons of different temperature (***Godyak , 1993***) . The temperatures of the first group of electrons are about 1-3 eV , while those of the second group are about 5-12 eV .

The electron energy distribution function F(E) was thus calculated using equation (5-1) . Figures (37) , (38) , (39) and (40) show F(E) as a function of the probe retarding potential Vp (which can be considered as the electron energy) . Two well defined maxima are observed at about 5 and 15 eV for Ar glow discharge and at about 9 and 21 eV for He glow discharge .

The presence of two groups of electrons at the edge of the cathode fall and in the negative glow region can be explained as follows :-

The primary electrons emitted from the cathode will be accelerated by the electric field before entering the negative glow region forming what is called "runaway electrons" . As these accelerated electrons enter the negative glow region the majority of them will be subjected to electron - atom collision (inelastic collision) and loosing most of their

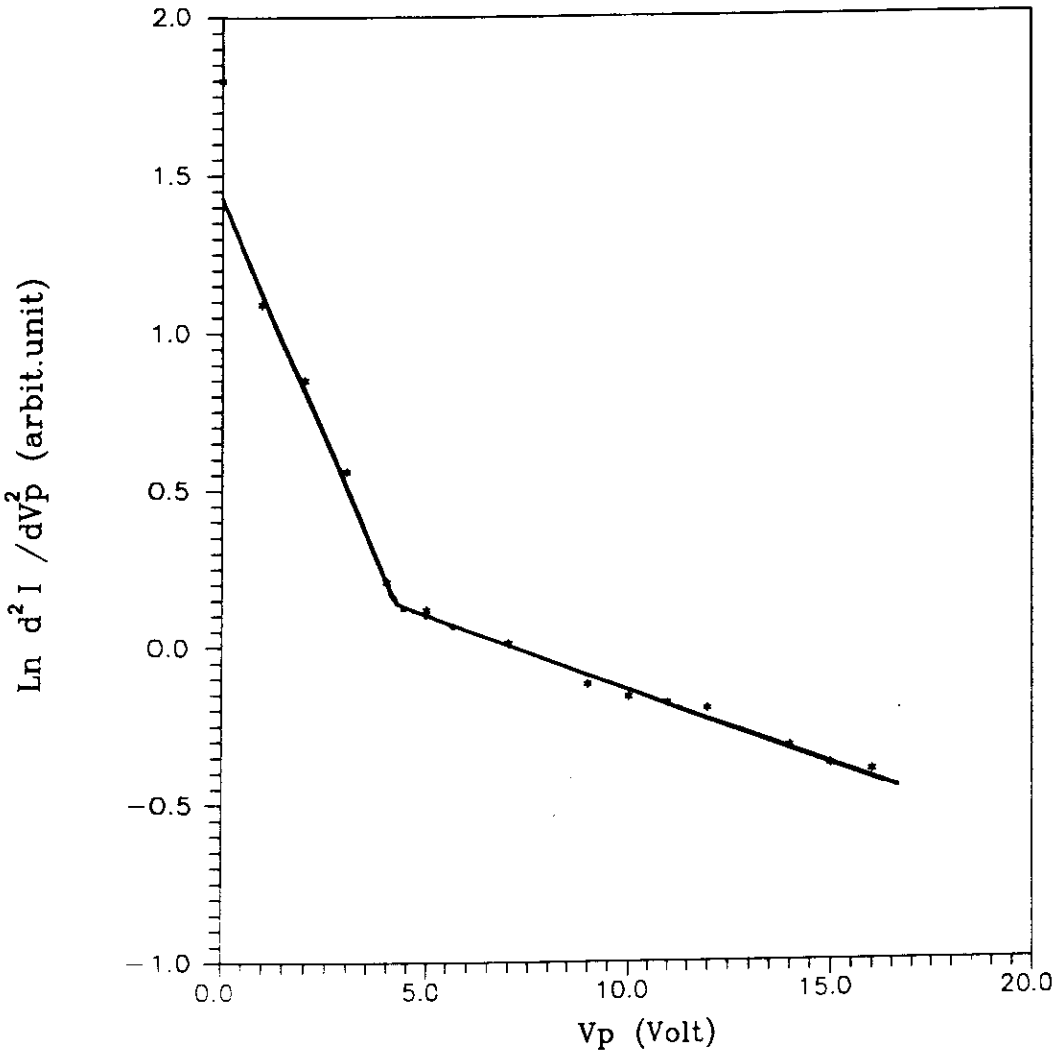

Fig.(33) The semi-log of the second derivative of electron current for the cath.fall region of Ar-discharge.

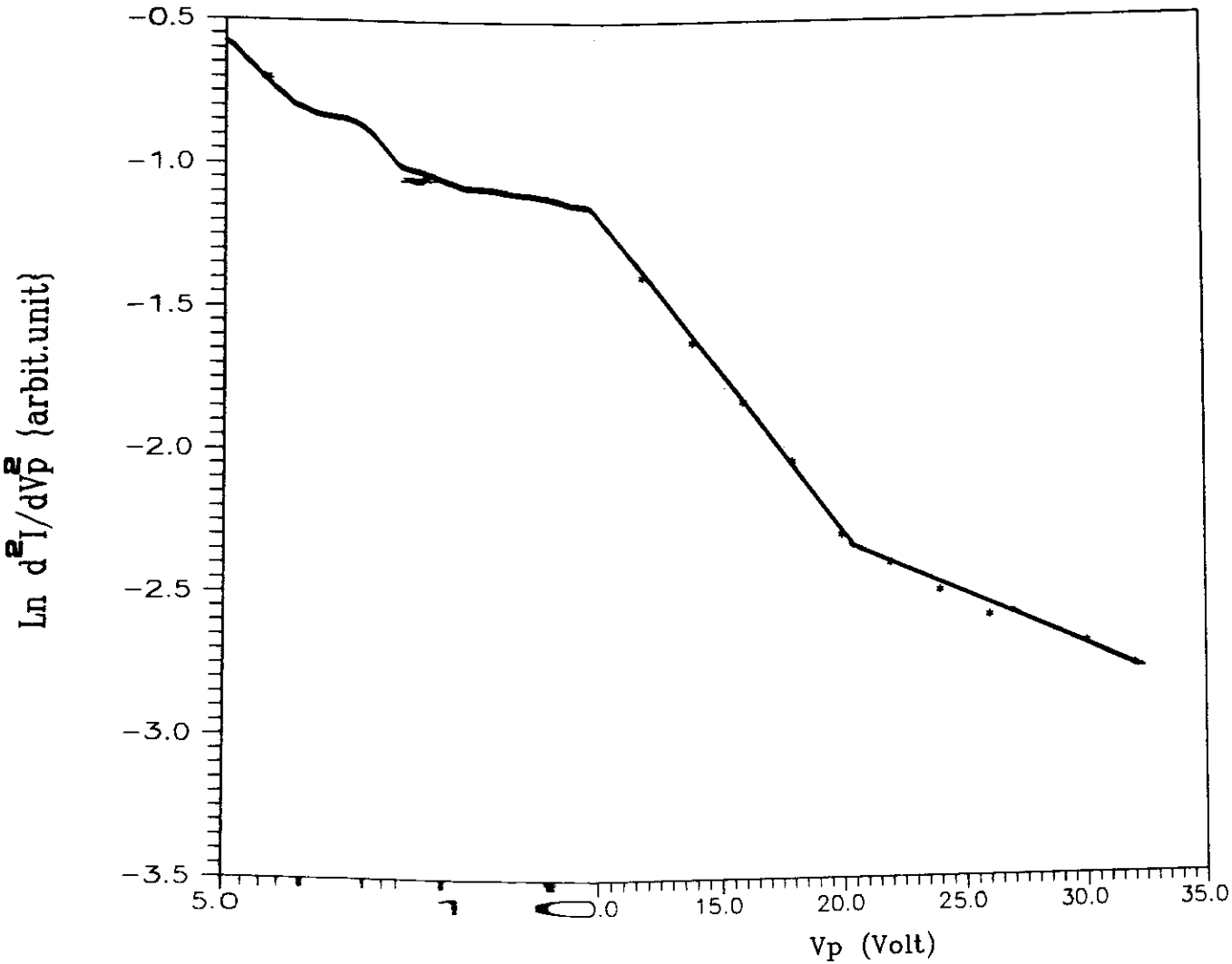

Fig.(34) Semi-log of the second derivative of the electron current for cathode fall region in He discharge.

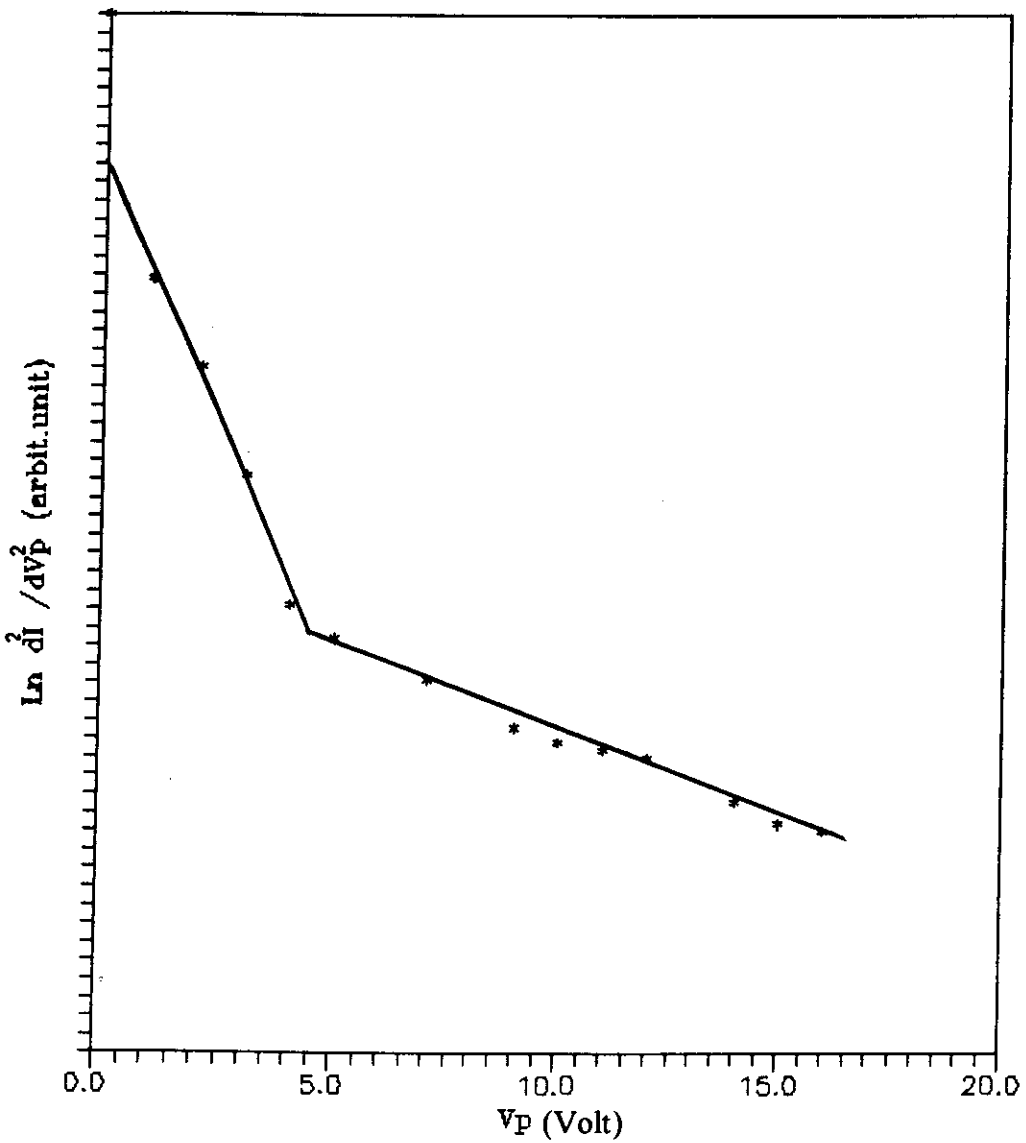

Fig.(35) The semi-log of the second derivative of electron current for negative glow region (Ar-glow discharge).

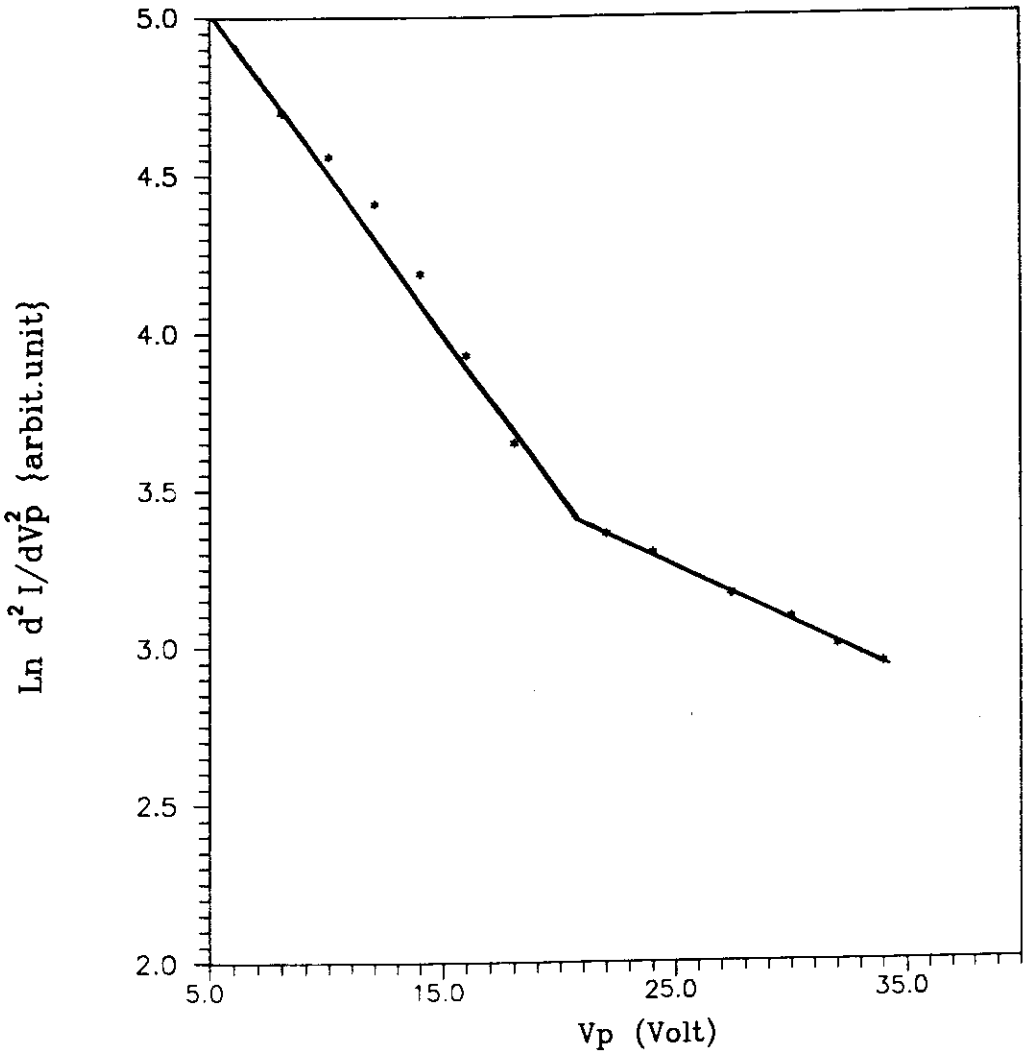

Fig.(36) Semi–log of the second derivative of the electron current for negative glow region in He discharge.

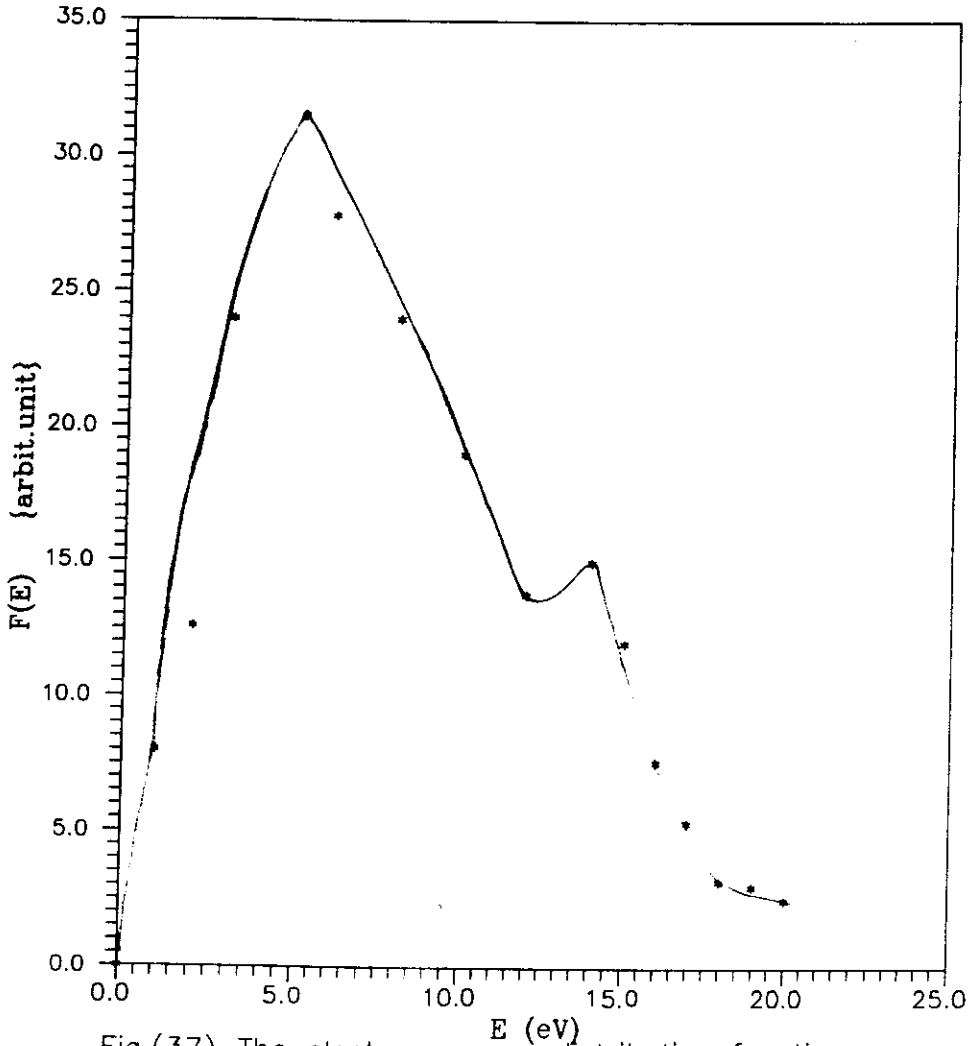

Fig.(37) The electron energy distribution function of the cathode fall region of Ar discharge (at P= 4.0 mbar) .

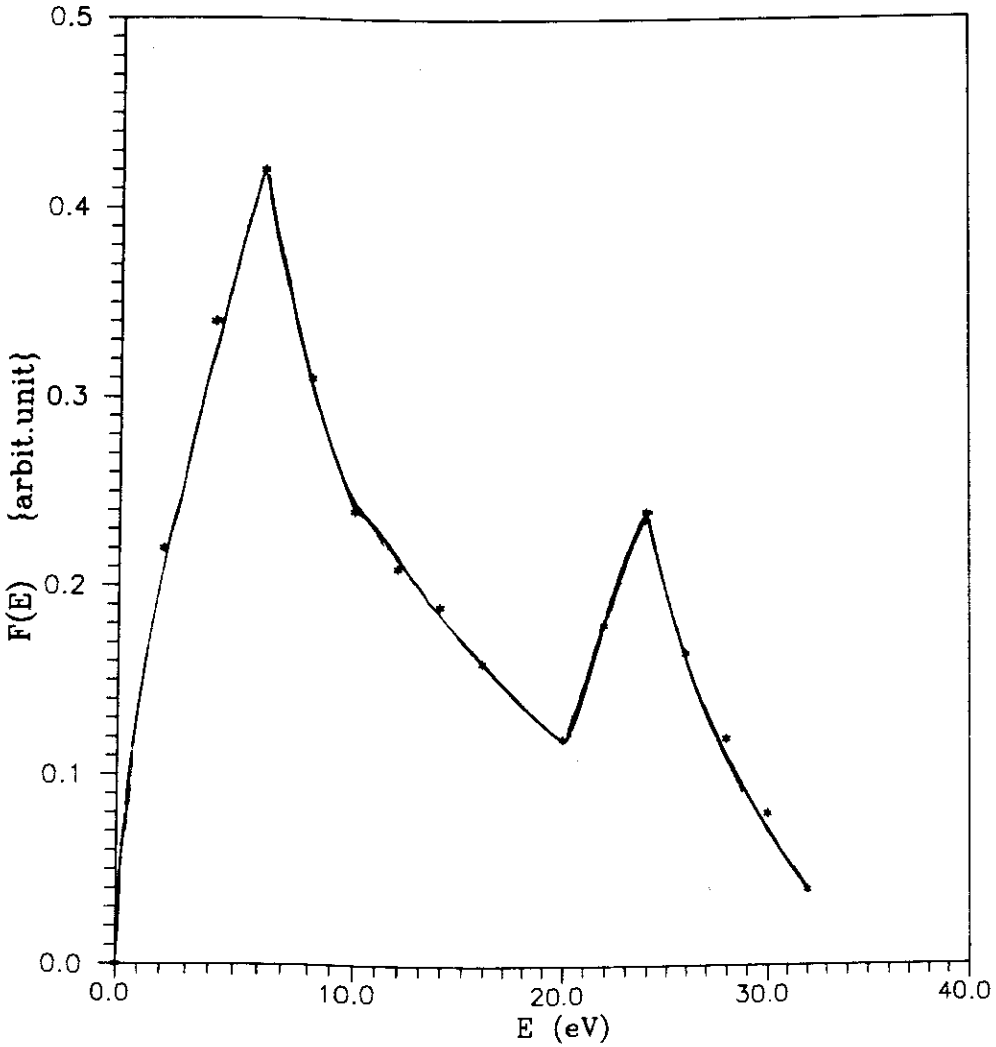

Fig.(38) The electran energy distribution function of the catnade fall region of He discharge (P=3.0 mbar).

energy and hence , forming the low energy group . However , the minority of these electrons will be escape without inelastic collisions and hence , forming the high energy group .

Ecker and Muller , (1961) found that the electrons could "runaway" in a partially ionized gas as a result of the applied field E . The value of $(E/P.T_g)$ must exceeds a critical quantity which depends upon the electron velocity v_e and the collision cross-section $Q_{e\text{-}n}(v_e)$. In fact $(E/P.T_g)_c$ is the maximum of the term $\{0.55 \times 10^4 v_e^2 Q_{e\text{-}n}(v_e)\}$ when it is plotted against v_e^2 . When the applied values of $(E/P.T_g)$ are less than that , electrons can "runaway" only if their initial velocity v_0 is higher than a limit which is determined graphically . Values of $Q_{e\text{-}n}(v_e)$ were taken from ***Puech and Torchin , (1986)*** .

For Ar , $(E/P.T_g)_c$ is about 30×10^4 volt.K°/cm.torr , which is less by a factor of 30 than the applied value at the edge of the cathode fall region . This confirms that some of the accelerated electrons could "runaway" as a result of the formed electric field and gain high energy . For He , $(E/P.T_g)_c$ is 7×10^4 , which is less , by an order of magnitude , than the applied value in the present experiment . Thus electrons gain their energy from the electric field and escape (or runaway) from the cathode region before making a collision .

The time required for the fast electrons to form a displaced Maxwellian distribution (self collision time) is given by (***Spitzer , 1967***):-

$$t_c = 0.266 . \frac{T_e^{3/2}}{N_e} . \ln(\lambda_D/\rho_0)$$

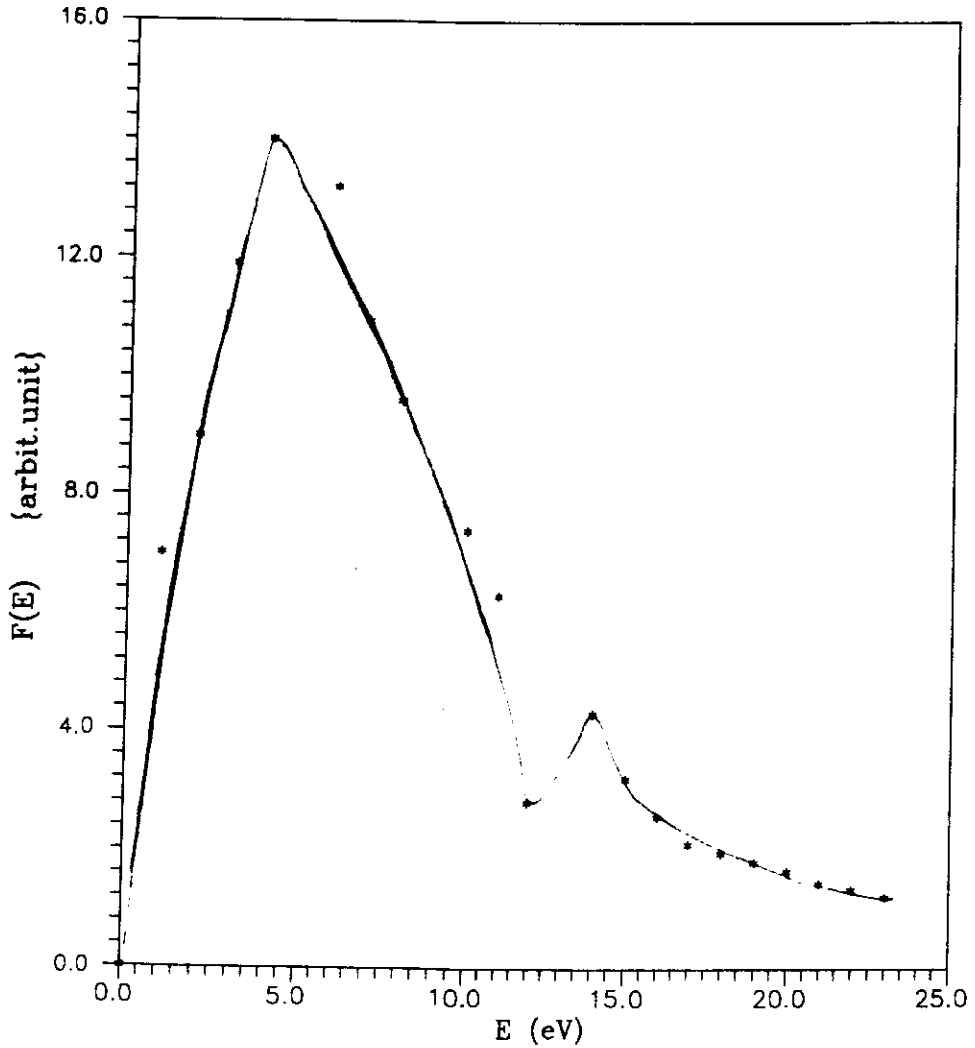

Fig.(39) The electron energy distribution function of negative glow region of Ar discharge (at P=2.0 mbar) .

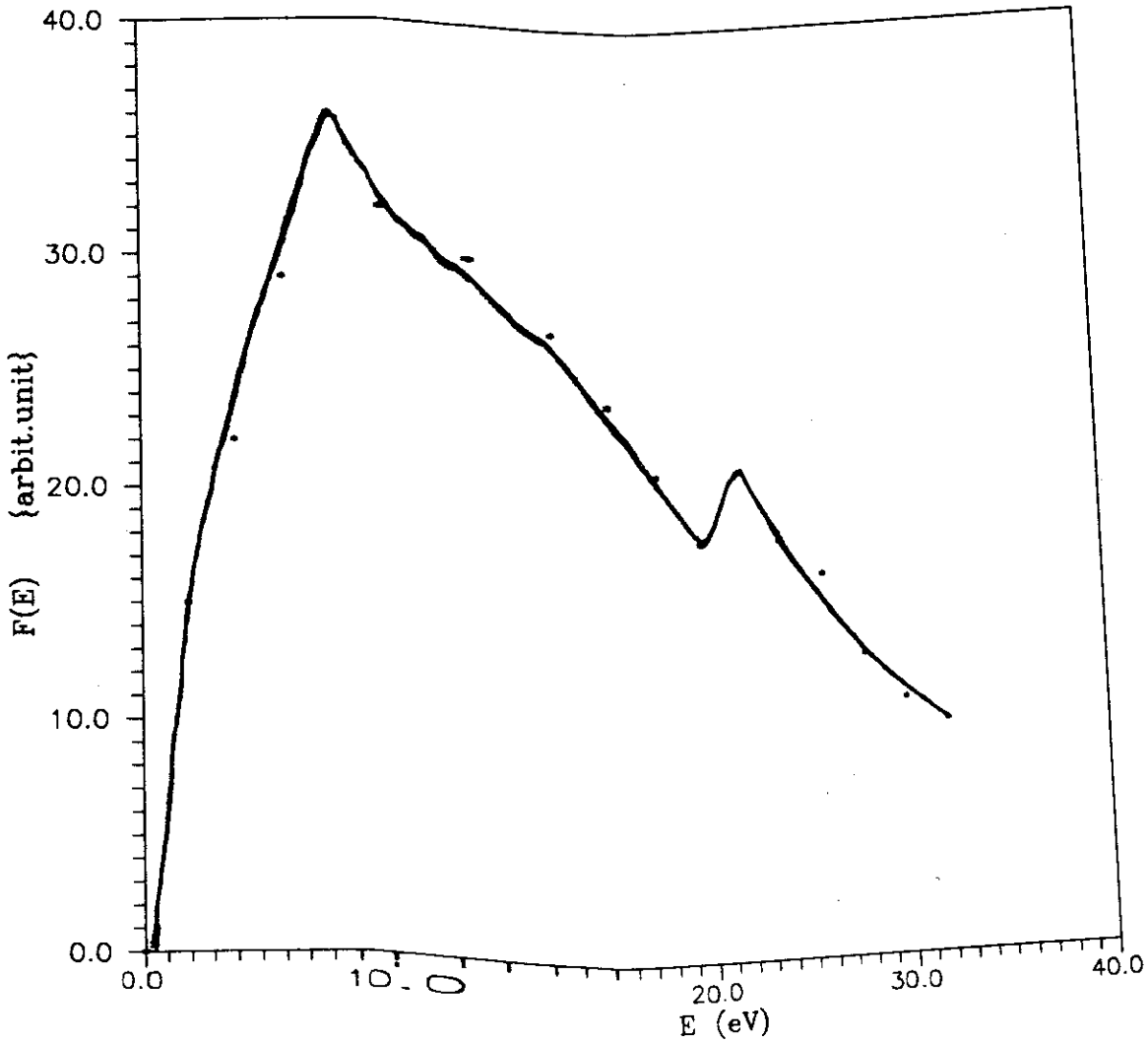

Fig.(40) The electron energy distribution function of the negative glow region of He discharge (P=3.0 mbar).

Where :-

λ_D is the Debye length in meters ,

ρ_o is the average impact parameter for a 90° Coulomb deflection and ,

T_e is the electron temperature in K° .

Values of ln (λ_D/ρ_o) were taken from ***Spitzer , (1967)*** . "t_c" for the present work is about 2.4 x 10^{-9} sec . The fast electrons would not have a chance to redistribute themselves in a displaced Maxwellian distribution before leaving the cathode fall region since the cathode fall thickness was about 0.35 cm and the electron moved with a velocity of about 1.5 x 10^8 cm/sec. thus , the time required for electrons to leave the cathode fall region $t_{electrons}$ was about 9.8 x 10^{-10} sec. which is 2-3 times less than t_c . Figure (41) shows the relation between t_c and $t_{electrons}$ as a function of the gas pressure . Also , there was no chance for equilibrium to occur between the two groups of electrons . The time required to approach an equilibrium between two groups of electrons is given by ***Spitzer (1967)*** :-

$$t_{eq} = \frac{t_{e1e2}}{1 + N_{e1} / N_{e2}} \qquad \text{sec.}$$

Where :-

$$t_{e1e2} = 17X10^4 \frac{(T_{e1} + T_{e2})^{\frac{3}{2}}}{N_{e1}} . \ln(\frac{\lambda_D}{\rho_o})$$

t_{e1e2} is the time at which equipartition of energy is established between two groups of electrons . T_{e1} and T_{e2} and N_{e1} and N_{e2} are the electron temperatures and densities of the two groups , T_e is in eV . t_{eq} was about 10^{-7} sec. for the present work , which was 100 times more than

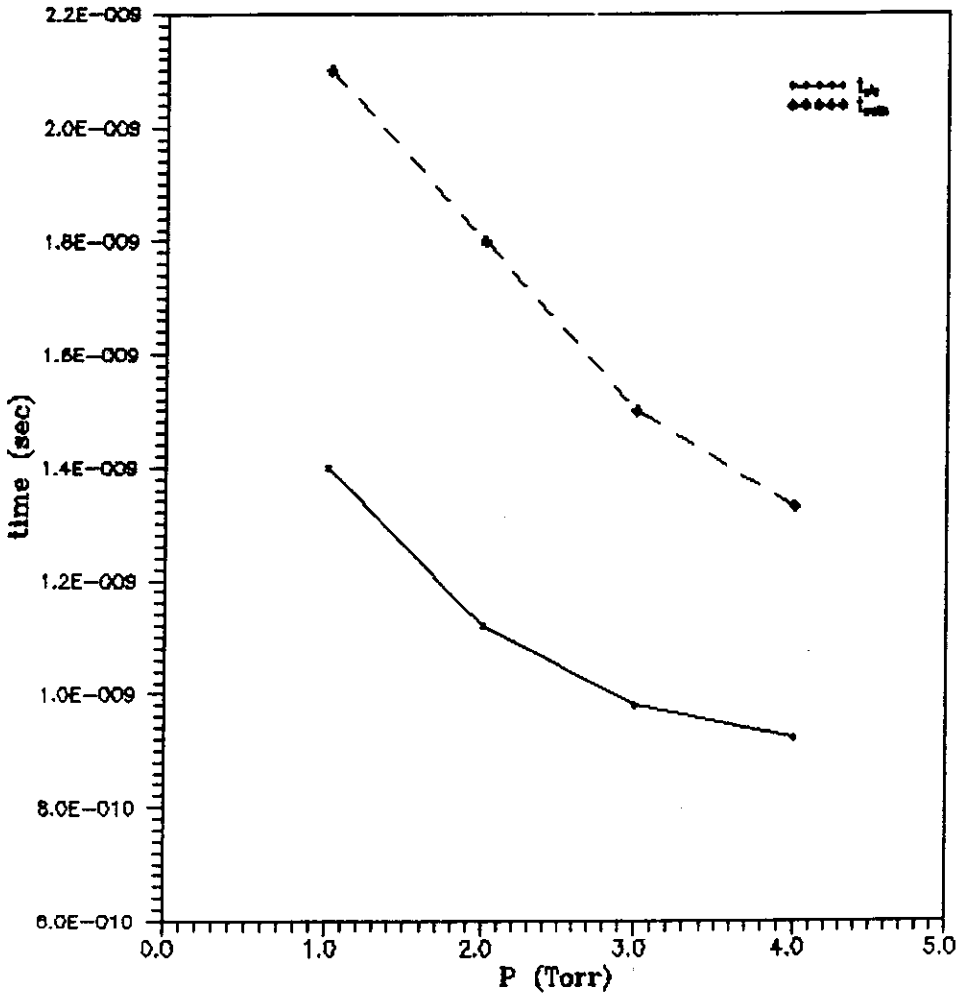

Fig.(41) The relation between the thermalization time of electrons and tc for Ar discharge .

that taken by the electron to leave the cathode fall region . Consequently , the two groups must have left the cathode fall region before reaching equilibrium with each other .

Runaway electrons were also noticed by ***Howatson and Topham , (1976)*** and were related to the fact that the energy gained by the electrons from the electric field in the cathode sheath was not usually matched by the energy lost by inelastic collision processes . Also , ***Djakov (1989)*** demonstrated that , the runaway electrons may play an important role in the cathode region of a vacuum arc , provided the plasma is fully ionized . Moreover , ***Carman and Maitland , (1987)*** show that , the state of nonequilibrium between the electrons and the electric field gives rise to a non- Maxwellian electron energy distribution in both the cathode sheath and the negative glow regions . Three distinct groups of electrons were detected :-

(i) Primary electrons from the cathode that pass through the cathode sheath region without collisions .

(ii) Secondary electrons corresponding to the tail of the flux distribution with energies greater than the ionization potential .

(iii) Ultimate slow electrons with energies below the ionization potential .

In the present work , only two groups of electrons were detected . So , more sensitive diagnostic tools may be needed . Also , at very low degrees of ionization , the electron energy gained in the electric field is essentially transferred to the neutral atoms by elastic and inelastic collisions , leading to individual distribution functions for the particular discharge in question {***Behringer and Fantz (1994)***} . This is not the case in the present work, since the mean free path is much longer than the discharge thickness .

5.2.2- Positive Column Region:-

Figures (42) and (43) show the I-V characteristic curves of the single probe of the positive column region for Ar and He plasmas, respectively .

The semi-log curves of the electron current as a function of the probe voltage at pressures of 2.0 , and 3.0 mbar for Ar-plasma , and at 2.7 , 4.0 , 5.0 mbar for He plasma are shown in Figs.(44) and (45) . Straight lines, which may indicate Maxwellian distributions,are observed. The reproducibility of the results was checked by repeating the experiment several times and the same data were observed .

Figures (46) and (47) show $\ln(\frac{d^2I_e}{dV_p^2})$ curves as a function of the probe voltage V_p for the positive column region of the Ar and He plasmas , respectively . Straight lines are obtained which may be indicate the presence of Maxewellian distributions .

A comparison between the experimental data of F(E) , as a function of V_p , and that of the theoretical Maxwellian curves are shown in Figs. (48) and (49) for Ar and He-plasmas of the positive column region ; receptively . A good agreement is obtained from these curves , indicating the presence of Maxwellian energy distribution function in the positive column region of Ar and He-plasmas at these pressures . Also , since the length of the positive column region is about five times greater than the cathode fall length , so electrons would have a longer time to redistribute (thermalized) themselves to form a Maxwellian distribution .

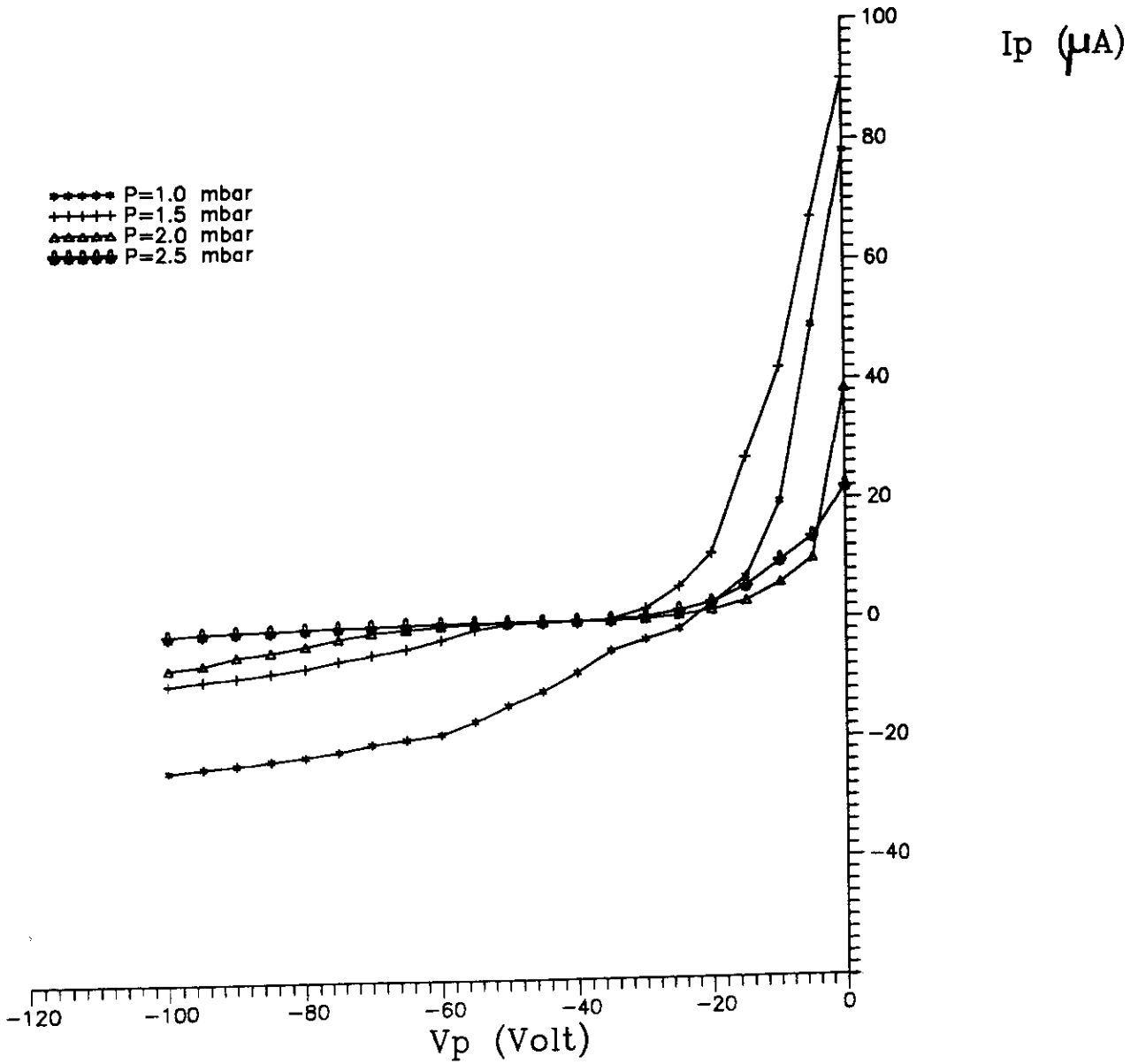

Fig.(**42**) I–V curves of the single probe for positive column region at different Ar perssures .

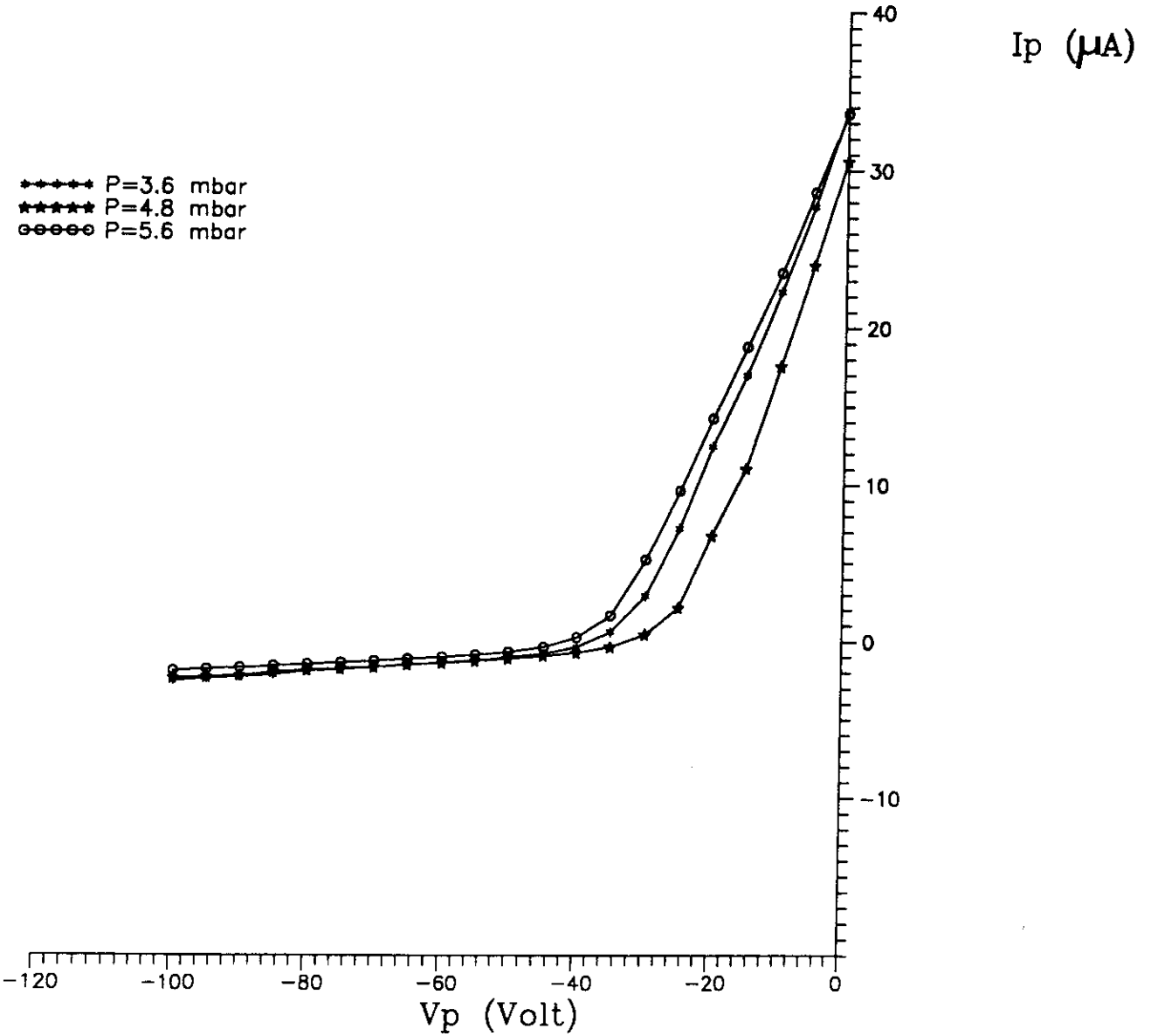

Fig.(43) I–V curves of the single probe for positive column region at different He perssures .

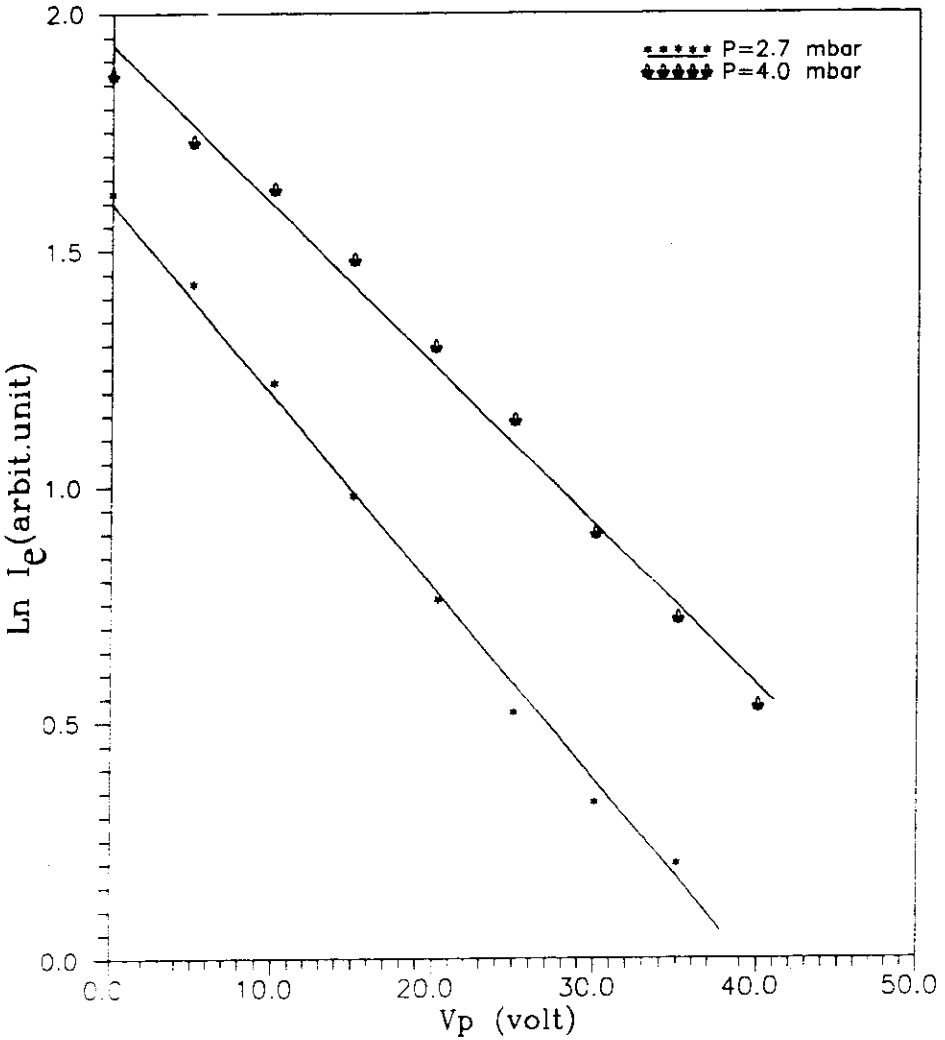

Fig.(45) Semi-log curves for the electron current as a function of the probe retarding potential , measured in the positive column region of He discharge .

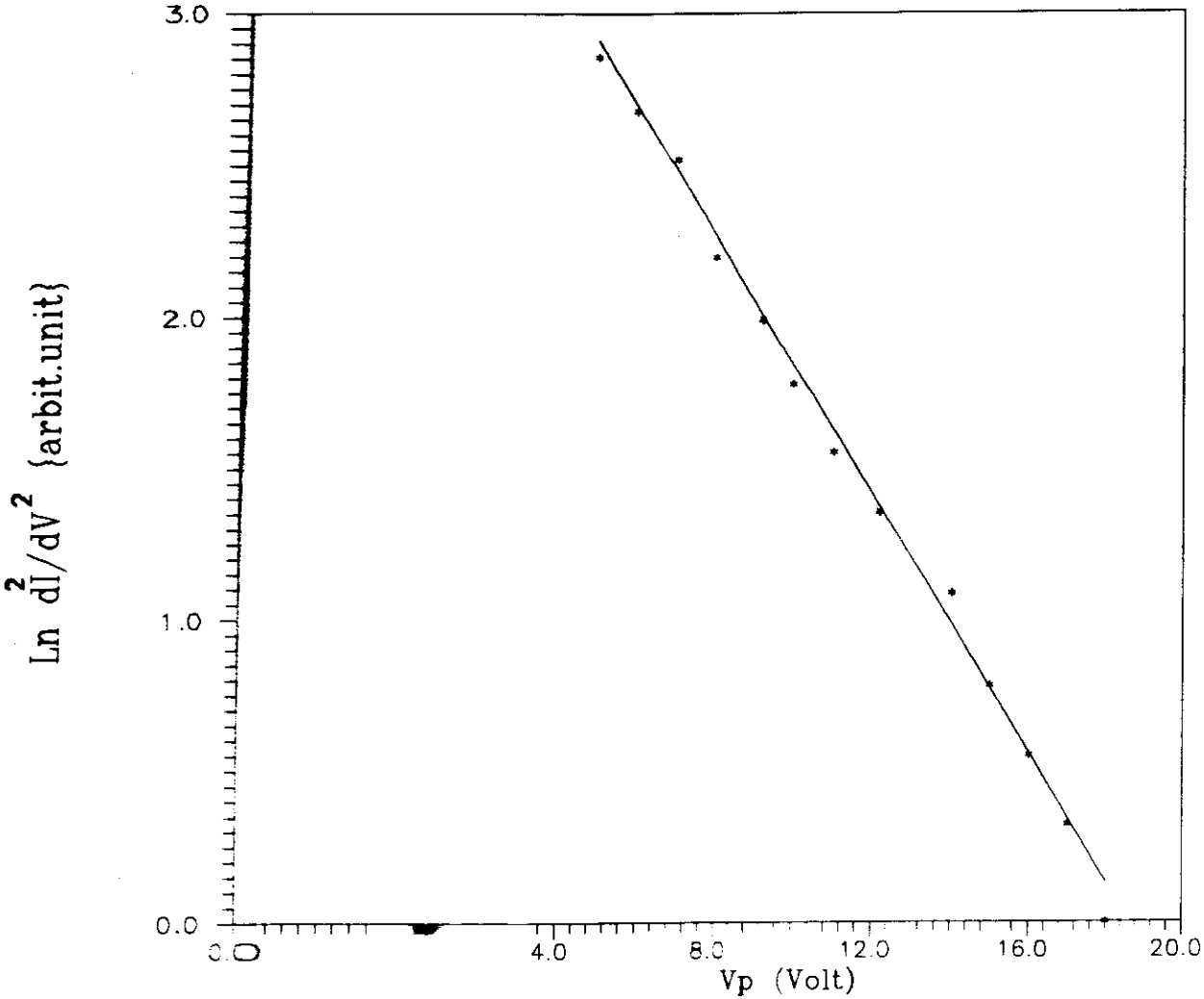

Fig.(46) The semi-log of the second derivative for the positive column in Ar glow discharge.

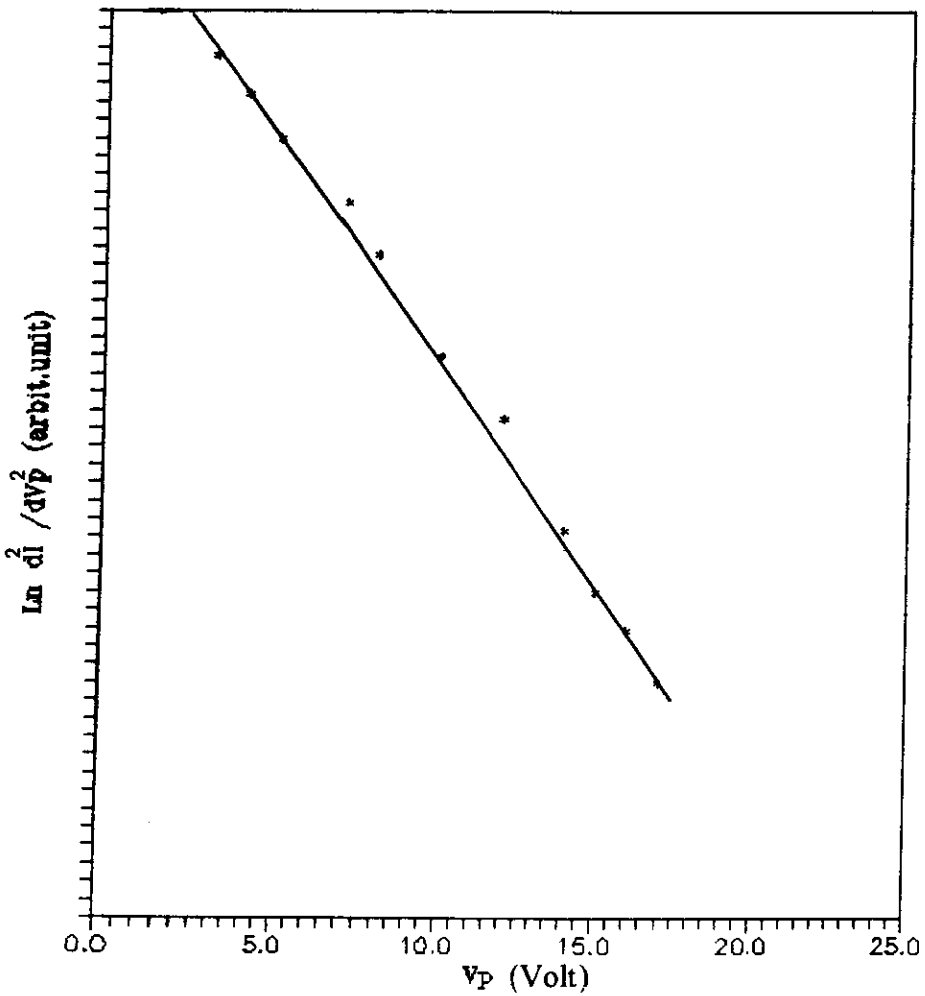

Fig.(47) The semi-log of the second derivative of electron current for positive col. region (He-glow discharge).

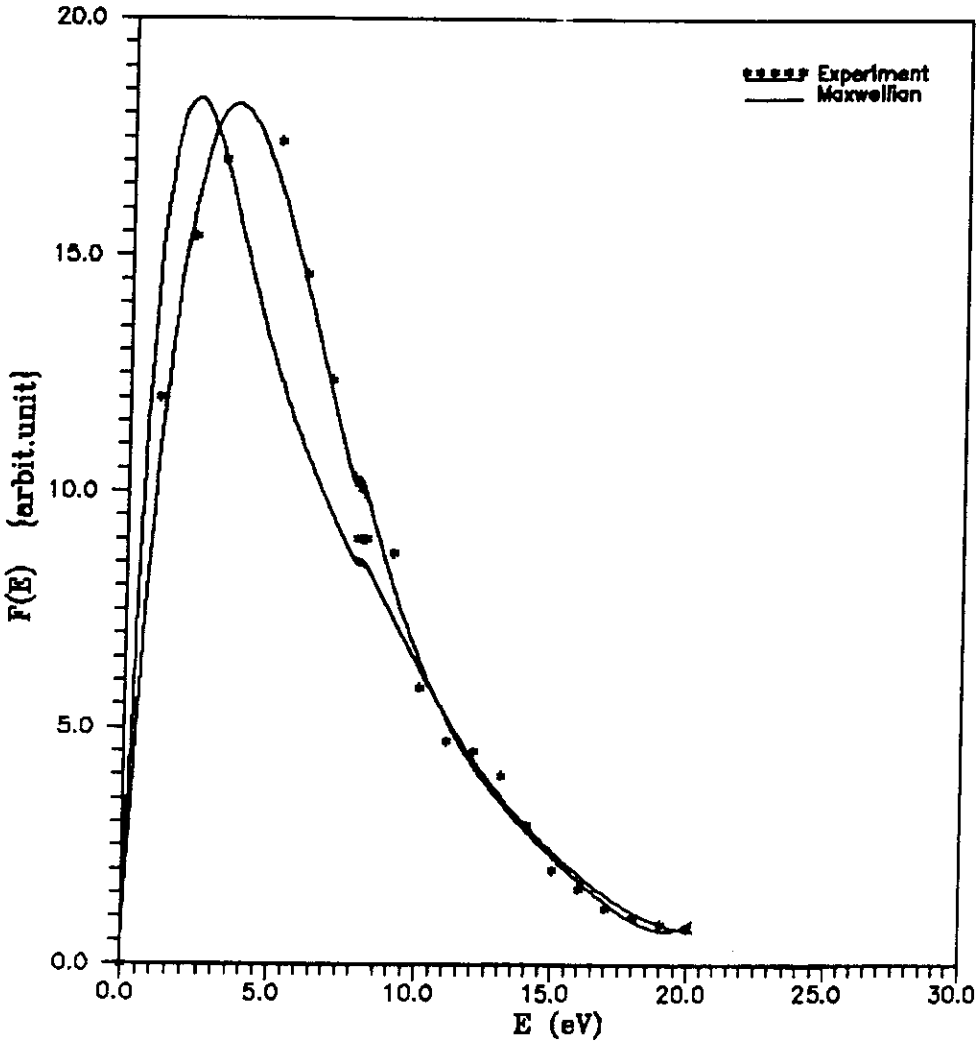

Fig.(48) The electron energy distribution function of positive column region of Ar discharge (at P=3.0 mbar) .

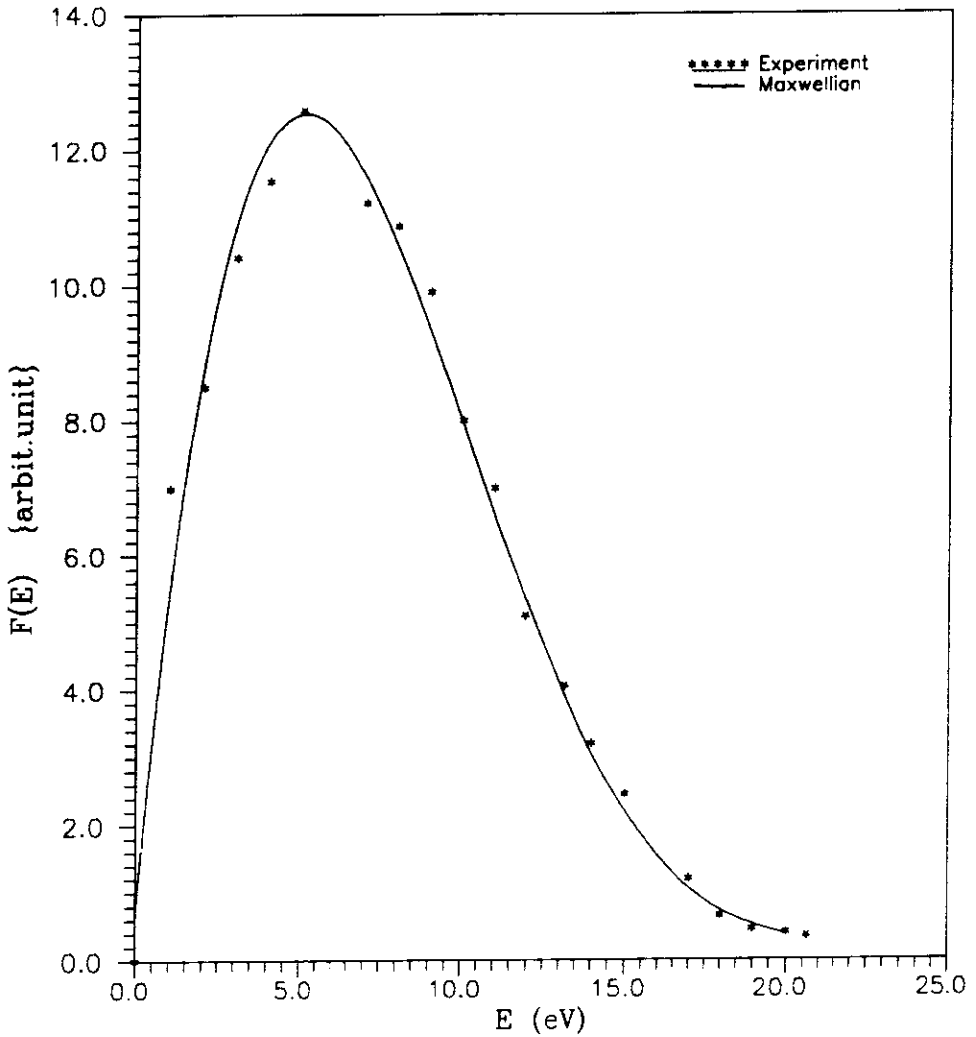

Fig.(49) The electron energy distribution function of positive column region of He discharge (at P=4.0 mbar).

5.3-ELECTRON TEMPERATURE MEASUREMENTS .

The recent widespread use of DC- glow discharge plasmas for microelectronics fabrications has enhanced interest in related plasma behaviour . The most important parameter for defining the characteristics of the DC-glow discharge is the electron temperature T_e . The electron temperature , in the present work , was determined by different techniques e.g. single and double probes and also spectroscopic techniques . Unless its area is extremely small , the single probe may draw sufficient electron current , when operating close to the space potential , and disturbs the plasma ***(Konuma , 1992)*** . The advantage of using a double probe is that it has a negligible influence on the plasma and it produces reliable temperature measurements , ***(Uckan 1988)*** . These methods have been described in details in chapter (3) . The results will be discussed in this section and a comparison between them is given .

5.3.1- Single Probe Measurements :-

The slope of the semi-log curves of the probe current in the retarding region against the probe voltage , which was explained earlier in sec. 5.2 , produced values of the electron temperature T_e .

Two lines with different slopes may appear providing that two groups of electrons are presented in the discharge . Samples of the semi-log curves of the electron current for Ar and He-glow discharges are given

in Figs. (29) , (30) , (44) and (45) , respectively . The measurements were carried out in the pressure ranges of 0.5-4.0 mbar for Ar-glow discharge , and 2.7-5.6 mbar for He-glow discharge .

5.3.1.1- Cathode Fall Region :

The I-V characteristic curves of the single probe at the edge of the region of the cathode fall region , for Ar and He-glow discharges , at different pressures are shown in Figs. (25) and (26) , respectively . The ion saturation current is increased as the gas pressure increased . Figure (50) shows values of electron temperature for Ar-discharge at different gas pressures whenever I_a (discharge current) = 4.0 mA . For He-discharge , values of T_e are shown in Fig. (51) at $I_a = 5.0$ mA . Values of T_e were varied from 8.7 ± 0.96 eV to 5.7 ± 0.6 eV for Ar glow discharge in a pressure range of 0.5-4.0 mbar . For He glow discharge T_e was found to vary from 8.0 ± 0.83 eV to 5.5 ± 0.52 eV in a pressure range of 2.7 - 5.6 mbar . Figures (50) and (51) show that , T_e decreased as the gas pressure was increased .

5.3.1.2- Negative Glow Region :-

A typical family of I-V probe characteristic curves , in the negative glow region for Ar and He-glow discharges , at different pressures are shown in Figs.(27) and (28) , respectively . Values of the electron temperature measured by using of the single probe as a function of the

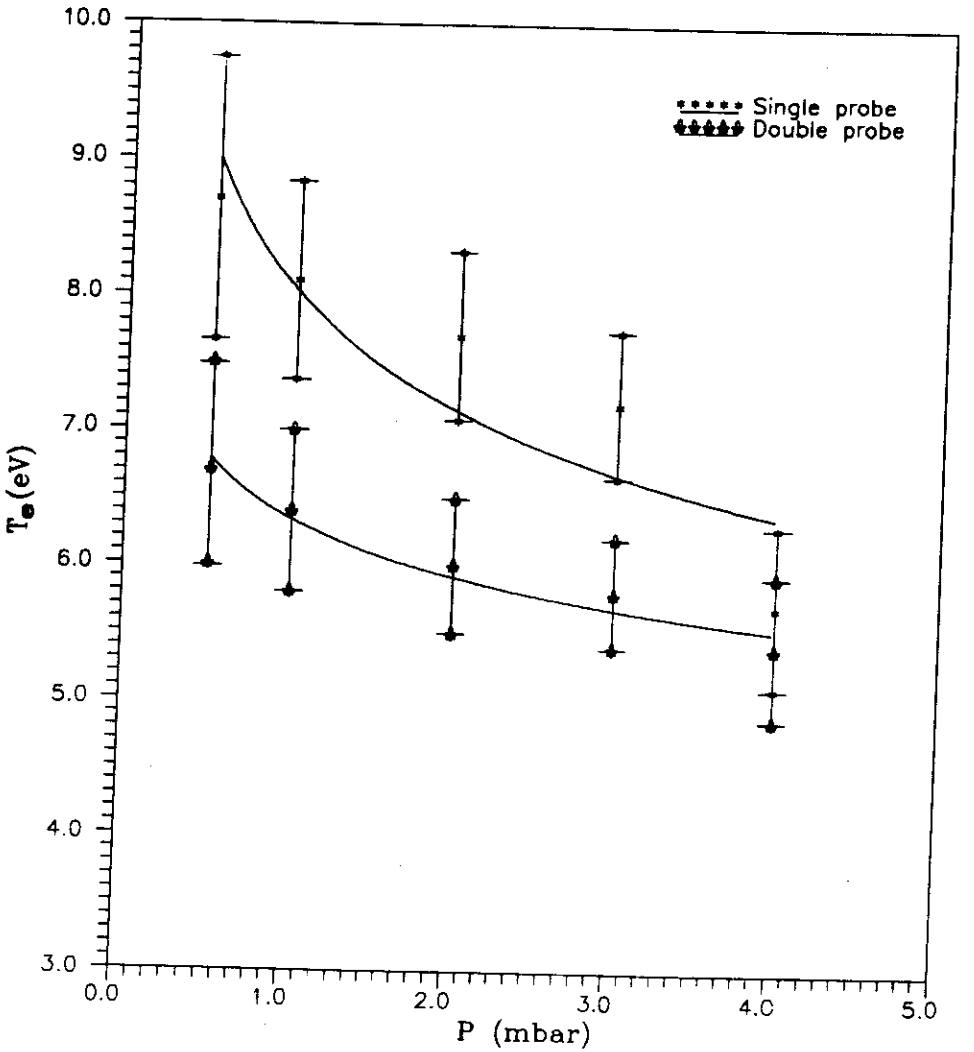

Fig.(50) Comparison between the T_e values , measured by single and double probes of the cathode fall region at different Ar pressures .

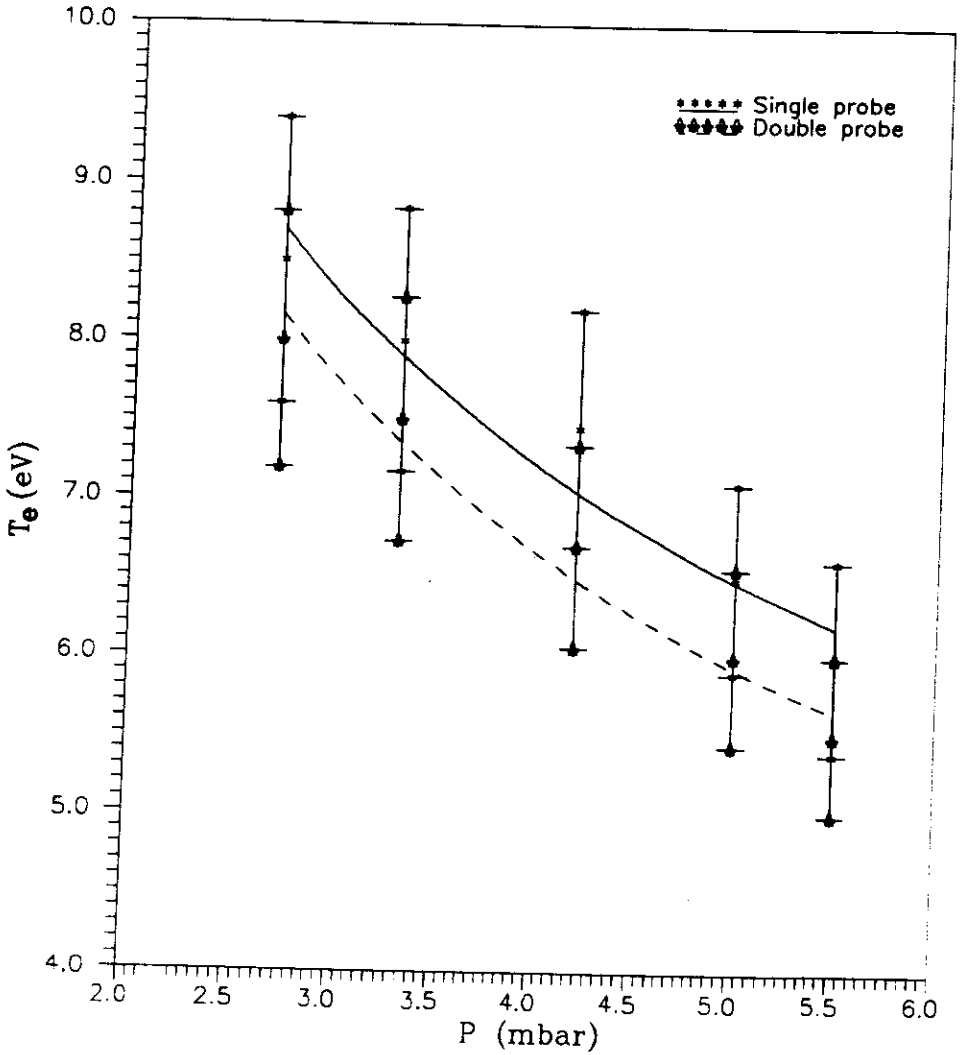

Fig.(51) Comparison between the T_e values, measurec by single and double probes, of the cathode fall region at different He pressures .

gas pressures for Ar and He-glow discharges are shown in Figs. (52), (53) , respectively . Values of T_e are in the range of (8.4 - 5.9 eV) for Ar glow discharge in a pressure range of (0.5 - 4.0 mbar) and (6.9 - 4.4 eV) for He glow discharge in a pressure range of (2.7 - 5.6 mbar) .

Electrons emitted from the cathode surface were accelerated through the cathode fall edge and enters the negative glow region . The intense light characterizes this region is related to the high rate of collisional excitation processes . The length of the negative glow region is determined by the dissipation of the electron energy due to inelastic collisions with neutral atoms ***(Hintz , 1990)*** .

5.3.1.3- Positive Column Region :-

The I-V characteristic curves of the single probe immersed in the positive column region of Ar and He plasmas , at different pressures , are shown in Figs. (42) and (43) , respectively . Figures (54) , (55) show values of T_e as a function of gas pressure for Ar and He gas discharge , respectively . Values of T_e , for- Ar plasma , varied from 8.8 ± 0.91 to 5.8 ± 0.62 at a pressure range of (0.5 - 4.0) mbar , while for He plasma , T_e varied from 7.0 ± 0.67 to 4.67 ± 0.51 at a pressure range of (2.7 - 5.6) mbar .

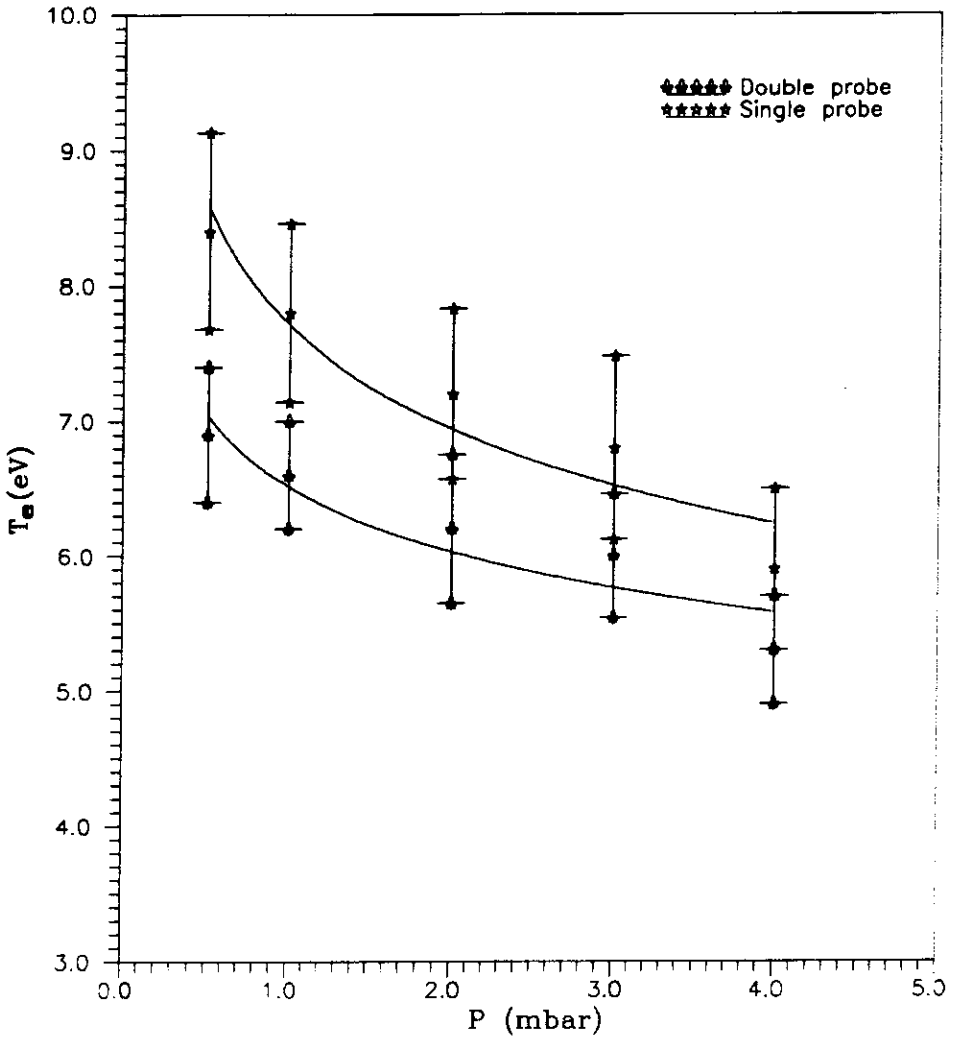

Fig.(52) Comparison between the T_e values , measured by single and double probes of negative glow region at different Ar pressures .

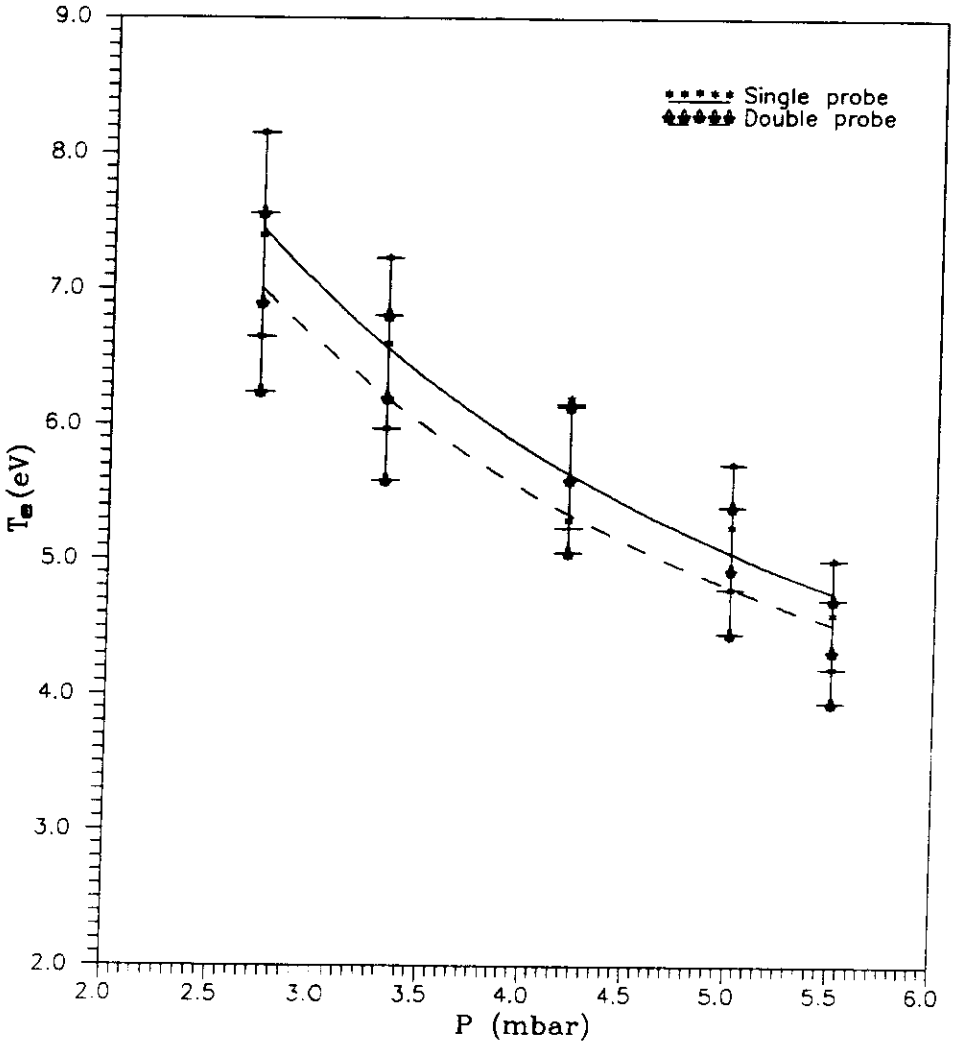

Fig.(53) Comparison between the T_e values, measured by single and double probes of the negative glow region at different He pressures .

5.3.2- Double Probe Measurements :-

The double probe consists of two identical cylindrical tungsten wires of 0.8 mm diameter and 2.0 mm length . They were held , so that , the distance between their centers was 3.0 mm . The separation distance was large enough to avoid the interference of the sheath around each electrode , i.e. larger than twice the Debye shielding length (λ_D) . The two electrodes were placed normal to the plasma path , so that , the plasma arrived at both electrodes at the same instant . The double probe was placed into the different regions of the glow discharge . The electric circuit of the double probe is shown in Fig. (9) . The two electrodes were connected together via a 50 KΩ , 10 turns potentiometer , to allow accurate measurements of the I-V characteristic curves . These curves were obtained by varying the probe bias from 0 to +100 volts between the two probes , using the potentiometer .

As explained earlier in chapter (3) , the electron temperature using the double probe method , can be calculated using the relation (***Swift and Schwar , 1970***) :-

$$T_e = \frac{1}{4}\Delta V_a F(\frac{S}{X})$$

where :-

ΔV_a is the voltage between the two points of curvature { points B and D in Fig. (10) } . The correction factor F(S/X) was introduced since the ideal double probe characteristic is extremely difficult to obtain

(experimentally) because of the sheath formation around the probe surface (***Hutchinson , 1990***) . The correction factor is given by :-

$$F(\frac{S}{X}) = \frac{[1 - 0.85(S/X)]}{[1 + 0.50(S/X)]}$$

Where :-

S is the slope of parts DC` or DE` and , X is the slope of line BD {Fig.(10) , chapter (3)} . (N.B. F (S/X) value was between 0.45-0.75).

Variation of the electron temperature , in the three regions for Ar and He-glow discharges as a function of gas pressure is compared with the single probe measurements .

5.3.2.1- Cathode Fall Region :-

Typical examples of the double probe (I-V) characteristic curves , for Ar and He-glow discharges , at different pressures are shown in Figs. (56) and (57) , respectively . Figure (56) shows that the ion saturation current of the probe is increased by increasing the gas pressure . The results shown in Figs (56) and (57) were obtained by increasing the probe voltage step by step .

Figure (50) and (51) show a comparison between values of T_e for Ar and He glow discharges , respectively , obtained by single and double probes , as a function of gas pressure . Values of T_e obtained by single probe is higher than those of the double probe , for Ar-discharge especially at the lower values of the gas pressure . However , this is not the case for He-discharge which is always operated at higher pressures .

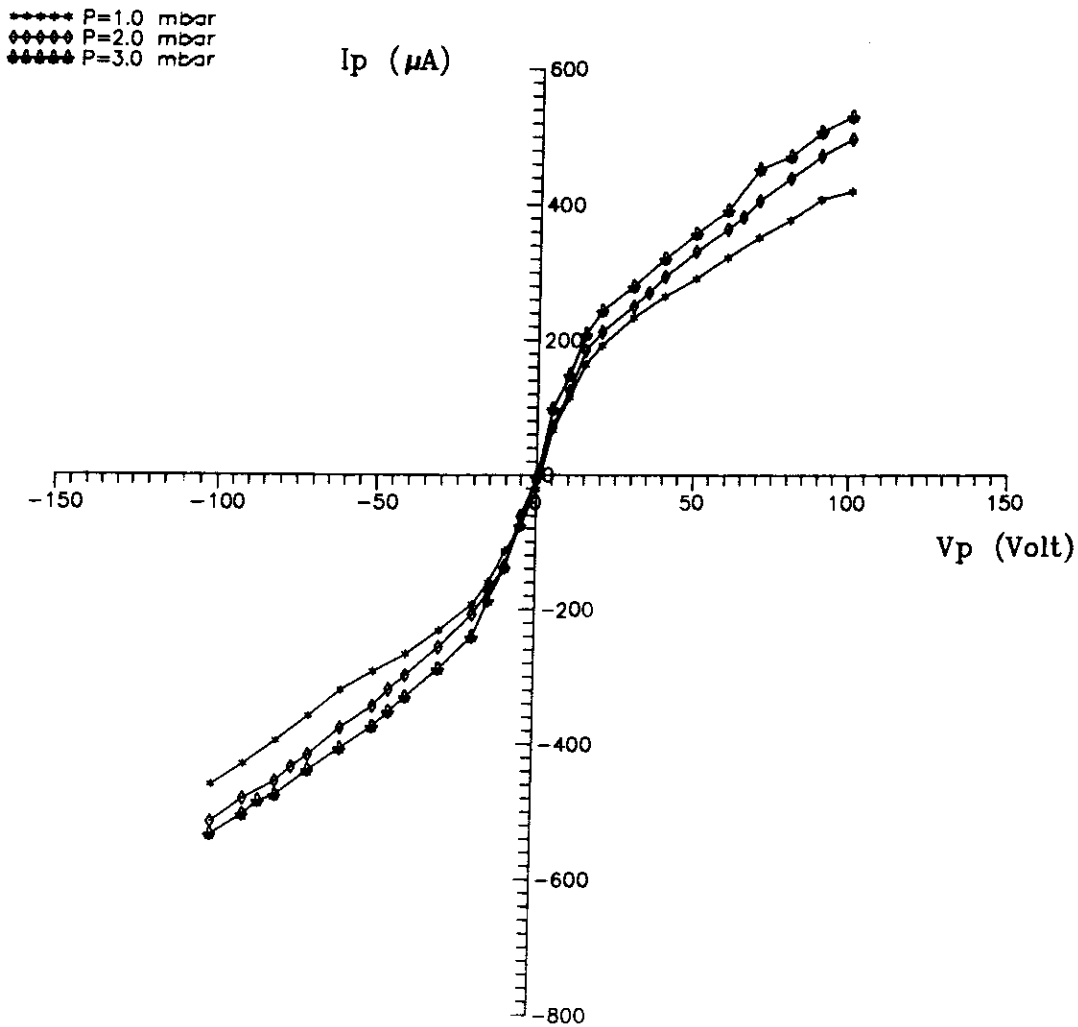

Fig.(56) The I–V curves of the double probe for the cathode fall region of Ar discharge at different pressures .

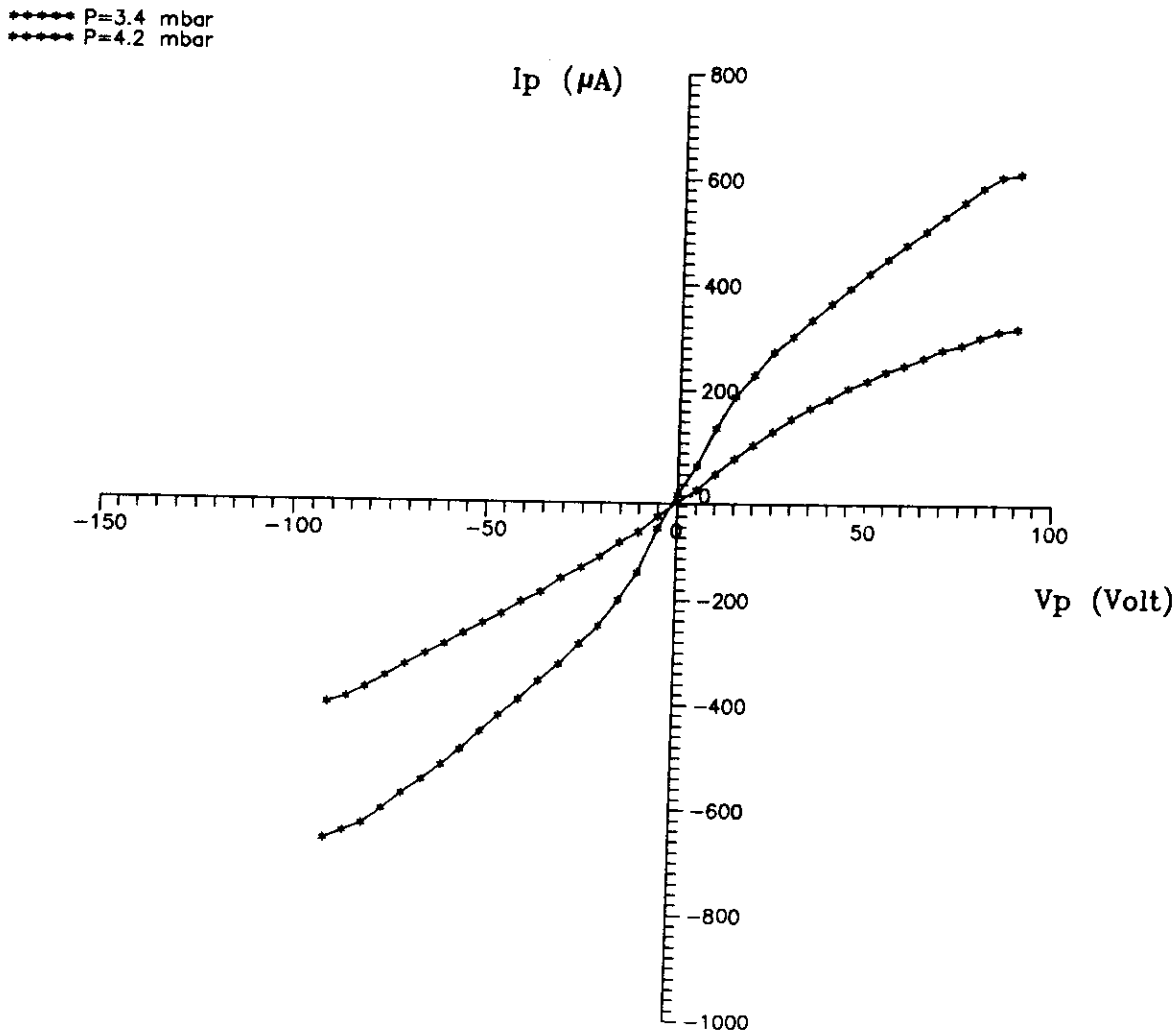

Fig.(57) The I–V curves of the double probe for the cathode fall region of He discharge at different pressures.

5.3.2.2- Negative Glow Region :-

The I-V characteristic curves using double probe in the negative glow region for Ar and He-glow discharges are shown in Figs. (58) and (59) , respectively . The electron temperature values are about (6.9-5.3 eV) ; in a pressure range of (0.5-4.0 mbar) for Ar-discharge , and (7.4-4.4 eV) for He-discharge in a pressure range of (2.7-5.6 mbar) .

Figures (52) and (53) , show a comparison between values of T_e , measured by single and double probe methods , in Ar and He-glow discharges ; respectively .

5.3.2.3- Positive Column Region :-

Samples of the I-V characteristic curves using double probe immersed in the positive column region for Ar and He-plasmas , are shown in Figs. (60) and (61) , respectively . For Ar-plasma , an increase in gas pressure is accompanied by a large change in both the magnitude of ion saturation current and of the slope of the current at the origin .

Figures (54) and (55) show a comparison between T_e values obtained by using single and double probes as a function of gas pressure for Ar and He positive column regions , respectively . A good agreement between T_e results is noticed as shown in Figs. (54) and (55) for Ar and He-plasmas ; respectively .

Figures (50) , (51) , (52) (53) , (54) and (55) confirm that , T_e decreased as the gas pressure was increased , this can be explained as follows :-

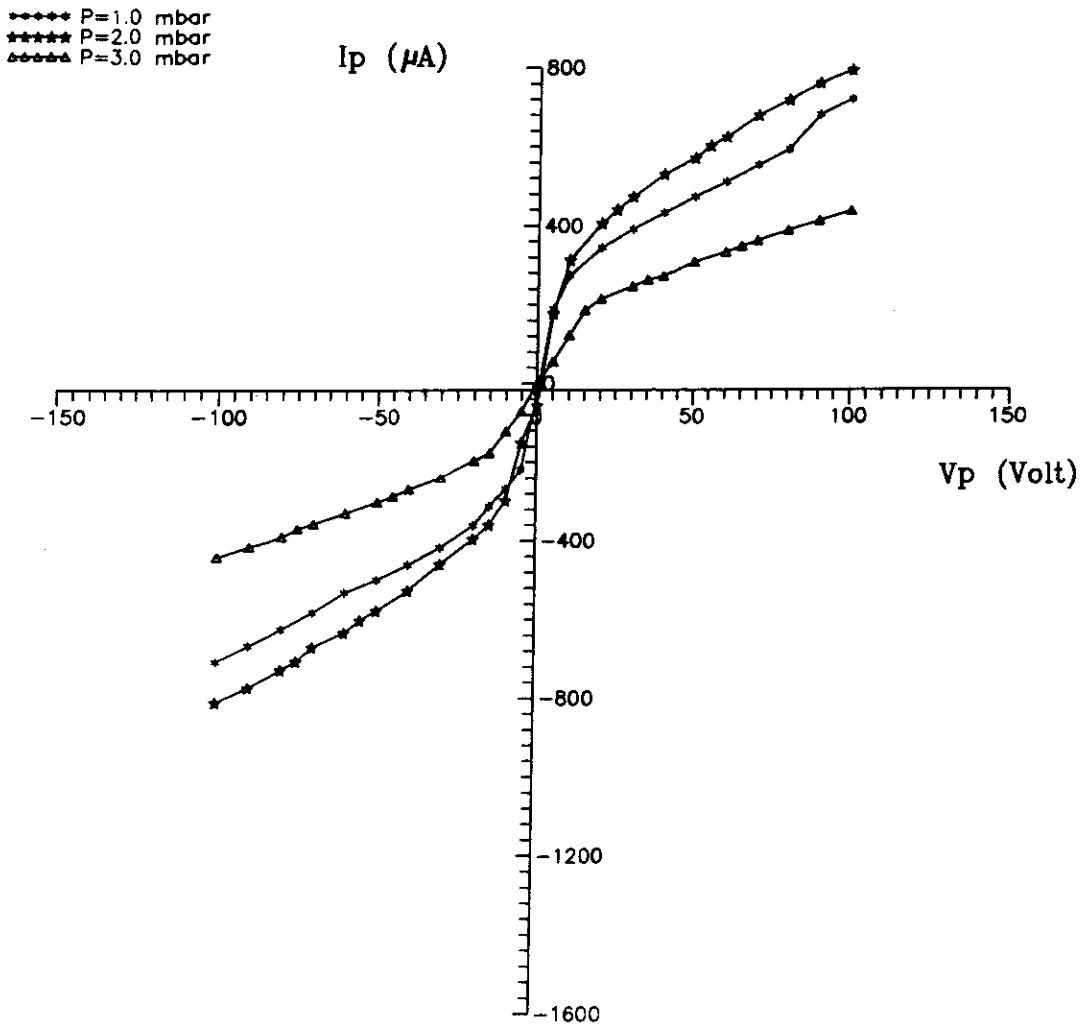

Fig.(58) The I–V curves of the double probe for the negative glow region of Ar discharge at different pressures .

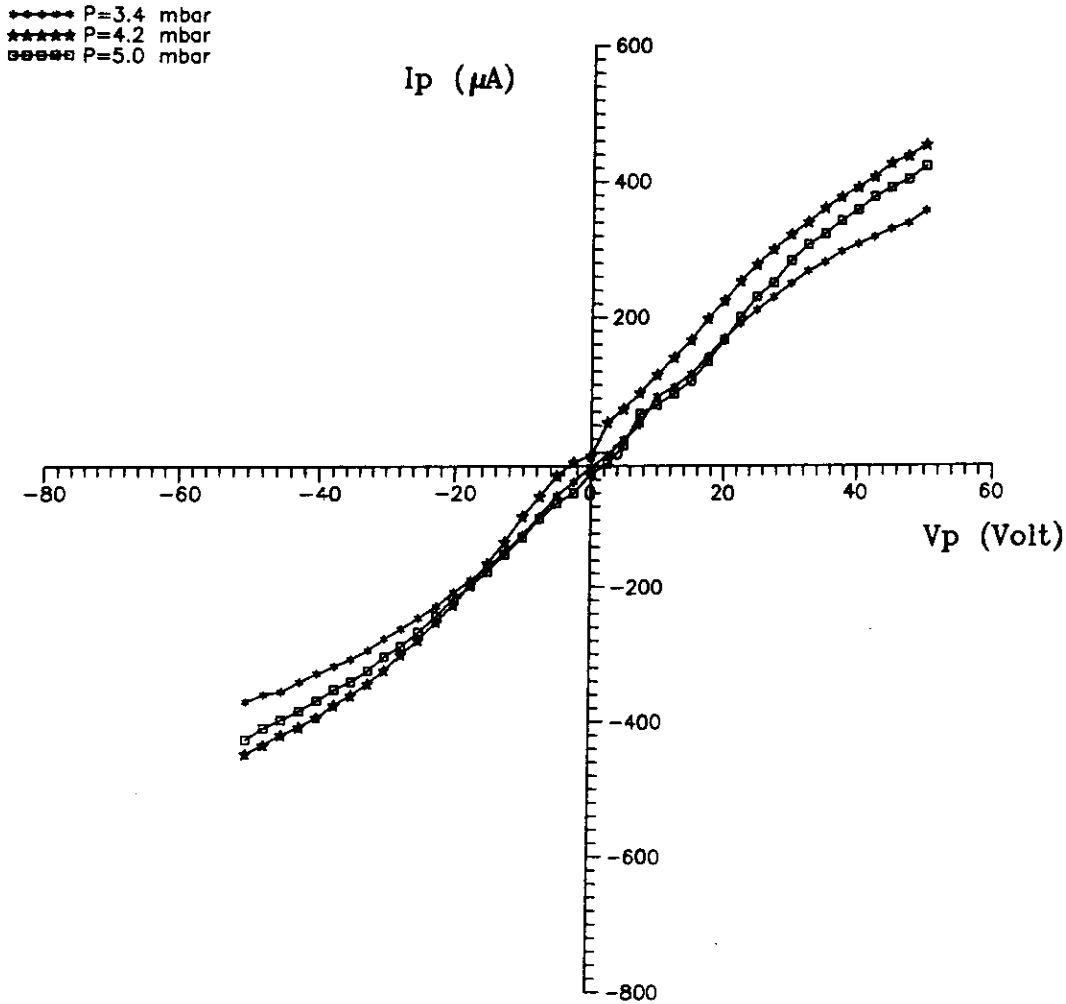

Fig.(59) The I–V curves of the double probe for the negative glow region of He discharge at different pressures.

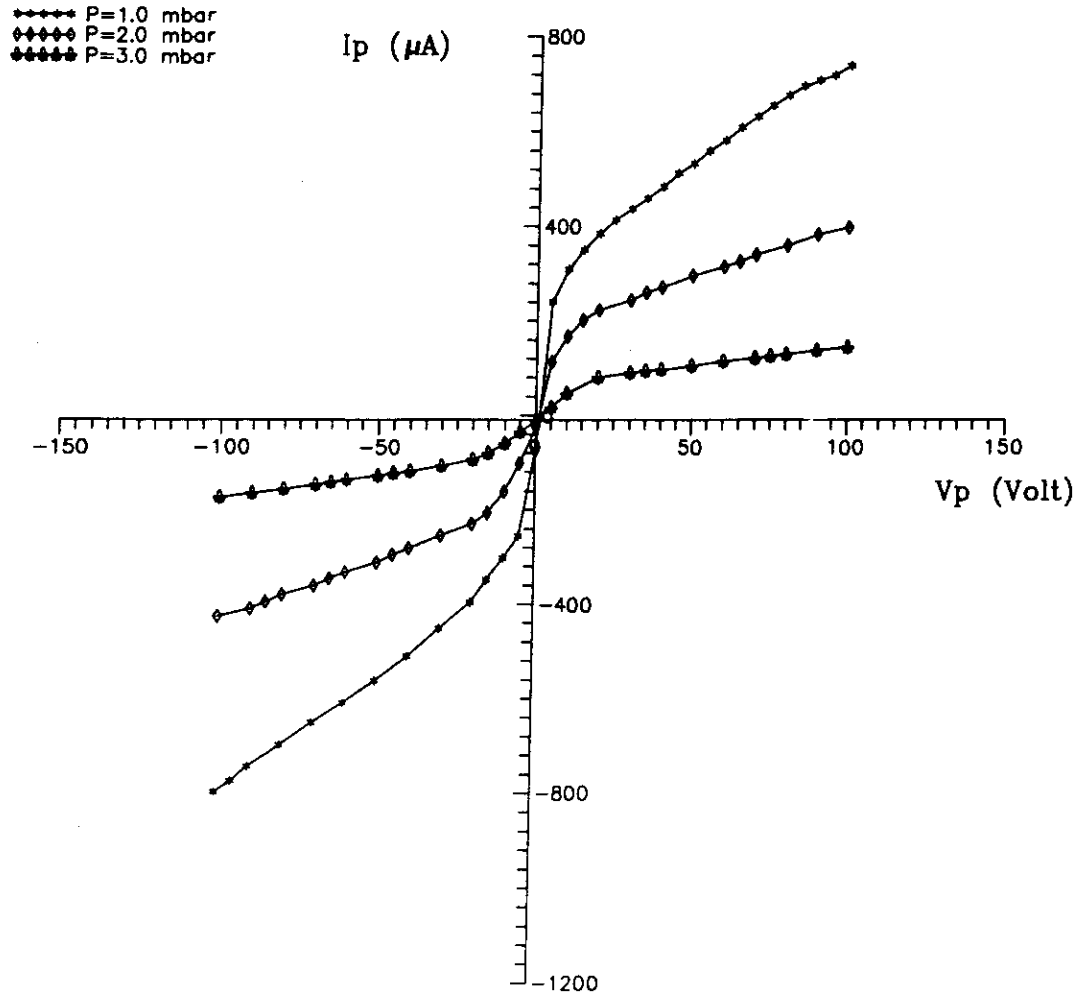

Fig.(60) The I–V curves of the double probe for the positive column region of Ar discharge at different pressures.

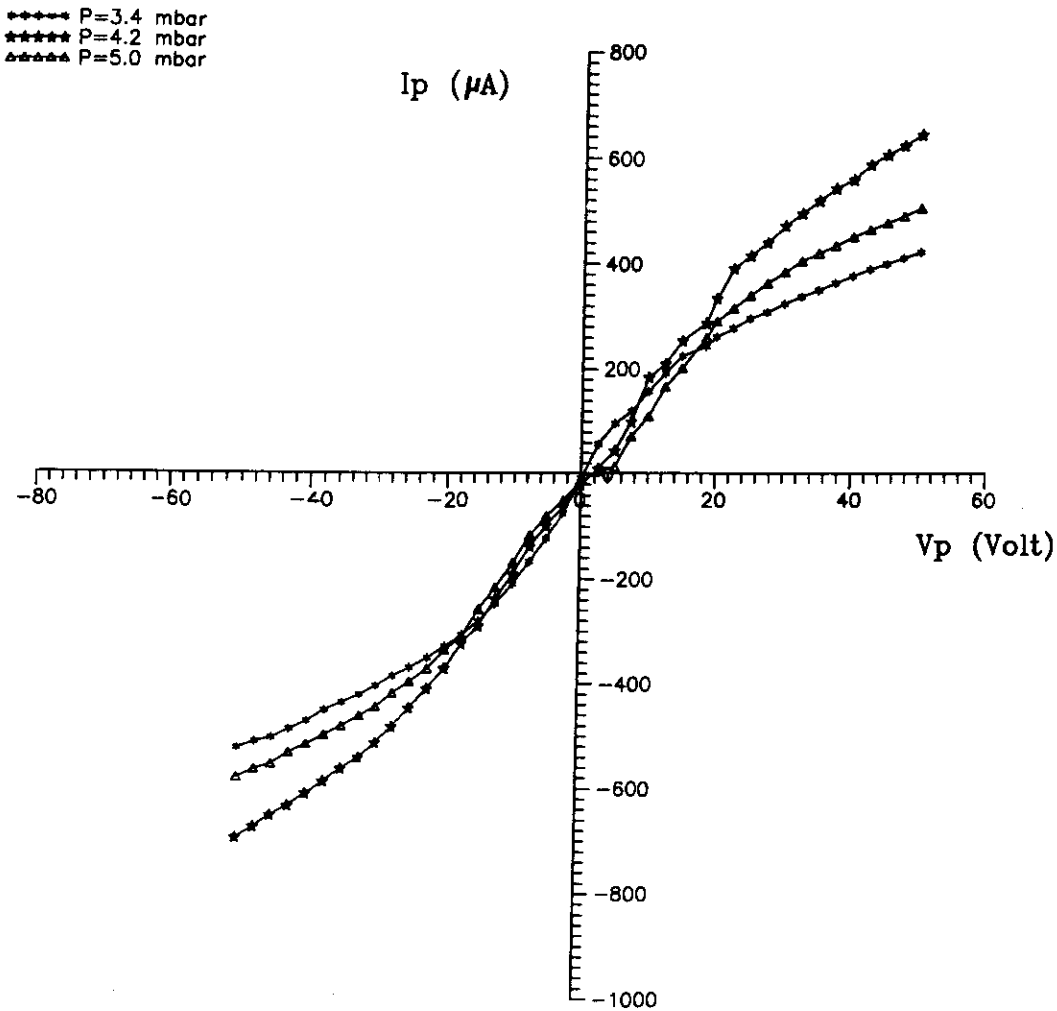

Fig.(61) The I–V curves of the double probe for the positive column region of He discharge at different pressures.

At low gas pressure , the electron-neutral particles collision frequency $\upsilon_{e\text{-}n}$ is small and the mean free path $\lambda_{e\text{-}n}$ is high . At high pressure , the collision frequency $\upsilon_{e\text{-}n}$ increases { see Figs. (62) , (63) } and hence , the loss of electron energy is high , thus T_e decreases . The collision frequency ν was calculated using the relation :-

$$\upsilon_{e\text{-}n} = N_n < Q_{e\text{-}n} (v_e) v_e >$$

where :-

N_n is the number of neutral particles , $Q (v_e)$ is the electron-neutral particle collision cross section and v_e is the electron velocity . N_n is given by $3.55 \times 10^{16} P$, where P is the gas pressure in torr .
The electron mean free path is given by :-

$$\lambda_{e\text{-}n} = 1/ N_n Q (v_e)$$

i.e. it is inversely proportional to the gas pressure .

The primary source of uncertainty in the electron temperature measurements is the absence of Maxwellian distribution which leads to higher values of T_e , since all theories of the single probe assumed the presence of Maxwellian distribution ***(Konuma , 1992)*** .

Adsorbed gas layers cause contact potentials such that the actual potential of the collecting surface is different from that applied to the probe from the circuit . Impurities on the probe surface , resulting in a changing or inhomogeneous work function , have a similar effect .

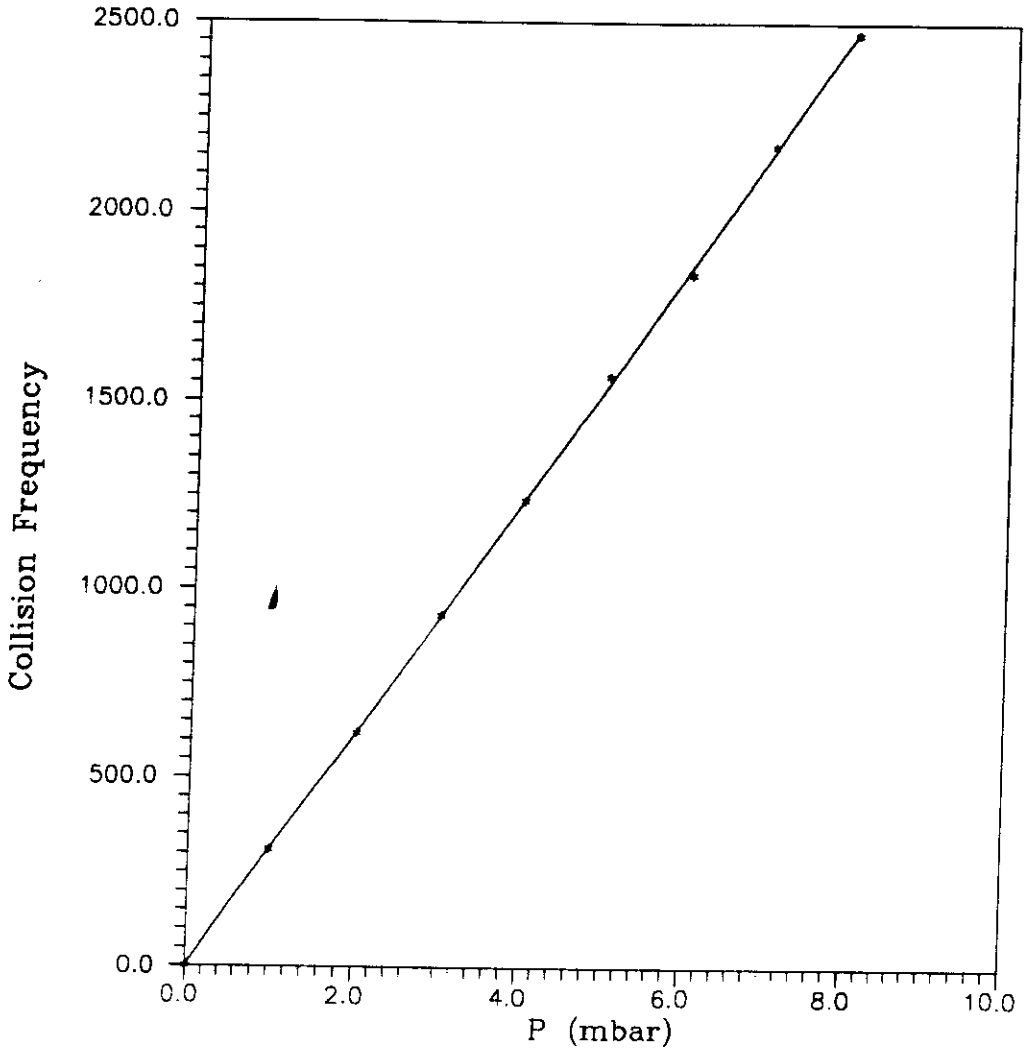

Fig.(62) The relation between the collision frequency and the Ar gas pressures .

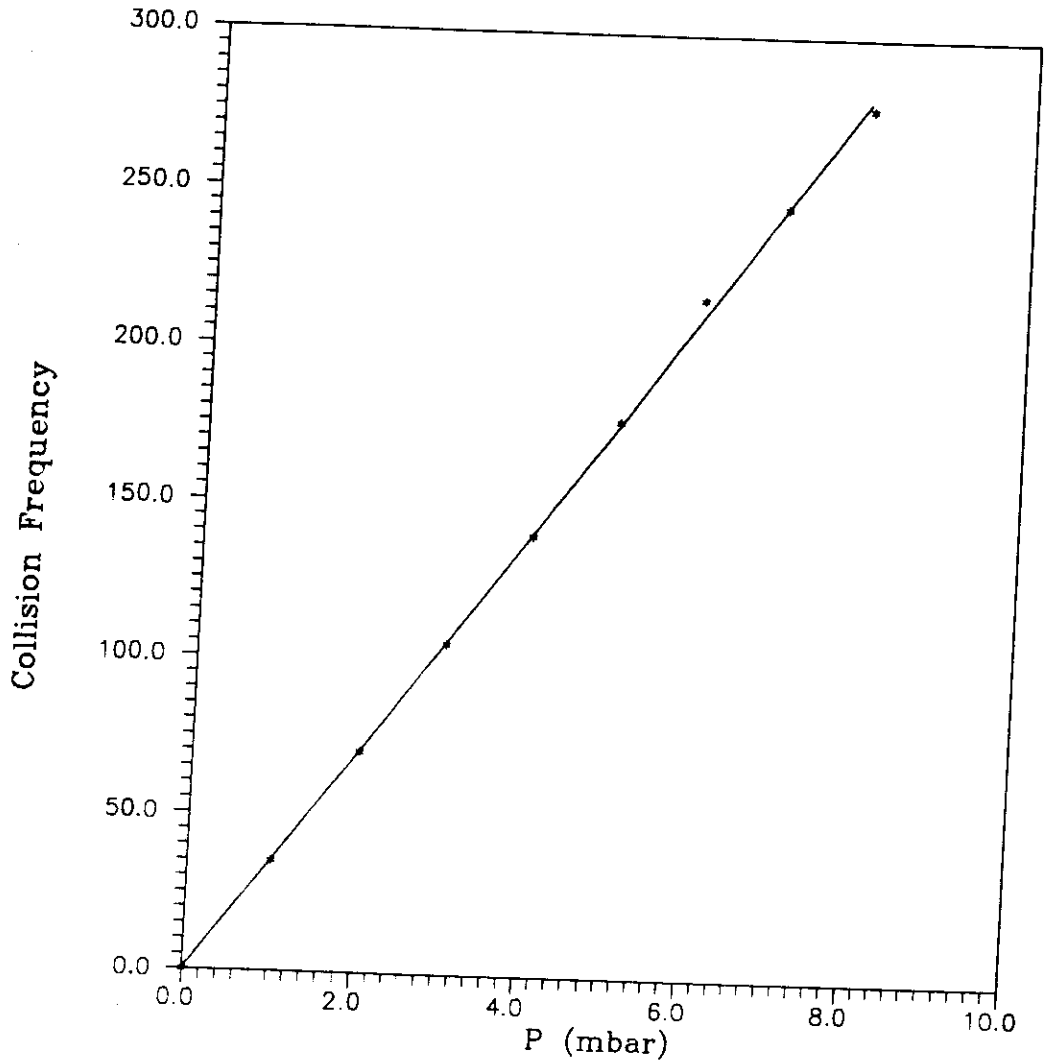

Fig.(63) The relation between the collision frequency and the **He** gas pressures .

Another source of uncertainty in T_e measurements is related to probe size . Too large probe size must introduce , essentially , geometric distortion in the discharge gap . However , even if the ion part of the probe characteristic is used , whereas the probe current is much small , the probe must be sufficiently small .

Contamination of the probe surface may also change the work function of the probe material or form surface layers with large ohmic resistance . If the probe current is small and the probe is cold , deposition is formed on the probe surface . With increasing the negative probe potentials , the ion bombardment becomes appreciable , and contaminations are evaporated from the surface ***(Kagan and Perel , 1964)*** .

Also , the oscillations of the plasma potential in the vicinity of the probe can greatly deform the electron current and the start point of the ion part of the characteristic curve . If the frequency of these oscillations is not too high , so that , the electron current can reach steady state within one period , then the instrument averages the current . The strong non linearity of the probe characteristic causes distortion , then , the temperature T_e will be overestimated (***Swift and Schwar , 1970***) .

The probe characteristic can be made perfectly reproducible if it is measured sufficiently slow , otherwise the characteristic will be deformed (***Kagan and Perel , 1964***) . Variation of the probe potential registed by the voltmeter will differ from the variation of the potential at the surface of the probe , if the work function , or the potential drop on the surface layer , changes at the same time , (***Kortshagen , 1991***) . To prevent this distortion it is necessary to clean the probe by emery paper or by electron or ion bombardment before the measurements , and to perform the measurements quit rapidly . The electron bombardment method was

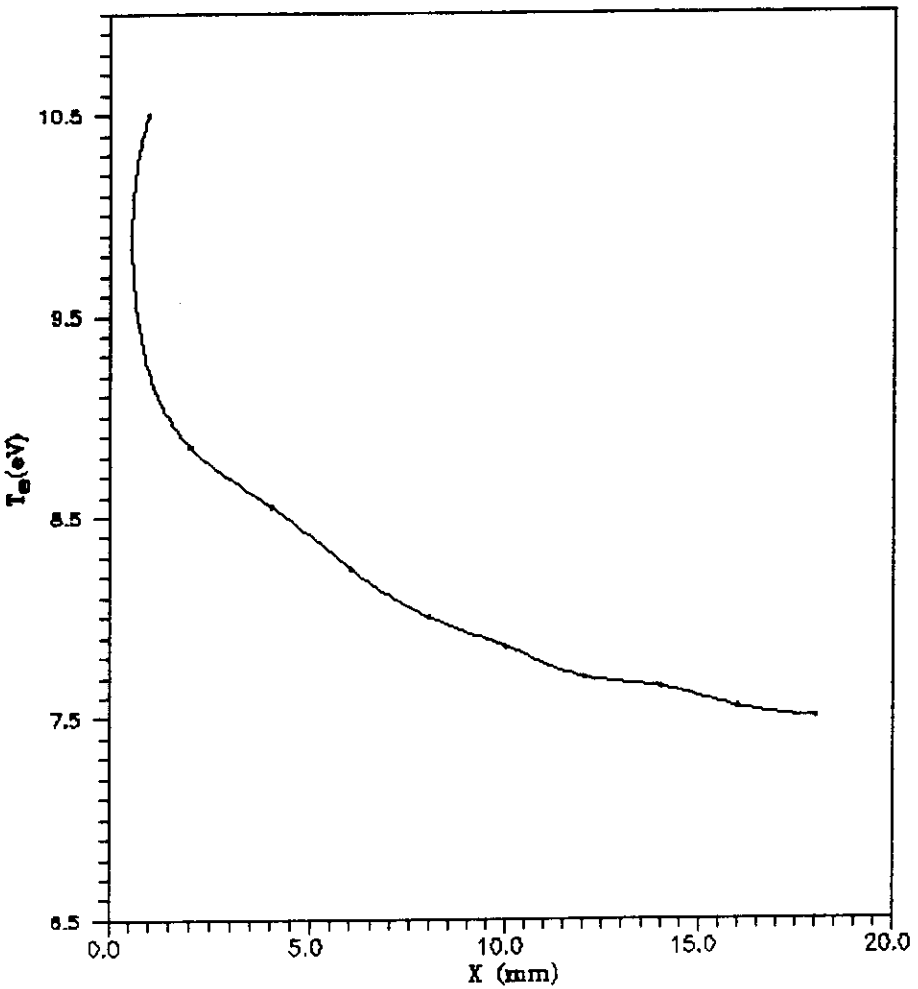

Fig.(64) The axial electron temperature distribution of the Ar glow discharge .

On the other hand , in the regions behind the cathode fall region , the electric field drop dramatically and the electrons undergoes many inelastic collision with atoms where they loose energy .

In the positive column region , the electric field is very weak and nearly constant because of the presence of the quasi-neutrality between the charge carriers densities , the electron temperature is nearly constant .

The present behaviour of electron temperature distribution agrees with that of ***Parker et al. (1993)*** .

The relation between the electron temperature T_e and the gas pressure P takes the form :-

$$T_e = (P^{-0.066} \times 6.5)$$

On the other hand , in the regions behind the cathode fall region , the electric field drop dramatically and the electrons undergoes many inelastic collision with atoms where they loose energy .

In the positive column region , the electric field is very weak and nearly constant because of the presence of the quasi-neutrality between the charge carriers densities , the electron temperature is nearly constant .

The present behaviour of electron temperature distribution agrees with that of ***Parker et al. (1993)*** .

The relation between the electron temperature T_e and the gas pressure P takes the form :-

$$T_e = (P^{-0.066} \times 6.5)$$

5.4- PLASMA DENSITY MEASUREMENTS .

a) Single Probe Method :-

The density was measured using different techniques , so as to overcome the uncertainty of each theory . These theories were explained earlier in chapter (3) .

The plasma density was calculated using values of the ion saturation current of the single probe by different methods . The most popular approach introduced by ***Langmuir (1923)*** , was first used . Also , the orbital motion limit (OML) theory derived by ***Laframboise (1966)*** was then used . The method is easy to use and it does not require knowledge of either the electron temperature or the plasma potential. The density was also calculated using ***Kagan and Perel theory (1964)*** . This method is more convenient to use than the other theories . They considered that outside the sheath , in the quasineutral region , there is a surface whenever ions reach it they strike the probe . Consequently , the ion strikes the surface of the sheath almost radially . The potential on the surface of the sheath layer (V_S) should be of the order of kT_e , since the sheath begins where the electrons concentrate . If $T_i < T_e$, where T_i is the ion temperature , then the velocity of the ion on the boundary of the sheath is given by the ion sound speed (i.e. $2kT_e / m_i)^{1/2}$. The ion current is thus given by :-

$$I_+ = CN_i e\left(\frac{2kT_e}{m_i}\right)^{1/2} A_s$$

Where ;

A_S is the sheath area $= 4\pi r_s^2$ for the spherical probe , and r_S is the sheath radius , N_i is the density in the quasineutral plasma and C is a constant $= 0.8$ for spherical probe , and $= 0.4$ for cylindrical probe .

The surface area of the sheath (A_S) can be chosen in practice to be equal to the area of the probe surface . In fact , (A_S) increases somewhat with the increasing of the probe potential , and therefore the ion part of the characteristic does not have a strict saturation . To estimate the sheath radius (r_S) , the probe current I_+ was calculated at the applied voltage Vp .

The space potential V_S was thus calculated using the relation :-

$$\frac{eV_s}{kT_e} = \ln\left(0.25\sqrt{\frac{m_i}{m_e}}.\frac{1}{C}\right)$$

Therefore ;

$$I_+ = 4\sqrt{\frac{2}{9}}.\sqrt{\frac{e}{m}}.\frac{(V_p - V_s)^{\frac{3}{2}}}{\sigma^2}$$

σ^2 was calculated and consequently r_S was obtained using ***Langmuir`s Tables (1923)*** . V_S was also estimated using the second derivative $\frac{d^2I_e}{dV_p^2}$ curves (see sec. 5-2) .

The plasma density N_e was also estimated using the double logarithmic extrapolation (DLE) method , (***Van de Motter and Peter , 1989***) , of ion saturation current I_+ using the relationship :-

$$I_+ = A \cdot I_{+0} (\eta + 1)^{\alpha} \quad ; \quad (0 \leq \alpha \leq 1 : 1 \leq A \leq 2/\sqrt{\pi}) .$$

I_{+0} was determined by (DLE) method i.e. log I_+ vs. log $(\eta + 1)$, where :

$$\eta = \left| \frac{e(V_p - V_s)}{kT_e} \right|$$

η being the normalized probe potential .

Values of N_e from "DLE" are lower by a factor of 2 to 3 than those obtained by usual linear extrapolation (LIN) . The electron density can be estimated also using the corresponding integrals of the electron energy distribution function (EEDF) , i.e. :-

$$N_e = \int_0^{\infty} F(E) dE$$

Where :-

F(E) is the electron energy distribution function .

The "EEDF" was obtained either by differentiating the I-V characteristic curves twice , or by electrical method , (i.e. :- a.c. signal method , see sec. 5.2) . This method is the most certain and reliable to get the true values of N_e , (***Godyak et al. , 1993***) . Values of N_e obtained by the use of these methods were compared with ***Kagan and Perel Theory*** ; this will be discussed latter .

b) Double Probe Method :-

The plasma density N_e was also measured using the I-V characteristic curve of the double probe for each region in the glow discharge . N_e was calculated using the following formula (***Hutchinson, 1990***) :-

$$N_e = \frac{I_i}{e(2kT_e / m_i)^{1/2}.A_p}$$

Where : -

I_i is the ion saturation current and it was determined by the linear extrapolation of lines C`B and E`D in Fig. (10) , chapter (3) . For accurate measurements , average of the parts AF and AG should be taken , Ap is the area of the probe and T_e is the electron temperature which was determined previously . In the following , the results of the plasma density obtained by both the single and double probe methods , in the three regions of the glow discharge are compared and discussed .

5.4.1- Cathode Fall Region :-

Figures (65) and (66) show values of the plasma density N_e , calculated using the single and the double probes , as a function of gas pressure in the range of 0.5 - 4.0 mbar for Ar-glow discharge and 2.7-5.6 mbar for He-glow discharge . Single probe measurements include :-

1- Kagan and Perel method , (LIN) ,

2- Log-log method (DLE) , and

3- Integration of (EEDF) method .

Figures (65) and (66) indicate that plasma density increases by increasing gas pressure . This is attributed to the increase in the number of electron-atom collisions (and consequently increases the ionization rate) .

Figures (65) and (66) show that values of the plasma density N_e , calculated using ***Kagan and Perel*** theory are higher by a factor of 2-3 , than the other methods , this may be attributed to :-

i) Deviation of electron energy distribution function from being Maxwellian , may lead to higher values of N_e (***Kagan and Perel , 1964***).

ii) The assumption that ions enter the sheath with a velocity of $(kT_e/m_i)^{1/2}$ may not be exactly valid .

iii) Ideal ion saturation current did not achieve as a result of the screening effect which is related to the change of the effective collecting area . Sheath area A_S must be considered in place of the geometrical area of the probe Ap (***Hutchinson , 1990***) . However , a reasonable agreement was obtained by using of the log-log method which depends upon orbital limit theory and the integration of EEDF method . Both methods , overcome most of the above shortcomings .

5.4.2- Negative Glow Region :-

Figures (67) and (68) show a comparison between N_e values obtained by using of the single and the double probes as a function of the gas pressure for Ar and He glow discharges in the negative glow regions , respectively .

An agreement between integration of EEDF and log-log methods with the double probe is obtained . However , in both cases , the ion

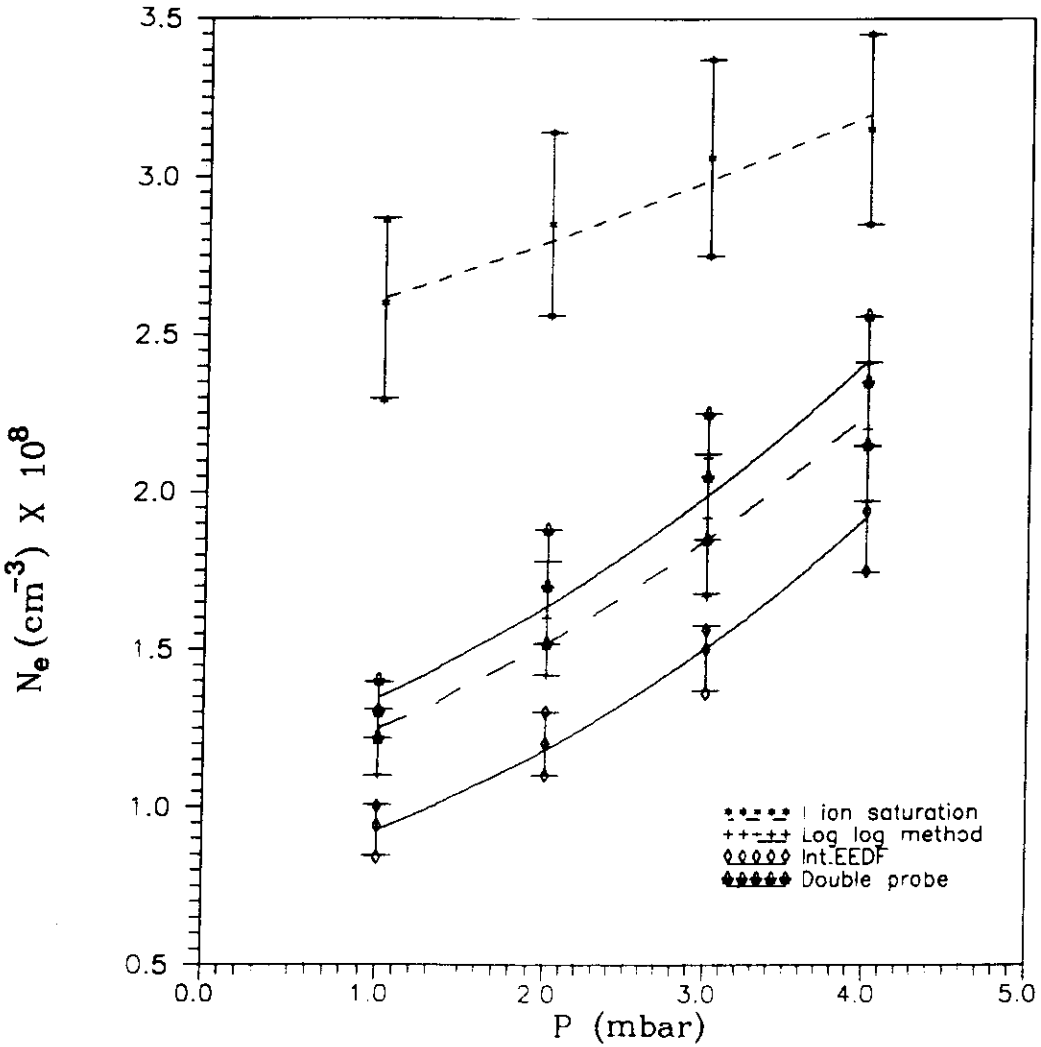

Fig.(65) Comparison between plasma density measurements by the different method, for the cathode fall region, as a function of the Ar gas pressures.

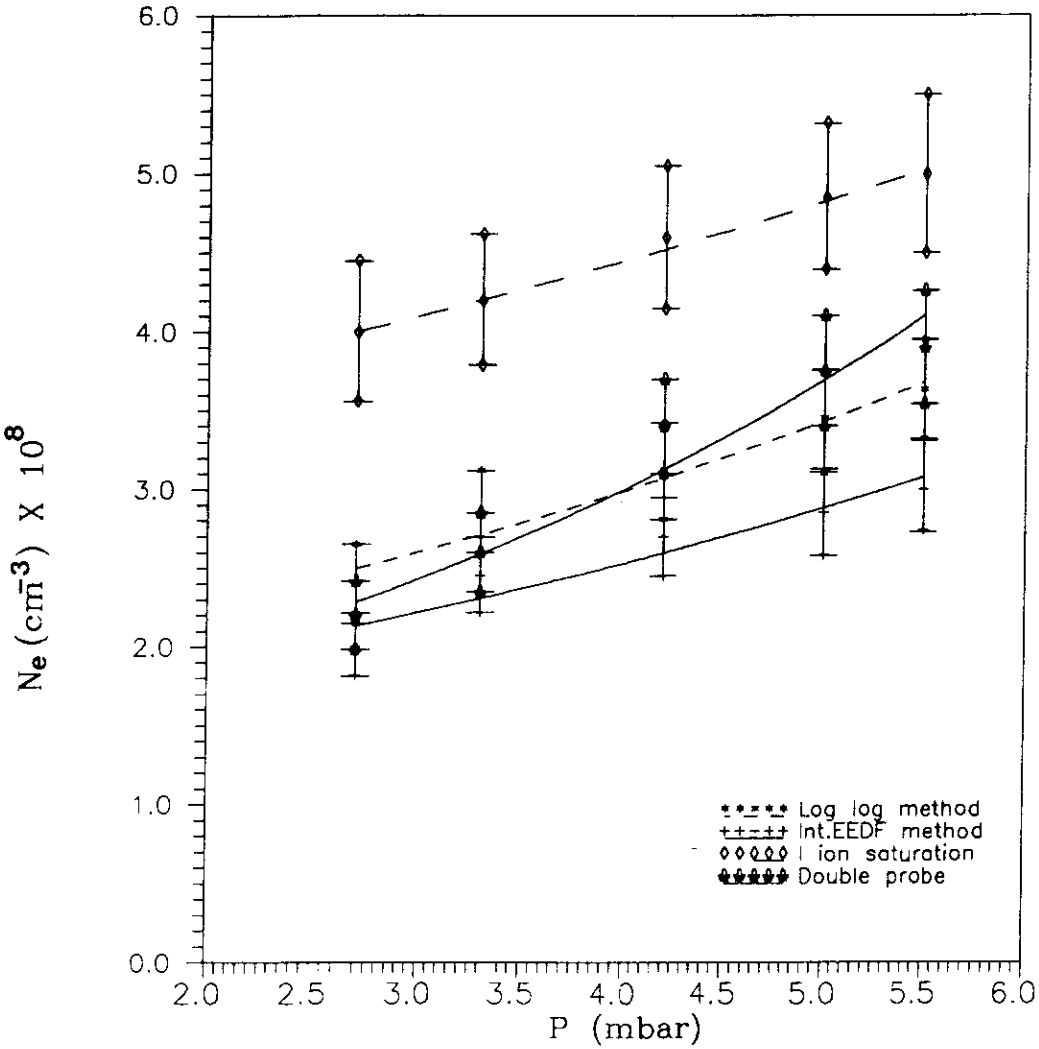

Fig.(66) Comparison between plasma density measurements by the different method, for the cathode fall region, as a function of the He gas pressures.

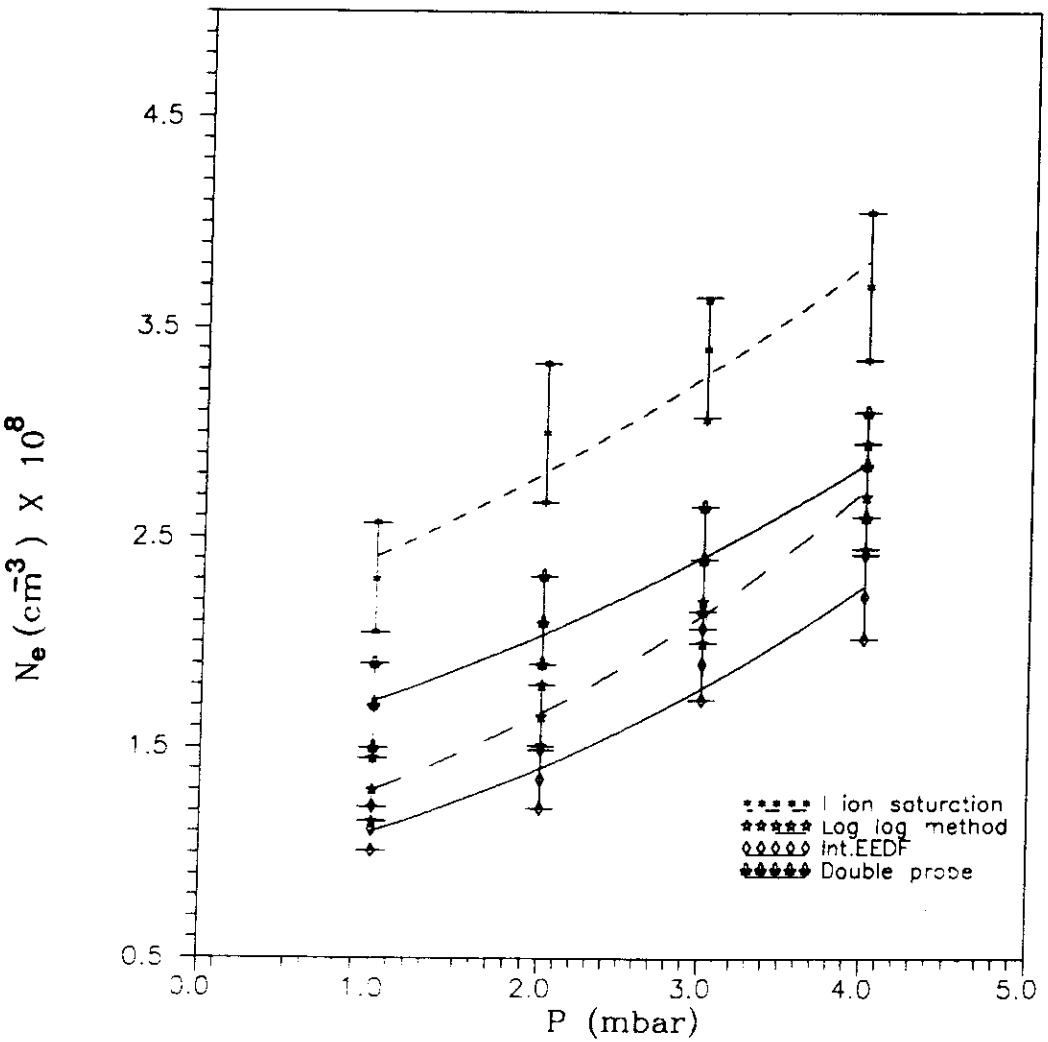

Fig.(67) Comparison between plasma density measurements by the different method, for the negative glow region, as a function of the Ar gas pressures.

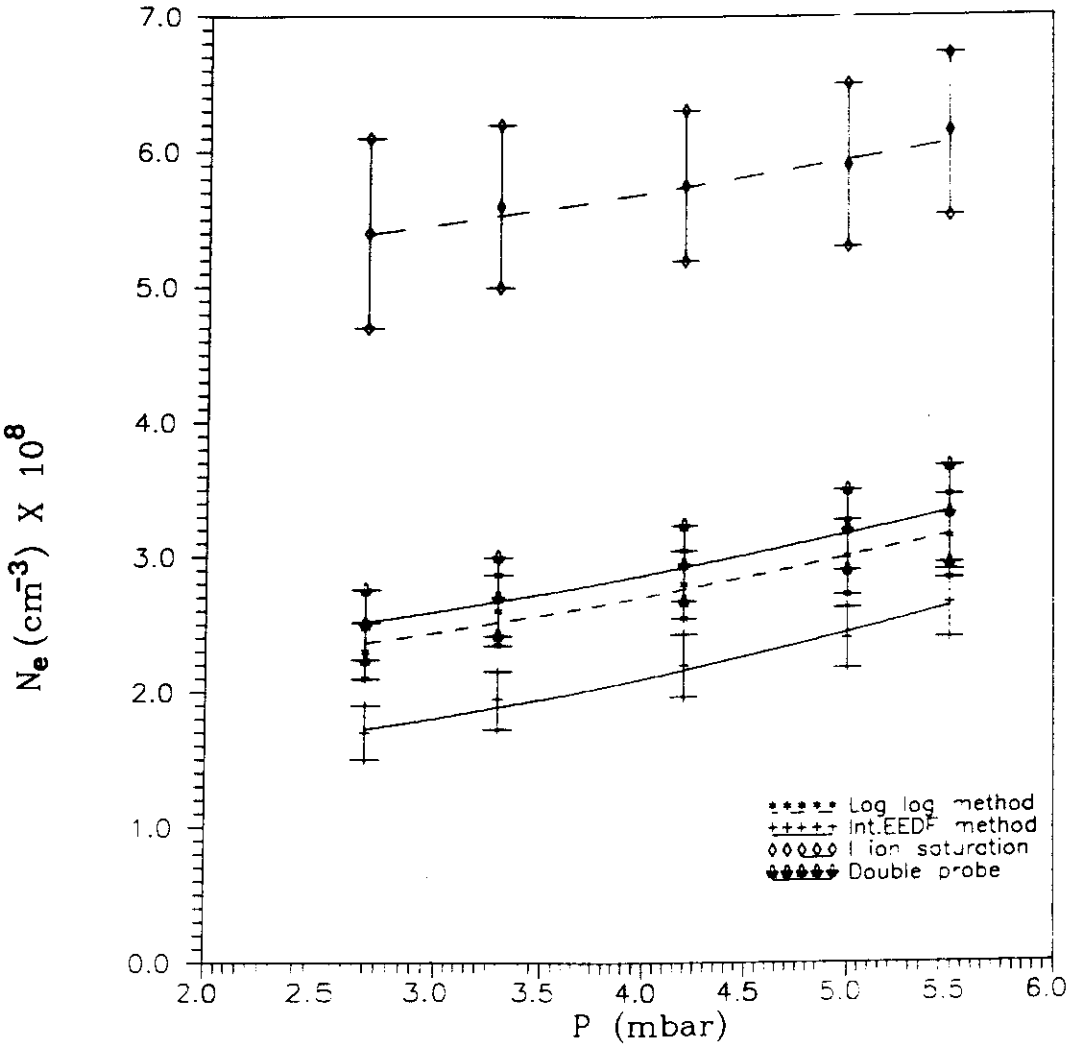

Fig.(68) Comparison between plasma density measurements by the different method, for the negative glow region, as a function of the He gas pressures.

saturation current (***Kagan and Perel***) method produces higher values than the other methods .

5.4.3- Positive Column Region :-

Figures (69) and (70) show a comparison between N_e values obtained by using of the different methods in the positive column region for Ar and He plasmas . An agreement is found between the N_e values obtained from integration of EEDF, log-log method with the double probe measurements .

The main source of error in measuring N_e is related to the emission of secondary electrons under the influence of ions , photons and metastable atoms from the surface of the probe . This could result in an increase of the apparent ion saturation current . Therefore , total secondary electron current , as a result of all the above processes , must be subtracted from the total probe current .

Ions may be produced by ionization in a region around the probe surface by collision . An additional current equal to (ZNV) may thus increase the total current collected by the probe and consequently alters the true density , where V is the volume of the perturbed region by the probe and its defined by the ion impact parameter Z , given by(***Spitzer , 1967***) :-

$$Z = 0.8\left(\frac{2kT_e}{m_i}\right)^{1/2}.\frac{1}{R}$$

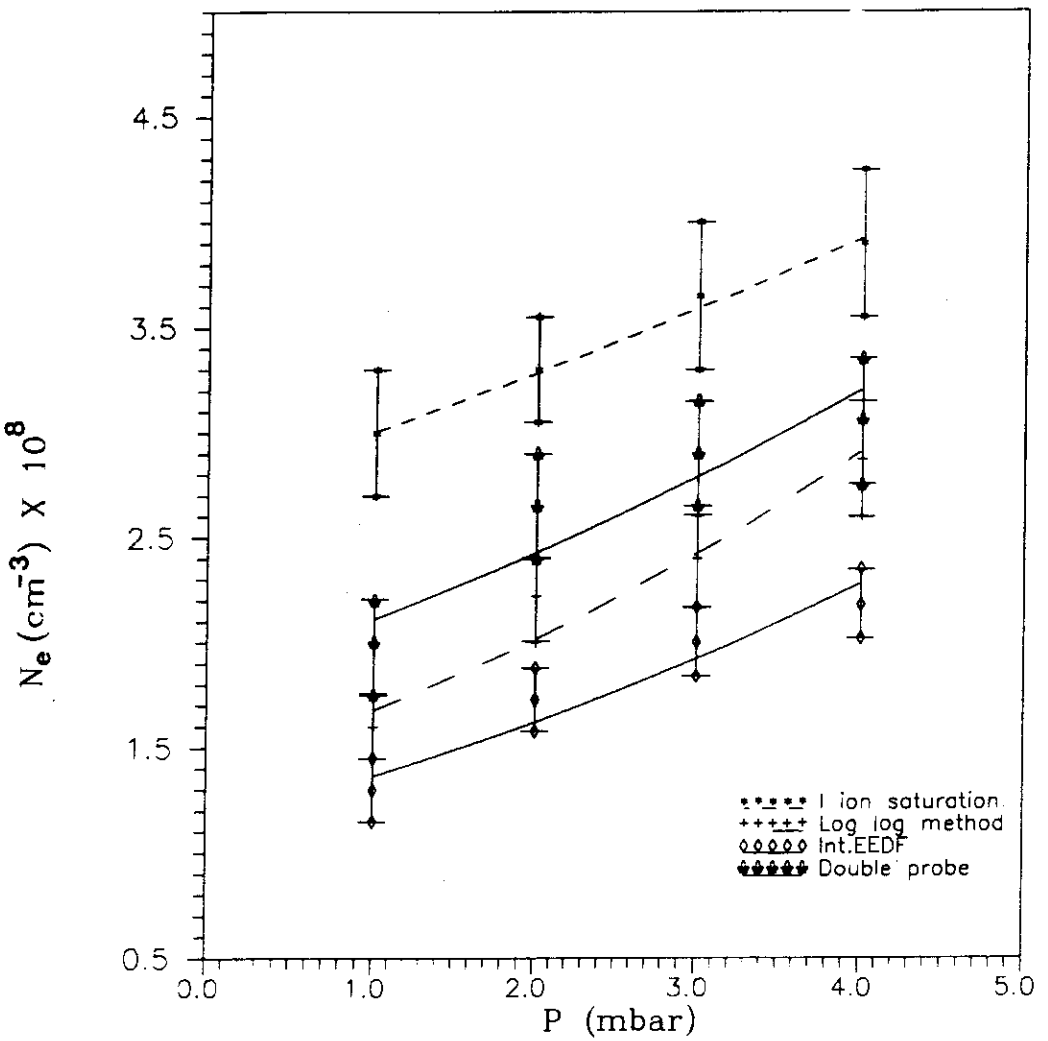

Fig.(69) Comparison between plasma density measurements by the different method, for the positive column region, as a function of the Ar gas pressures.

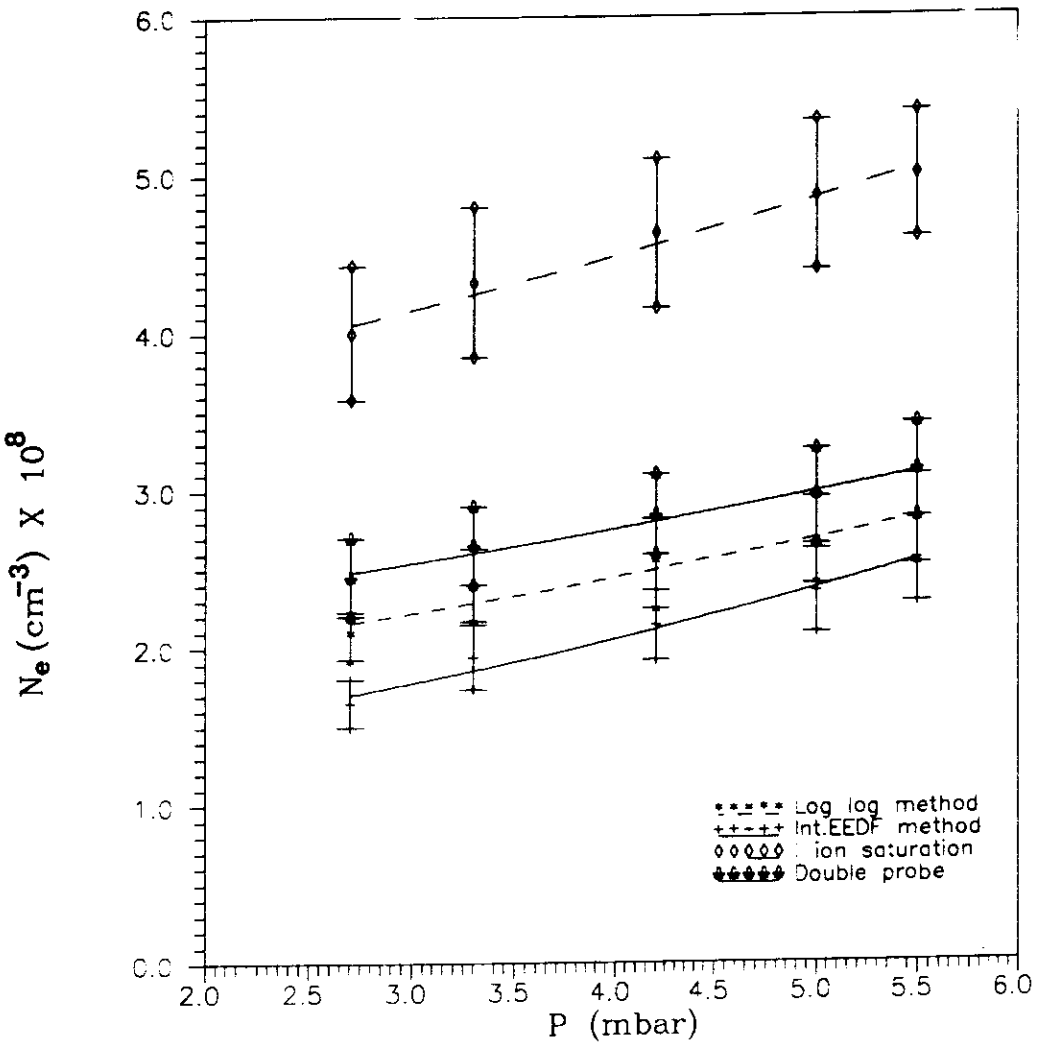

Fig.(70) Comparison between plasma density measurements by the different method, for the positive column region, as a function of the He gas pressures.

Where :-

R is the discharge tube radius . The current I_{ion} , is thus given by :-

$$I_{ion} = e\, Z\, N\, V$$

V was in the order of the probe volume ($V = 3/4\ \pi r_p^3$ for spherical probe). The electron emission from the probe surface due to the impact of positive ions , metastable atoms and photons was also calculated .
The current initiated by positive ion collision is given by ***(Spitzer , 1967)*** :-

$$I_{pos.ion} = \frac{1}{4}(N_i . e . v_i . A_p . \gamma)$$

Where :-

γ is the emission coefficient (=0.05 at 100 V { ***Kagan and Perel , 1964*** }) . A similar relationship must be used to calculate the current produced by metastable atoms collision , where γ is the emission coefficient as a result of this type of collision { ≈0.01 (***Spitzar , 1967***)} . An additional current of about 15 % must be subtracted from the total probe current as a result of all these processes .

5.4.4- The Electron Density Distribution Along the Glow Discharge .

Figure (71) shows the axial profile of the electron density distribution for Ar glow discharge . The density increased from the cathode fall region and reached a maximum value in the negative glow region , then it decreased again in the positive column region .

Electrons emitted from the cathode surface were accelerated through the cathode fall region (no inelastic collisions occurs) . The fast electrons enters the negative glow region ; excitation and ionization of the gas atoms are possible without additional energy gain by the weak electric field in this region . The adjoining Faraday dark space region is a transition region to the positive column region ; the electric field was small , electron energy and excitation/ionization of atoms were low , it serves for matching the electron density in the negative glow region by diffusion to that of the positive column region .

Coe and Lister , 1992 show that the accelerated electrons emitted from the cathode were the main cause of excitation/ionization processes in the negative glow region and hence , maximum electron density was expected in this region .

The relation between the plasma density N_e and the gas pressure P takes the form :-

$$N_e = \text{Exp.}\ (0.22xP) \times 1.45$$

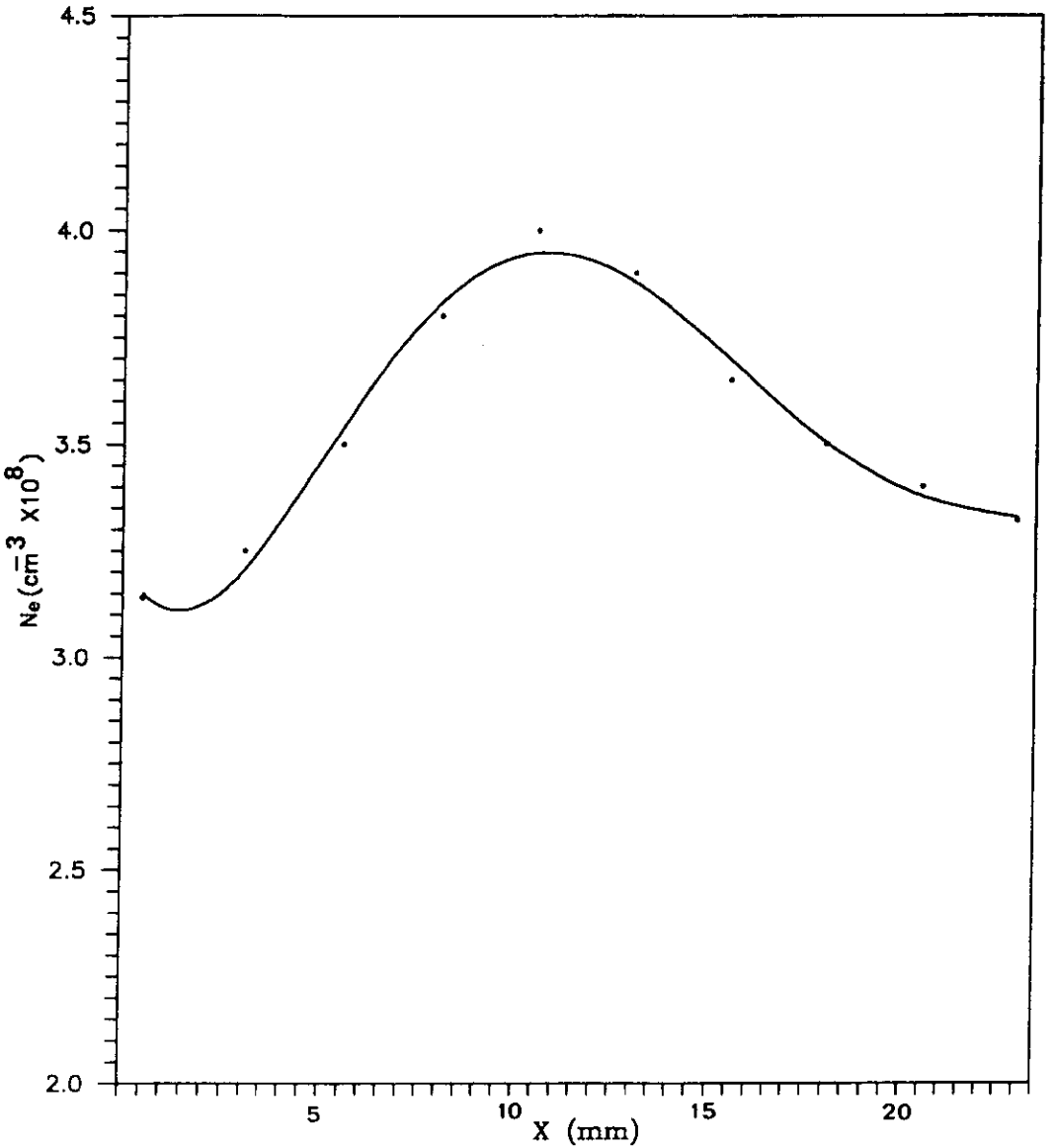

Fig.(71) The axial density destribution of the glow discharge.

5.5-THE SPECTROSCOPIC MEASUREMENTS :-

Introduction :-

The intensities of light output of the plasma from He and Ar glow discharges were measured using a Mc-Pherson monochromator (Model 270) . A schematic diagram of the spectroscopic instrumentation is shown in Fig.(72) . The monochromator was positioned so as to observe the plasma beam at 40 cm from the discharge tube .

The intensity of the emitted spectral lines was measured by using of a photomultiplier tube type RC-128 . The quantum efficiency of the photomultiplier was taken into consideration . One of the important source of error is the calibration of the monochromator . Therefore , a mercury and sodium lamps were used to check the calibration of the monochromator . The resolution of the monochromator was tested by observing the sodium D lines and it was found to be less than 2.0 A° at a slit width 100 μ .

Scattering effect in the monochromator was negligible in the present measurements which may effect the intensity of the considered two lines (such as He lines) . Also , the absorption of the lines , may cause some uncertainty in the calculation of the total line intensity (e.g. for He lines 5048 and 4713 A°) , a correction factor of about 5% must be used as suggested by ***Griem (1964)*** .

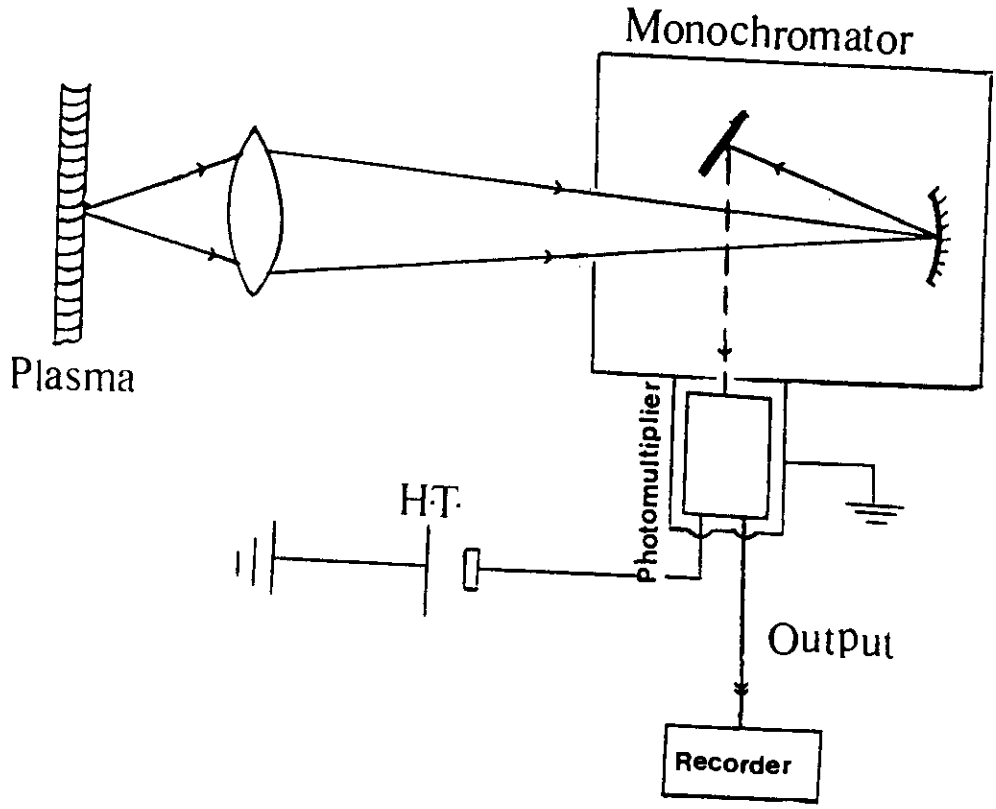

Fig.(72) Schematic Diagram for the Optical Arrangement .

Models of the formed plasma in the glow discharge (at the different three regions) have been investigated . The degree of ionization was also determined by measuring the He ionic to atomic lines intensity ratio .

5.5.1- The Spectra of the Ar and He-Glow Discharge :-

Tables (2) and (3) show the spectra of Ar and He glow discharges in the region of (3840 - 5500 A°) and (3600 - 5200 A°) , respectively . The appearance of He lines may be attributed to the direct one step impact between the electrons , (which have energies more than 19 eV) , and the neutral atoms (the first excitation energy of He is 19.75 eV) .

Also , Fig. (73,a) shows the intensity of lines 4686 , 4713 , 4921 , 5016 and 5048 A^0 of He discharge as a function of gas pressure . For each curve of these lines , the line intensity increases to reach a maximum value at P = 5.6 mbar , then it decreases as the gas pressure increases . This behaviour was confirmed by calculating the theoretical line intensity using the relationship :-

$$I = N_e N_n Q_e (v_e) v_e \ .$$

where :-

$$N_n = 3.55 \times 10^{16} \ P \ .$$

, $v_e = (2kT_e / m_e)^{1/2}$.

P is the gas pressure in torr , T_e is the electron temperature in eV and N_e is the electron density . Figure (73,b) shows an agreement between the measured and computed line intensity I .

Table (2) :- Spectra of Ar Glow Discharge .

λ (A°)	I (arbit.unit)	λ (A°)	I (arbit.unit)
5494.2	0.22	4499.8	0.19
5185.4	0.17	4427.4	0.16
5160	0.18	4369.4	0.24
4963.2	0.27	4345	0.31
4886.4	0.15	4338	0.18
4859.4	0.56	4331	0.24
4804.2	0.26	4298	0.22
4762.6	0.66	4275.6	0.64
4734	0.18	4256	0.56
4724.6	0.35	4196	0.56
4655.6	0.42	4188	0.22
4608	0.52	4156	0.47
4587	0.31	4129	0.32
4577.4	0.23	4069	0.25
4543.6	0.47	4042	0.17
4508.6	0.26	3842	0.11

Table (3) :- Spectra of He Glow Discharge .

λ (A°)	I (arbit.unit)	λ (A°)	I (arbit.unit)
3962	0.45	4278.5	0.77
4024	0.56	4338.4	0.75
4057	0.16	4368	1.17
4100	0.36	4437	0.40
4119.4	0.69	4471	12.7
4140	0.48	4512	0.27
4157	0.23	4521	0.22
4166	0.44	4549	0.33
4194	0.39	4560	0.21
4221	0.22	4711	0.31
4233	0.58	4919	0.78
4255	0.33	5014	5.55
4275	1.30	5046	0.31

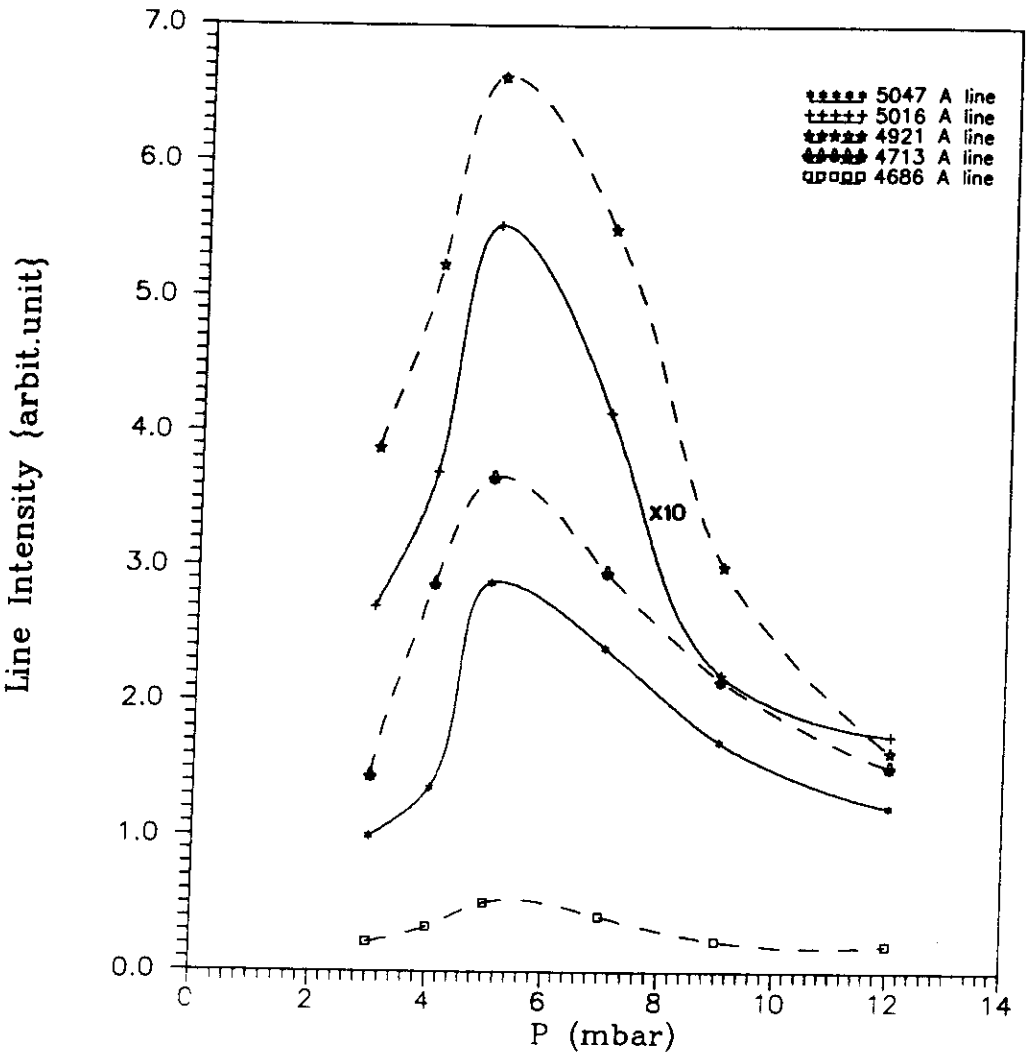

Fig.(73):a) The dependence of some He lines intensity on the gas pressure .

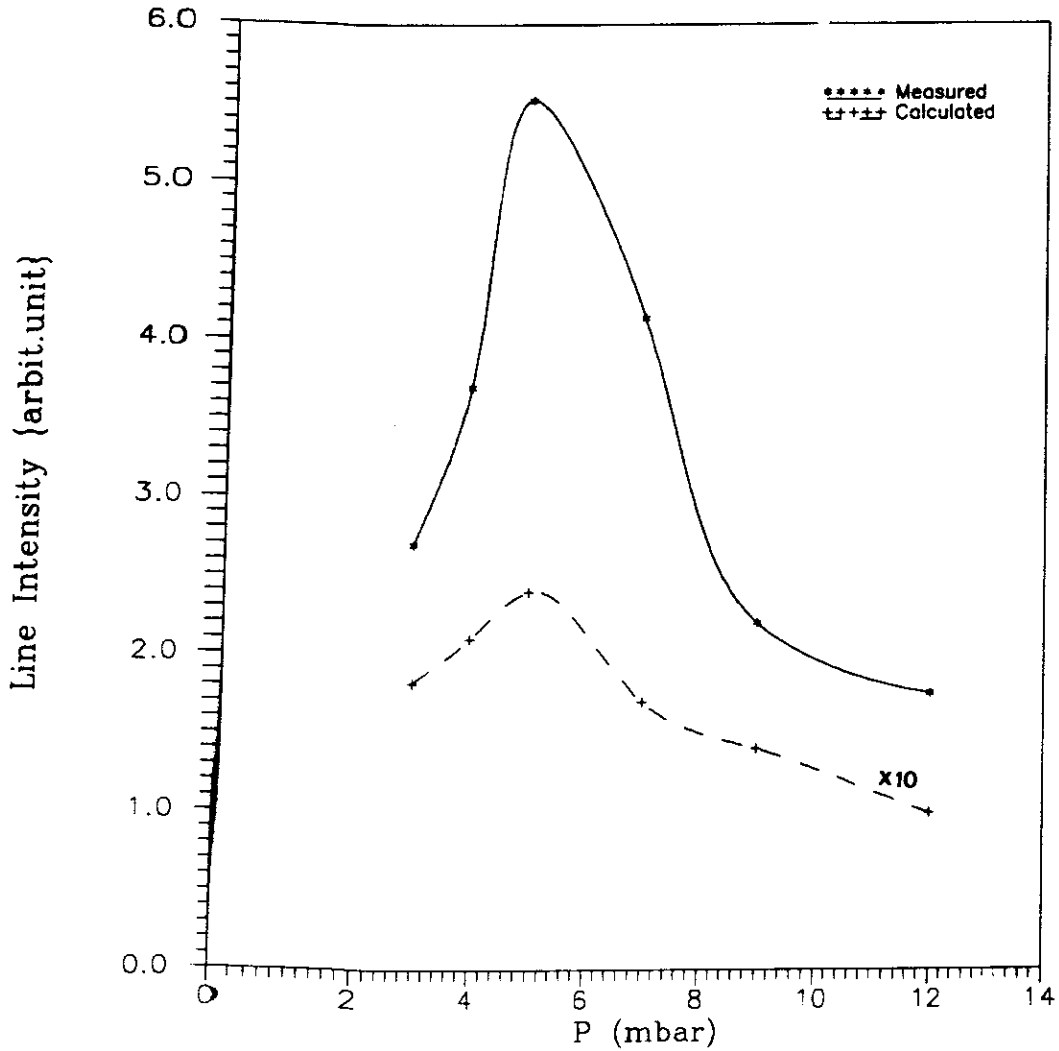

Fig.(73):b) Comparison between the measured and calculated (4921 A^0) He line intensity.

5.5.2- Electron Temperature Measurements :-

Three methods were used to determine the electron temperature using the spectroscopic techniques , these methods were described earlier (see chapter 3) . In the present work , the line to line intensity ratio was used to determine the electron temperature T_e for the negative glow and positive column regions of the Ar and He-glow discharges .

5.5.2.1- T_e Assuming The Plasma in "LTE" Model .

A test for T_e measurements under LTE model was performed by the use of the intensity ratio of Ar lines (e.g. 4259 and 4765 A^0) according to equation (3-13) . If the LTE model criteria are violated , unreliable results would be expected . The electron temperature was given by equation (3-13) , ***(Griem , 1964)*** :-

$$kT_e = \frac{E' - E}{\ln(I\lambda^3 g' f' / I'\lambda'^3 gf)}$$

Where :-

f and λ are the oscillator strength and wave length of the line , g is the statistical weight calculated using J`-J values , E` and E are the excitation energies for the higher and lower ionization stage . The values of the above parameters were taken from ***(Griem , 1964)*** .

T_e values obtained by this method , were in the range of 0.8- 1.6 eV in Ar glow discharge in the range of 1-3 mbar . These result are

obviously too low than those determined by probes . This suggests that the plasma formed in the glow discharge was not in "LTE" model .

5.5.2.2- T_e Assuming The Plasma in Steady State Corona Model

Accurate spectroscopic measurements of T_e could be obtained using calculations based on the radiation intensity ratio of two spectral lines , one emitted by ionized atoms and the other by neutral atoms . For Ar-glow discharge , T_e can be obtained from the ratio of the ion and neutral line intensities (i.e. 4042/4259 A° ratio) using the relation (3-15) ***(McWhirter , 1965)*** :-

$$\frac{I'}{I} = \frac{f'g'\lambda^3}{fg\lambda'^3}\exp\left(\frac{E'_\infty - E' - E_\infty + E}{kT_e}\right)\cdot\frac{S}{\alpha}$$

Where :-

E_∞' is the ionization energy of the higher ionization stage and E_∞ that of the lower stage , E` , E are the excitation energies for the higher and lower ionization stage and S and α are the ionization and recombination coefficients with respect to the next higher ionization stage {see equations (3-9 , 3-10) , section [3.1.1.2] } .

Tables (4) and (5) show values of T_e in the negative glow and positive column regions as a function of the gas pressure in Ar glow discharge . As explained previously in section 5.3 , T_e values decreases as the gas pressure increases .

Table (4) :- T_e Values For Negative Glow Region of Ar Glow Discharge .

P (mbar)	T_e (eV)
1.0	6.50
2.0	6.32
3.0	6.10
4.0	5.93

Table (5) :- T_e Values For Positive Column Region of Ar Glow Discharge .

P (mbar)	T_e (eV)
1.0	6.35
2.0	6.17
3.0	6.05
4.0	5.82

For He discharge , T_e was also deduced by using the relative intensity ratio of singlet and triplet lines ***(Cunningham , 1955)*** .

The intensity of a line resulting from a (p ,q) transition is given by :-

$$I(p,q) = N_e N_o < Q(p,q)(v_e) v_e > .$$

Where :-

Q (p,q) (v_e) is the excitation cross-section for the p-q transition averaged over the Maxwellian distribution , v_e is the electron velocity ($v_e = \{2kT_e/m_e\}^{1/2}$) , N_o is the neutral atoms density and N_e is the electron density . Thus , the intensity ratio for two spectral lines can be given by :-

$$X_0 = \frac{I_{p,q}}{I_{m,n}} = \frac{N_e N_o \langle Q_{p,q}(v_e) v_e \rangle}{N_e N_o \langle Q_{m,n}(v_e) v_e \rangle}$$

The brackets indicate a value average over the velocity distribution . Cunningham's calculations were not accurate, since they neglected the secondary effects such as :-

a) production of metastables with subsequent deexcitation ; b) excitation exchange and c) cascade radiation .

Gabriel and Heddle , (1960) reported that the secondary processes mentioned above may have a major effect on certain lines intensity but other lines are affectedness at all . For example , the 5048 and 4713 A° transitions lines are much less sensitive to these effects than the 4921 A° line .

In the present work , the ratio of the singlet line 5048 A° to the triplet line 4713 A° was calculated and the T_e was deduced by the help of the theoretical curves due to ***Sovie (1964) and Eastuland et al.(1973)***. T_e was also obtained at different gas pressures . Tables (6) and (7) show values of T_e for both negative glow and positive column regions of the He-glow discharge at different gas pressures . Values of T_e obtained by using Sovie's curve are higher than those estimated using Eastuland's curve . This may be attributed to the secondary processes which occur at high pressures . Moreover , Eastuland calculations depend upon Gabriel and Heddle cross sections .

In order to evaluate the effect of the secondary processes , lines 5016 and 3889 A° were used . The choice of the 5016 and 3889 A° lines is attributed to the fact that the secondary processes,such as electron impact induced transitions between excited levels or excitation from metastable levels are well estimated . It is impossible to determine the influence of these secondary processes for the other He I lines due to the lack of atomic data ***(Brenning , 1980)*** .

The 3889 A° line is among the very few lines for which the influence of secondary processes can be calculated , since reliable experimental and/or theoretical determinations exist of all the necessary data . The transitions that determining the 3889 A° line intensity are shown in Fig.(74) . For the 5016 A° line ($3^1P \rightarrow 2^1S$) the analysis is simpler than that for the 3889 A° line . The reason for this is that the upper level 3^1P has a large cross-section for excitation from the ground state and a short natural life time . These facts combine to make the intensity of the 5016 A° line very little influenced (always less than 10 %) by the secondary processes ***(Brenning , 1980)*** . The influences from

Table (6) :- T_e Values For Negative Glow Region of He Glow Discharge Using Eastuland and Sovie Curves .

P (mbar)	T_e (eV) Eastuland	T_e (eV) Sovie
2.7	14	17
4.0	10	12
5.0	10	12
6.2	7.5	10

Table (7) :- T_e Values For Positive Column Region of He Glow Discharge Using Eastuland and Sovie Curves .

P (mbar)	T_e (eV) Eastuland	T_e (eV) Sovie
2.7	16	18
4.0	11	16
5.0	9	13
5.6	10	14
6.2	8.5	11

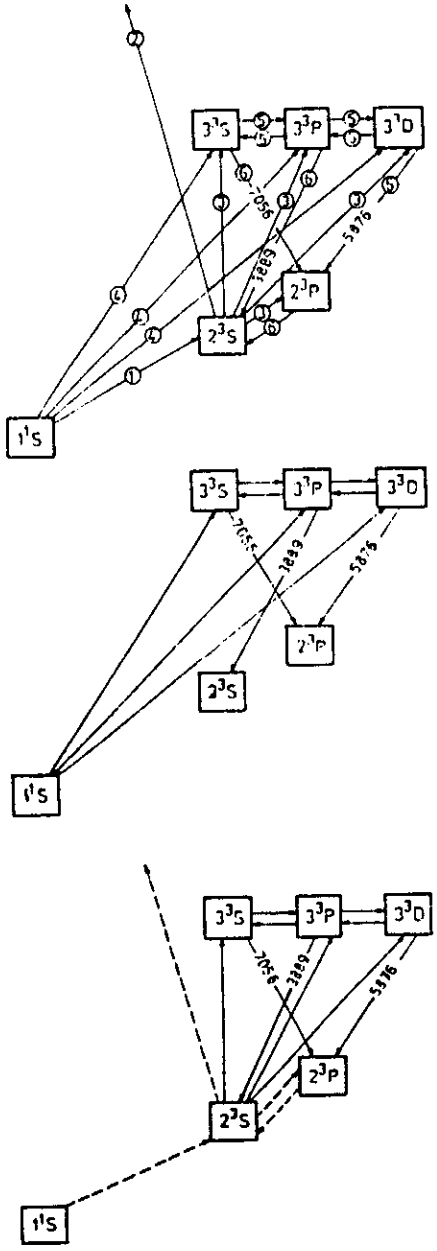

Fig.(7.4): The processes that determine the 3889 Å line excitation rate. (1) Excitation $1^1S \rightarrow 2^3S$ by electron impact, directly or via other triplet level excitations followed by cascading to 2^3S. (2) Ionisation from 2^3S by electron impact. (3) Excitation from 2^3S by electron impact. (4) Excitation from 1^1S by electron impact. (5) Excitation transfer by electron impact. (6) Radiative transitions.

the secondary processes on these two lines were thus calculated using *(Brenning , 1980)* data . The influence on the line intensity from these secondary processes can be , in principle , calculated from the coupled rate equations for population and depopulation of all levels concerned . Unfortunately , this is generally not possible to do for most gases due to lack of atomic data . This can be exemplified with the case of He gas due to the fact that the He atom is one of the most studied and best known .

The intensity ratio of lines 5016 and 3889 A° is computed using the relation :-

$$X_0 = \frac{I_{5016}}{I_{3889}} = \frac{\langle Q_{5016}(v_e)v_e \rangle}{\langle Q_{3889}(v_e)v_e \rangle}$$

To obtain the quantities $< Q_{5016}(v_e)\, v_e >$ and $< Q_{3889}(v_e)\, v_e >$, the excitation cross-section as a function of the electron velocity was multiplied by the electron velocity and averaged over a Maxwellian energy distribution . The cross-section values of the 3889 and 5016 A° lines were taken from ***Gabriel and Heddle , 1960*** . "X_0" was thus plotted against the electron temperature T_e , this is shown in Fig. (75) . In order to obtain T_e , one merely needs to observe the intensity ratio X_0 of the two indicated lines (i.e.5016 and 3889 A°) and obtain T_e from Fig. (75) .

Tables (8) and (9) show T_e values obtained for the negative glow and positive column regions of He glow discharge using Fig. (75) . Again , T_e decreased by increasing the gas pressure .

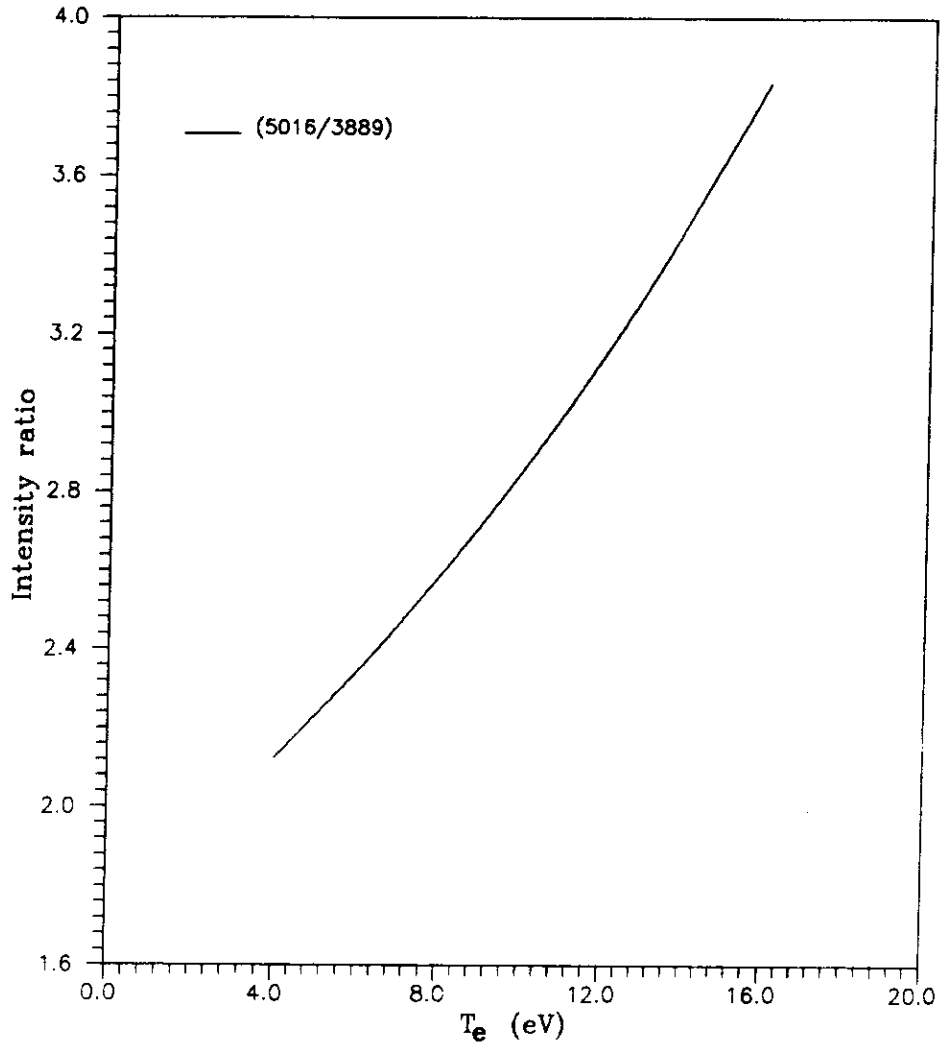

Fig.(75) The (5016/3889) line intensity ratio as a function of T_e .

Table (8) :- T_e Values For Negative Glow Region of He Glow Discharge .

P (mbar)	T_e (eV)
2.7	11.5
3.3	10.2
4.2	9.30
5.0	5.80
5.6	4.90

Table (9) :- T_e Values For Positive Column Region of He Glow Discharge .

P (mbar)	T_e (eV)
2.7	9.80
3.3	9.20
4.2	8.00
5.0	5.40
5.6	4.50

Figures (76) and (77) show a comparison between T_e values obtained using different techniques (probes & spectroscopy) for the negative glow and the positive column regions of Ar glow discharge . A good agreement was obtained . For He glow discharge , a fair agreement was obtained as shown in Figs. (78) and (79) for the negative glow and the positive column regions . This may be attributed to the uncertainty in the cross-section values of the He transition lines .

5.5.3- The Degree of Ionization :-

The degree of ionization in the plasma can be calculated from the ratio of the intensity of the ionized He II line 4686 A° and the neutral line 5048 A° (see sec. 3.2.4) . Using equation (3-22) , the degree of ionization is given by :-

$$S = \frac{100}{1 + \frac{F(kT_e)}{X^*}}$$

Where :-

F (kT_e) is the kinetic electron function which can determined from Sovie's curves {Fig.(6) } and X^* is the ratio of the lines intensity .

The degree of ionization can also be deduced from the ratio of charged to neutral particles . The number of neutrals N_n is given by :-

$$N_n = 3.55 \times 10^{16} P \quad .$$

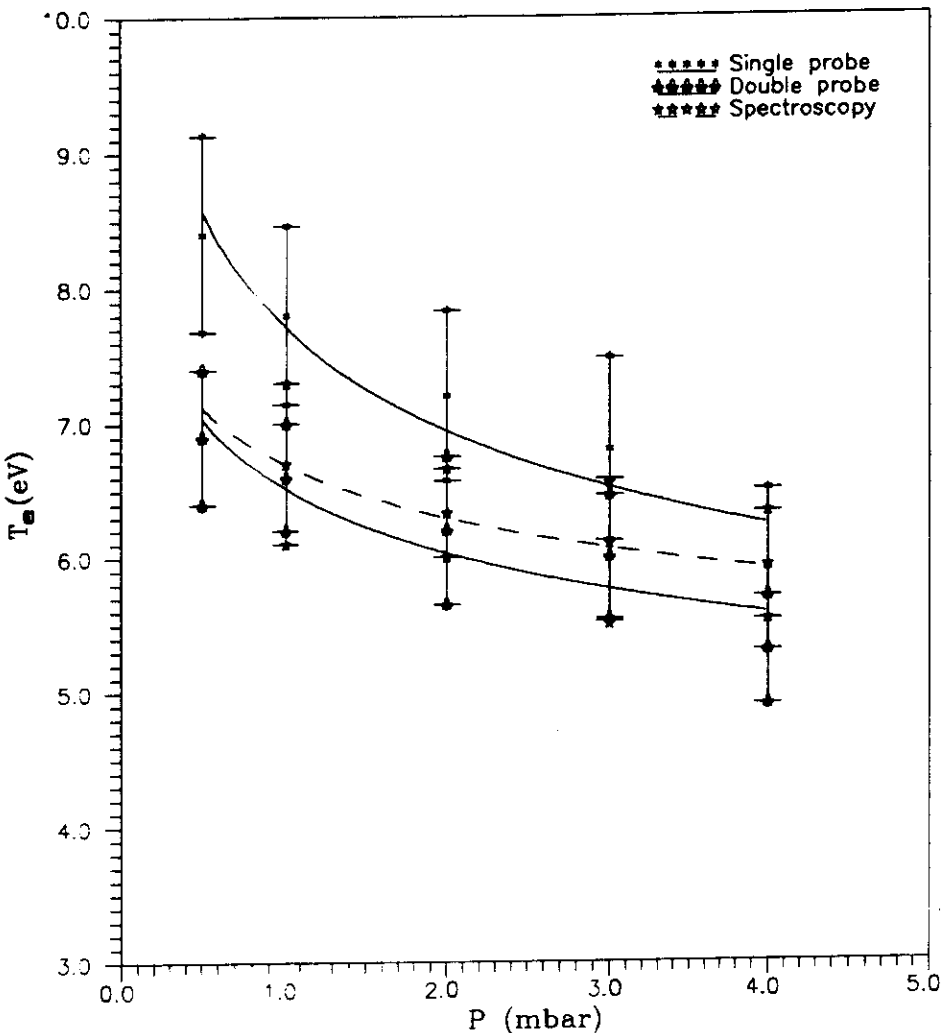

Fig.(76) Comparison between the T_e values , measured by electric probes and spectroscopy of negative glow region at different Ar pressures .

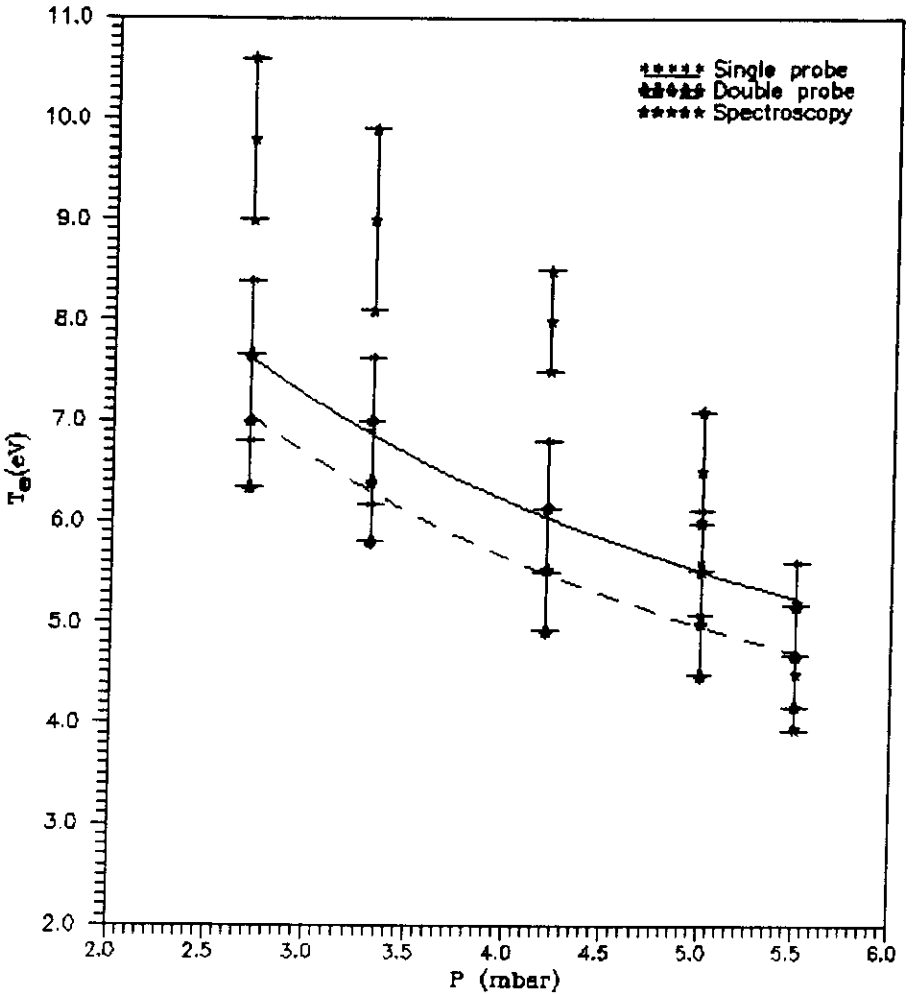

Fig.(79) Comparison between the T_e values, measured by electric probes and spectroscopy of the positive column region at different He pressures .

P is the gas pressure in torr . The degree of ionization using this calculation was found to be less than 6×10^{-6} .

It can be noticed that the degree of ionization obtained by these two different methods are so weak and can be said that the plasma in the present work was partially ionized .

5.5.4- Plasma Modeling :-

Because of the deviation from a Maxwellian energy distribution , it is difficult to describe the plasma model in the cathode fall and negative glow regions of the Ar and He-glow discharges .

Moreover , it is concluded that the plasma in the positive column region of Ar and He glow discharge is in a Steady State Corona model according to the following :-

1- The electrons have a Maxwellian energy distribution function , (see section 5.2) for Ar-plasma in a pressure range of (0.5-4.0 mbar) and for He-plasma in a pressure range of (2.7-5.6 mbar) .

2- The plasma was in a steady state . The positive column region of the glow discharge may be represented as a continuous flow of plasma .

3- Since , the electron temperature was higher than the expected ion temperature in the glow discharge , therefore , ion-ion collisions were negligible .

4- The electron-atom collisions were dominated because $N_e << N_n$, electron - electron collisions were negligible .

5- The plasma was optically thin and the radiation escaped without interacting with it .

6- The corona model criterion ($N_e \leq 10^{11}$ cm^{-3} , equation [3-12]) was well satisfied , since the electron density in the present work was in the order of 10^8 cm^{-3} . This density was much less than the LTE and C-R models .